Norwegian University
of Life Sciences

Master's Thesis 2024 60 ECTS
Faculty of Environmental Sciences and Natural Resource Management

Molting inhibition in *Calanus finmarchicus* from exposure to the chitin synthesis inhibitor teflubenzuron

Celine Våga
Environmental Science

Acknowledgment

This thesis has been a collaboration between the ecotoxicology departments of the Norwegian Institute of Water Research (NIVA) and SINTEF Trondheim. The work has been done as a part of NIVAs EXPECT project with funding from the Norwegian Research Council (Forskningsrådet). The cumulated work and effort have resulted in this master's thesis.

A special thanks is given to my helpful local hosts at the NIVA lab. Thank you, Simon, you helped me greatly by introducing me to the NIVA lab, the protocols, and the chitin analysis, although you were so tired of it. And thank you Li, you showed me how to not destroy the Bioassay lab and fought valiantly with bureaucracy for my entrance chip. Without your help and expertise, I would surely have failed far more often.

To my helpful co-supervisors at Trondheim, Bjørn Henrik Hansen at SINTEF Ocean and Dag Altin at NTNU, thank you for the animals and your experience. My incredible skills in non-sedated imaging of *Calanus* will always be at your disposal. Thanks also to the EMBRC-ERIC Laboratory for Low-Level Trophic Interactions at NTNU SeaLab for access to the culture of *Calanus finmarchicus.*

One must not forget Knut-Erik Tollefsen, who guided Hanne and me through the overwhelming jungle of structured science, meetings, and TEAMS. Thank you for your knowledge, patience, feedback, life advice, and time.

And lastly, to the girls who made these last five years unforgettable with love, tears, laughter and memories. Life is better with you guys.

Abstract

Within the aquaculture industry, various chemotherapeutics and treatment strategies have been applied to protect farmed fish in open cages against parasites and diseases. Among the most common strategies for management of parasitic copepods is the use of chitin synthesis inhibitors (CSI) such as teflubenzuron. In addition to controlling salmon lice infestations of salmon, exposure to teflubenzuron can cause adverse effects in non-target organisms within the surrounding marine environment. Teflubenzuron causes inhibition in the synthesis of chitin resulting in premature molting and molting-associated mortality. In the marine boreal ecosystems, the copepod *Calanus finmarchicus* is essential in interconnecting trophic levels and constitutes a substantial part of the total zooplankton biomass in the northern oceans. The copepod depends on molting between life stages to grow and is a potential non-target organism to teflubenzuron. As climate changes, an increase in environmental stress and anthropogenetic pollution in the arctic and boreal areas is expected. Likewise expected is the future need for knowledge of the potential effects increased anthropogenic activity and presence has on the northernmost environment and the life in it.

Adverse outcome pathways (AOPs) is a tool that provides insight into the mechanistic processes of complex systems by examining, evaluating, and organizing key events and the relationship between them into linear sequences of events. There is currently a wide network of AOPs used in hazard identification of numerous typical stressors. As a continuation of the work in AOP 360, "Inhibition of chitin synthase 1 leading to increased mortality in arthropods", this thesis aims to investigate the relationship between exposure to the veterinary insecticide teflubenzuron and the negative effects on molting in the copepod *C. finmarchicus*. To achieve this, an extended sub-acute exposure study of *C. finmarchicus* has been carried out, supplemented by a gene expression study of genes relevant to the molting process and its regulation. Additionally, a novel method is being developed for fluorescent chitin imaging and measurement of chitin content in marine copepods. Based on these sub-studies, this thesis aims to describe the effects of teflubenzuron on molting in *C. finmarchicus.*

The main findings suggest that exposure concentrations of 0.03 µg/L teflubenzuron and higher causes inhibition of normal development and growth, morphological deformities, and molting-associated mortality in *C. finmarchicus*. Correcting this effect concertation from nominal to measured (0.127 µg/L), our findings suggest that *C. finmarchicus* can experience substantial adverse effects on multiple levels of biological organization at environmentally relevant concentrations. Despite multiple indications of the possible effect teflubenzuron has on chitin synthesis in *C. finmarchicus*, no statistical significance was found for the expression of *chs1* at teflubenzuron exposures of 0.01 µg/L -0.03 µg/L. Thus, this study was unable to link molecular inhibition of chitin synthesis, by *chs1,* to the adverse effects found in the other levels of biological organization related to molting.

In summary, teflubenzuron causes adverse molting-associated effects in *C. finmarchicus* at environmentally relevant concentrations. Future efforts to link teflubenzuron to the inhibition of *chs1* are needed to assess the applicability of AOP 360 to *C. finmarchicus*.

Sammendrag

Innen akvakulturindustrien har ulike kjemoterapeutika og behandlingsstrategier blitt brukt for å beskytte oppdrettsfisk i åpne merder mot parasitter og sykdommer. Blant de vanligste strategiene for håndtering av parasittiske hoppekreps er bruken av kitinsyntesehemmere (KSH) som teflubenzuron. I tillegg til å kontrollere infestasjoner av lakselus hos laks, kan eksponering for teflubenzuron forårsake uønskede effekter hos ikke-målorganismer i det omkringliggende marine miljøet. Teflubenzuron forårsaker hemming i kitinsyntesen, noe som resulterer i prematurt skallskifte og skallskifte-assosiert dødelighet. I de marine boreale økosystemene er hoppekrepsen *Calanus finmarchicus* avgjørende for å koble sammen trofiske nivåer og utgjør en betydelig del av den totale zooplanktonbiomassen i de nordlige havene. Hoppekrepsen er avhengig av skallskifte mellom livsstadier for å vokse og er en potensiell ikke-målorganisme for teflubenzuron. Som følge av klimaendringer, forventes det et økt miljøstress og mer antropogen forurensning i arktiske og boreale områder. På samme måte forventes det et fremtidig behov for kunnskap om de potensielle effektene som økt antropogen aktivitet og tilstedeværelse har på det nordligste miljøet og livet i det.

Adverse Outcome Pathways (AOPs) er et verktøy som gir innsikt i mekanistiske prosesser i komplekse systemer ved å undersøke, evaluere og organisere nøkkelhendelser og forholdet mellom dem i lineære sekvenser av hendelser. Det er for øyeblikket et bredt nettverk av AOP-er som brukes i fareidentifisering av mange typiske stressfaktorer. Som en videreføring av arbeidet i AOP 360, "Inhibition of chitin synthase 1 leading to increased mortality in arthropods", har denne avhandlingen som mål å undersøke forholdet mellom eksponering for veterinærinsekticidet teflubenzuron og de negative effektene på skallskiftet hos hoppekrepsen *C. finmarchicus*. For å oppnå dette har det blitt gjennomført en utvidet subakutt eksponeringsstudie med *C. finmarchicus,* supplert med en genuttrykk studie av gener relevante for skallskifteprosessen og dens regulering. I tillegg utvikles det en ny metode for fluorescerende kitinavbildning og måling av kitininholdet i marine hoppekreps. Basert på disse delstudier har denne avhandlingen som mål å beskrive effektene av teflubenzuron på skallskiftet hos *C. finmarchicus*.

De viktigste funnene antyder at eksponeringskonsentrasjoner på 0.03 µg/L teflubenzuron og høyere forårsaker hemming av normal utvikling og vekst, morfologiske deformiteter og skallskifte-assosiert dødelighet hos *C. finmarchicus*. Ved å korrigere denne effektkonsentrasjonen fra nominell til målt (0.127 µg/L), antyder våre funn at *C. finmarchicus* kan oppleve betydelige uønskede effekter på flere nivåer av biologisk organisering ved miljømessig relevante konsentrasjoner. Til tross for flere indikasjoner på den mulige effekten teflubenzuron har på kitinsyntesen i *C. finmarchicus*, ble det ikke funnet statistisk signifikans for uttrykket av *chs1* ved teflubenzuron-eksponeringer på 0.01 µg/L -0.03 µg/L. Dermed kunne denne studien ikke knytte molekylær hemming av kitinsyntese, ved *chs1*, til de alvorlige effektene som ble funnet på de andre nivåene av biologisk organisering relatert til skallskifte.

Oppsummert forårsaker teflubenzuron uønskede skallskifte-assosierte effekter hos *C. finmarchicus* ved miljømessig relevante konsentrasjoner. Fremtidige arbeid for å knytte teflubenzuron til hemming av *chs1* er nødvendig for å vurdere anvendbarheten av AOP 360 for *C. finmarchicus.*

Glossary

Term	*Definition and description*
AF	Assessment factor
AO	Adverse outcome
BMDx	Benchmark dose of X% effect
CSI	Chitin synthesis inhibitor
ECx	X% effect concentration
IGR	Insect growth regulator
KE	Key event
KER	Key event relationship
LCx	X% lethal concentration
LOEC	Lowest observed effect-concentration
MFC	Mean fold change
MIE	Molecular initiating event
MoA	Mode of action
NOEC	No observed effect-concentration
PEC	Predicted effect concentration
PNEC	Predicted no-effect concentration

Outline

Acknowledgment II

Abstract III

Sammendrag IV

Glossary V

1 Introduction 1

1.1 Chemical Pollution from marine intensive aquaculture to the environment 1

1.2 Mode of action of CSI and effects on non-target organisms 3
1.2.1 Molecular mode of action of CSI and chitin metabolism 3
5
1.2.2 Non-target organisms and effects from CSI exposure 5

1.3 Calanus finmarchicus; a key species in northern marine ecosystems 6

1.4 Linkage of mechanistic information to regulatory relevant endpoints; Adverse Outcome Pathways 8
1.4.1 Relevant AOPs for molting inhibition in *C. finmarchicus* 8

1.5 Objective 10

2 Material and methods 11

2.1 Project overview 11

2.2 Sub-acute toxicity test of teflubenzuron on developing life stage C. finmarchicus copepods 11
2.2.1 Preparation phase 11
2.2.2 Culture conditions of *C. finmarchicus* 12
2.2.3 Experimental phase 12
2.2.4 Analysis phase 15

2.3 Calculation of ecotoxicologically relevant threshold levels 17

2.4 Statistical analysis of data 17

3 Results 18

3.1 Test Chemicals and chemical analysis 18

3.2 Acute toxicity test of teflubenzuron exposure 18
3.2.1 Mortality 18
3.2.2 RNA extraction 19
3.2.3 Gene expression by qPCR 19
3.2.4 Developmental stage distribution 22
23
3.2.5 Prosome length 23
3.2.6 Morphological deformities 24
25

3.3 Summary toxicological dose descriptors 25

4 Discussion 26

4.1 Ecotoxicological effects from teflubenzuron exposure on developmental stages of C .finmarchicus; main findings from this study 26
4.1.1 Apical endpoints: Mortality 26
4.1.2 Molecular endpoints: Expression of molting relevant genes in response to teflubenzuron exposure
27

4.1.3 Physiological and morphological endpoints: Developmental inhibition and deformities 29

4.2 Linking molecular effects to physiological deformities by AOP360; fitness of model *30*

4.3 Methods and study design; factors influencing results *31*
4.3.1 Calanus finmarchicus as a study species; practical limitations of scale 31
4.3.2 Life stage heterogeneity and size bias during sampling 32
4.3.3 Unexpected high mortality and implications for the gene expression study 32

4.4 Environmental relevance *33*
4.4.1 Bioavailability of teflubenzuron to *Calanus finmarchicus* in a laboratory setting and in the environment. 33
4.4.2 Current environmental standards and relevance to this study 34

4.5 Future prospects and potentials *34*
4.5.1 Optimization of study design based on experiences from this study 34
4.5.2 The potential of fluorescent high-content imaging in chitin content determination 35
4.5.3 Future development of AOPs 35

4.6 Summary and conclusion *36*

5 References **37**

Appendix **44**

I. Summary literature review *44*

II. Figures and tables *45*

III. Genes, primers and priority list *57*

IV. Image compilation: Dose-dependent morphological deformities in C. finmarchicus from teflubenzuron exposure *60*

1 Introduction

1.1 Chemical Pollution from marine intensive aquaculture to the environment

Marine aquaculture is one of Norway's most influential and largest industries that in addition to contributing to great national values economically, is a major source of chemical pollution to the environment it makes use of. Norwegian intensive fish farming is focused on a handful of species, mainly salmonoid fish such as Atlantic salmon (*Salmo salar*) and is located scattered along the Norwegian coast; from north to south. A major issue within the industry is the balance between high biomass production and controlling salmon lice infestations. A high biomass production, traditionally in open net pens, often entails more parasite infestations and reduced animal welfare (Grefsrud et al., 2023); tipping the balance scale towards increased pressure on farmed fish, wild fauna, and the marine environment. The development and implementation of chemical veterinary medicine and insecticides have played an important role in managing and solving the issue of parasite infestations (Burridge et al., 2010; Jansson et al., 1997; Matsumura, 2010; Merzendorfer, 2013; Sun et al., 2015). Veterinary chemotherapeutics in marine aquaculture are prescribed chemical treatments used to remove and manage parasitic copepods such as ectoparasitic salmon lice, *Lepeophtheirus salmonis* and *Caligus elongate* in the northern hemisphere, either as chemical bath treatments or as in-feed chemotherapeutics (Burridge et al., 2010; Langford et al., 2014; Myhre Jensen et al., 2020). Today, a wide catalog of chemical treatments with different molecular modes of action (MoA) and insecticidal activity is available for industrial purposes in pest control. Amongst the few regulated for use in Norwegian marine aquaculture are chitin synthesis inhibitors (CSI).

Chitin synthesis inhibitors (CSI) are a group of chemical insect growth regulators (IGR) that have an inhibitory effect on chitin synthesis and molting in arthropods. Molting (ecdysis) is defined as "the coordinated formation of a new exoskeleton and shedding of the old exoskeleton" (Harðardóttir et al, 2019). There are several groups of chemicals that act as CSI, such as pyrimidine peptides, oxazolines, tetrazines, and benzoylphenylureas (Merzendorfer, 2013). Of the benzoylphenylurea compounds, diflubenzuron and teflubenzuron are today the most widely used insecticides in both hemispheres to protect crops, trees, and livestock from nuisance pests (Merzendorfer, 2013; Sun et al., 2015). Teflubenzuron ([1-(3,5-dichloro-2,4-difluorophenyl)-3-(2,6-difluorobenzoyl) urea]) is commonly sold as the active ingredient in veterinary pharmaceuticals under brand names such as Ektoban vet® (Skretting, Norway) and Calicide® (Nutreco, Canada). The compound is mainly administered at a dosage of 10 mg/kg fish daily for seven days, and is advertised as effective against larval and nauplii stages of parasitic copepods by inhibition of chitin synthesis (Burridge et al., 2010; Felleskatalogen, 2018; A. E. Parsons et al., 2021; Samuelsen et al., 2015). In marine intensive aquaculture teflubenzuron is mainly used as an in-feed chemotherapeutic coated on feed pellets for salmonoid fish farming. As the farmed fish feed on the medicinal pellets, the active ingredients are taken up in the fish and distributed in the body. When the ectoparasitic salmon louse then feeds on the host fish's skin, mucus, and or blood, the chemotherapeutic is administered to the parasite, causing molting inhibition and mortality (Grefsrud et al., 2022a).

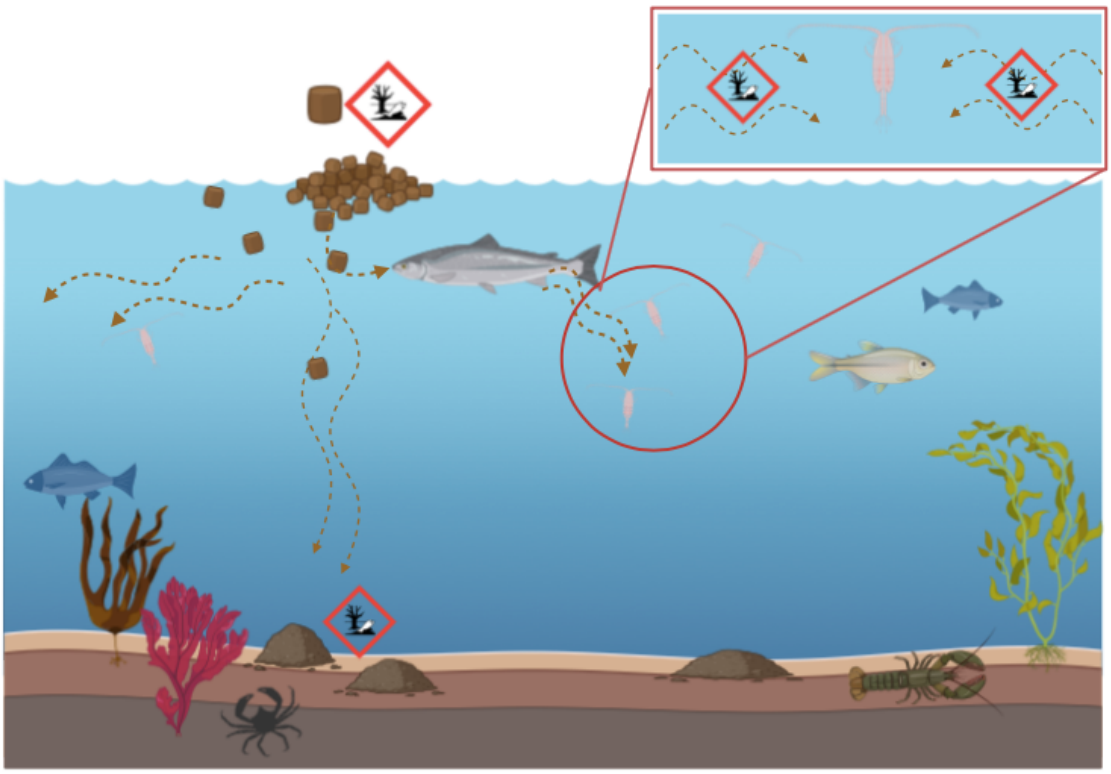

Figure 1: Schematic of the environmental fate of chitin synthesis inhibitors (CSI) such as teflubenzuron used as in-feed chemotherapeutics in marine aquaculture. The main routes of exposure to teflubenzuron are illustrated by the dashed lines and represent leaching to the water from spilled feed or through the excretory system (feces/urine) of farmed fish.

As chitin synthesis is an arthropod- and fungal-specific and highly conserved biological process, there is a beneficial low risk of hazard to mammals, birds, and fish (Merzendorfer, 2006, 2013; Zhu et al., 2016). In Norwegian marine aquaculture, CSI was introduced in the early 90s as a treatment against frequent salmon lice infestations (Macken et al., 2015; Myhre Jensen et al., 2020). The usage of CSI increased rapidly during the 2010s and reached an all-time high in 2015 and 2016 (Figure 1, Appendix II). During this peak, more than 9000 kg of the CSI compounds teflubenzuron and diflubenzuron were administered and released from Norwegian fish farms to the open marine environment (Folkehelseinstituttet, 2024; Grefsrud et al., 2022b). However, pharmacokinetic studies of veterinary insecticides in farmed fish have shown that as little as 10% of the active chemical is accumulated in the host organism, meaning that as much as 90% is released into the open environment by mainly feces and urine (Samuelsen et al., 2015; Strachan & Kennedy, 2021). Additionally, medicinal pellets that are not eaten by the fish during treatment will also contribute to the redistribution of the insecticides into the environment (A. Parsons et al., 2021; Samuelsen et al., 2015). Due to the low water solubility of teflubenzuron (K_{OW}≈ 5.4, (Grefsrud et al., 2022b)) the insecticide readily adsorbs to organic particles in the water column or accumulates in the sediments below the fish farms (Grefsrud, 2024; A.E Parsons et al., 2021; Samuelsen et al., 2015; Strachan & Kennedy, 2021). Surprisingly, the environmental data on the concentration of teflubenzuron in the water phase is scarce. The most current study mapping and reporting water-phase concentrations of teflubenzuron in Norway is Langford's study from 2014. Langford's team reported environmental concentrations of teflubenzuron at four sites near aquaculture

facilities, two in Northern Norway, two on the West Coast of Norway, and one non-aquaculture reference site in the Oslo Fjord. Here Langford's team reported concentrations higher than 1 µg/L teflubenzuron at sites in both Northern Norway and the West Coast of Norway. Additionally, the team also reported an extraordinary concentration of 12.9 µg/L teflubenzuron near one of the facilities in Northern Norway, ten times higher than the most serious EQS class limit for teflubenzuron in coastal waters at 1.2 µg/L (Langford et al., 2014; Miljødirektoratet, 2010).

Today, the usage of chemical treatments against salmon lice, both bath treatments and in-feed chemotherapeutics, has been reduced and shifted towards a preferred usage of mechanical strategies of parasite counter measurement. This strategic paradigm shift has reduced the overall chemical pollution from farming sites along the Norwegian coast, as well as prevented uncontrollable outbreaks of insecticide resistance in salmon lice (Myhre Jensen et al., 2020). As the concern about the environmental impact of the industry decreased, so did also the environmental monitoring of teflubenzuron concentrations in the environment. Thus, it is difficult to determine the degree of current teflubenzuron presence or pollution in the Norwegian marine environment. To add to the insecurity around teflubenzuron in the environment, the previous assumptions of the degree of persistence of teflubenzuron in the environment were shown by Parsons to be severely underestimated (A.E Parsons et al., 2021). Teflubenzuron was shown to be present for 8-22 months longer than the previously predicted environmental persistence (half-life of five to six months), and with a substantial distribution away from the original farming facility (Langford et al., 2014; A. E. Parsons et al., 2021). Such underestimate and the lack of updated environmental monitoring data shows that there is a wider knowledge gap when it comes to the role veterinary insecticides from marine aquaculture could, and do, play in the environment as chemical pollutants against non-target organisms.

1.2 Mode of action of CSI and effects on non-target organisms

1.2.1 Molecular mode of action of CSI and chitin metabolism

Until recently, the actual mode of action (MoA) of many CSIs remained uncertain. Over the years there have been several suggested explanations for the chitin-inhibitory effects of the benzoylphenylurea compounds. In Matsumura's review from 2010, it was suggested that the target site of diflubenzuron was the insect sulfonylurea receptor (SUR receptor) (Matsumura, 2010). Later in 2013 Merzendorfer further suggested in his review that benzoylphenylureas block a pre- or post-catalytic step in the chitin synthesis (Merzendorfer, 2013). Macken and others also suggested that the possible mode of toxicity of CSI is caused by the inhibition of expression of chitin synthetase enzymes during molting in the early life stages of arthropod development (Macken et al., 2015). This suggestion was further confirmed by Douris's team the year after. By utilizing genome editing the team eluded the MoA of benzoylphenylureas insecticides to directly interfere with the chitin synthase 1 (*chs1*) gene, causing inhibition in the chitin synthesis of arthropods (Douris et al., 2016).

Chitin synthases (CHS) are integral transmembrane proteins that have a key role in the synthesis of chitin in arthropods (Merzendorfer, 2013). In arthropods, there are mainly two chitin synthetases, CHS1 and CHS2. The former is located in the external cuticle and is important for chitin deposition on the exterior of the animal, the latter is found in the midgut

and lining of the intestine (Harðardóttir et al., 2021). The CHS1 translocates newly formed chitin across the plasma membrane and facilitates the higher structural organization of chitin into growing chains of polymeric chitin (e.g. into microfibrils). Eventually, the chitin is deposited onto the cell surface where it serves as a protective layer on the surface area of the organism (Merzendorfer, 2013; Zhu et al., 2016). In addition to creating a tough barrier against the potential harm of the outer environment, chitin in the cuticle and exoskeleton has a structural function of high relevance in the molting process. Sufficient chitin content in the shell and exoskeleton of crustaceans is necessary for successful molting and further development (Chang & Mykles, 2011; Zhang et al., 2021).

The importance of chitin in the molting process also becomes apparent when examining the expression pattern of chitin synthases during molting. The molting process itself can be described through five phases: initial shedding of the old exocuticle (ecdysis), a postmolt stage with completion of the new cuticle (metecdysis), an intermolt stage of maturation of the newly formed exocuticle (anecdysis) and a premolt stage (preecdysis). In this preparatory premolt phase the animal simultaneously synthesizes a new cuticle, degrades the connective tissue between the cuticle layers, and degrades the old exoskeleton for apolysis; as demonstrated in Figure 2 (Harðardóttir et al., 2021; Skinner, 1962). Previous studies of the

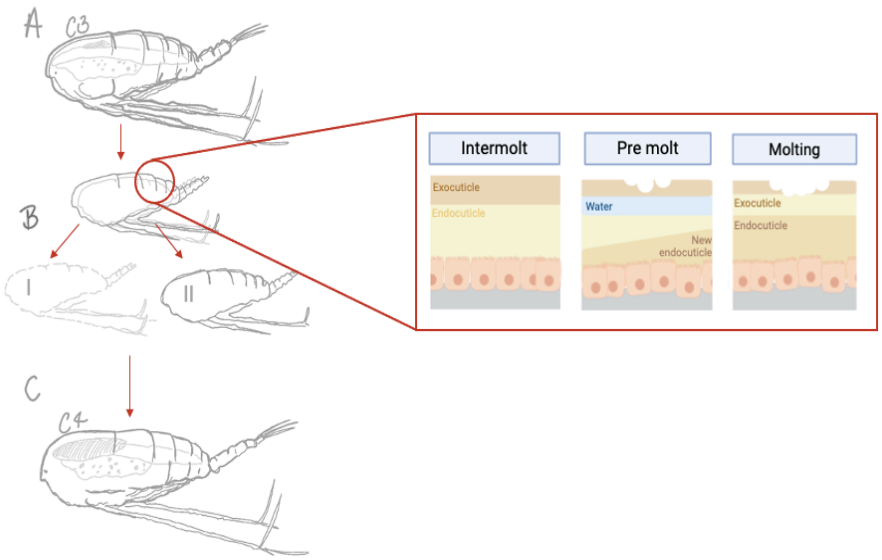

Figure 2: Schematic of the molting process in copepods (A-C). At the initiation of molting (A-B) the copepods cuticle layers (endocuticle and exocuticle) are replaced by simultaneous synthesis of a new inner cuticle (II) and degradation (I) of the connective tissues between the layers, in addition to degradation of the old external cuticle.

genetic expression pattern of CHS in whiteleg shrimp (*Litopenaeus vannamei)* demonstrate how the expression of CHS abruptly decreases in the premolt phase before a sharp up-regulation again in the postmolt stage (Zhang et al., 2021). This study, amongst others, demonstrates how the regulation of chitin synthesis follows, or leads, the need for structural integrity in the crustacean cuticle throughout the molting process of the animal. Therefore, the inhibition of chitin synthesis by the inhibition of CHS has implications for the success of molting and development in crustaceans (Harðardóttir et al., 2021; Schmid et al., 2022; Zhang et al., 2021). Not to forget, the chitin synthases are only the last enzymes in a long line of enzymes of importance in the chitin metabolism machinery and molting (Figure 3) (Zhang et al., 2021). Molting is not exclusively dependent on the activity of chitin synthases, but rather

on the dynamic balance between synthesis, degradation, as well as regulation. Understanding, as well as uncovering, the effects CSI has on the chitin metabolism machinery as a whole could be vital to grasp the full extent of the effects of chemical pollution in the environment and the susceptible species in it.

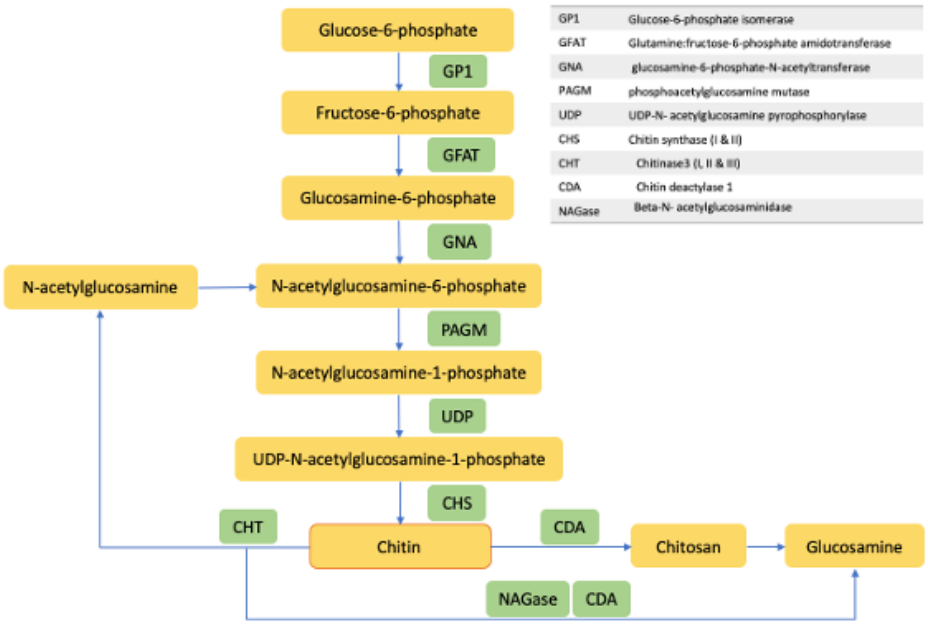

Figure 3: Schematic overview of the chitin metabolism pathway based on Zhang et.al. 2021. The main chitin synthesis pathway (downward) in relation to the chitin degradation pathways (left and right), as well as re-cycling of chitin back into the chitin synthesis pathway (left loop).

1.2.2 Non-target organisms and effects from CSI exposure

Since the implementation of chemotherapeutics and its use in aquaculture to target ectoparasitic pests, the concern of its influence on non-target organisms has been present. Especially, the concern of risk to marine crustaceans who share the dependency on chitin integrity and molting during development as the targeted pests. In response to this issue, there have been several studies on the effect of CSI compounds on both marine and aquatic crustaceans, including copepods, as non-target species (Macken et al., 2015; Olsvik et al., 2015; Song et al., 2016; Song et al., 2017; Willis & Ling, 2003). Generally, marine-oriented studies focus on economically important species such as lobster, shrimp, and crab, with fewer studies on ecologically important organisms such as zooplanktonic copepods as non-target species. Nevertheless, these studies on marine non-target organisms have uncovered a range of important effects from mortality, and morphological and behavioral changes, to molting inhibition and molting defects. Mortality in arthropods and crustaceans related to exposure to benzoylphenylurea is in most cases a result of the individual's inability to cast or escape its old exoskeleton during the molting process (Wright et al., 1996). An example of this is Samuelsen's study on teflubenzuron and non-target lobsters, where molting-associated mortality in *Homarus gammarus* juveniles after feeding on high-dosage teflubenzuron pellets was reported (Samuelsen et al., 2014). Other studies, such as Olsvik's from 2015, found morphological deformities in *H. gammarus* from both low and high exposure concentrations of teflubenzuron (Olsvik et al., 2015). The same study also found changes in the expression of

genes related to important biological functions such as molting and exoskeleton regulation, drug detoxification, and oxidative and cellular stress (Olsvik et al., 2015). A study done by Cresci in 2018 even found negative behavioral effects in *H. gammarus* from exposure to sub-lethal doses of teflubenzuron (Cresci et al., 2018).

1.3 *Calanus finmarchicus*; a key species in northern marine ecosystems

Calanus finmarchicus (Gunnerus, 1770) is a planktonic marine copepod of large ecological and biogeochemical importance in Northern Atlantic waters (Melle et al., 2014; Reygondeau & Beaugrand, 2011). The copepod represents a major link between trophic levels in the ocean as it connects and converts energy from primary producers to larger consumers in the marine food web (Møller et al., 2012). This interconnecting role is partly due to the high lipid content of the animal, contributing up to 50%-70% of its body weight (Aarflot et al., 2018), as well as its role during naupliar life stages as an essential food source for e.g., fish larvae in the marine ecosystem (Basedow et al., 2024). In addition to its important role ecologically*, C. finmarchicus* is also one of the largest contributors to planktonic biomass in the northern Atlantic oceans. In some areas, it represents more than 80% of the total zooplanktonic biomass (Hansen et al., 2008; Aarflot et al., 2018).

The accumulated knowledge of *C. finmarchicus* is extensive, and key biological processes such as development and growth have been thoroughly researched. The life cycle of *C. finmarchicus* is divided by molting into six naupliar (N1-N6), five juvenile copepodite (C1-C5), and one final adult copepod life stage (A/C6) (Figure 4). Physiological and morphological changes, such as an increase in lipid sac volume, cuticle tanning, biomass growth, and addition of segments on the prosome distinguish each life stage. During the first developmental stages (eggs to N6), the interval between each molt is shorter, each developmental life stage lasting between 2-3 days. At older life stages (C1-C5) the intervals between molting become longer, spending around 3-5 days at each developmental stage (Campbell et al., 2001); Table 1, Appendix II). Approximately 36 days after the eggs were hatched the copepods have developed into sexually mature individuals, completing their life cycle.

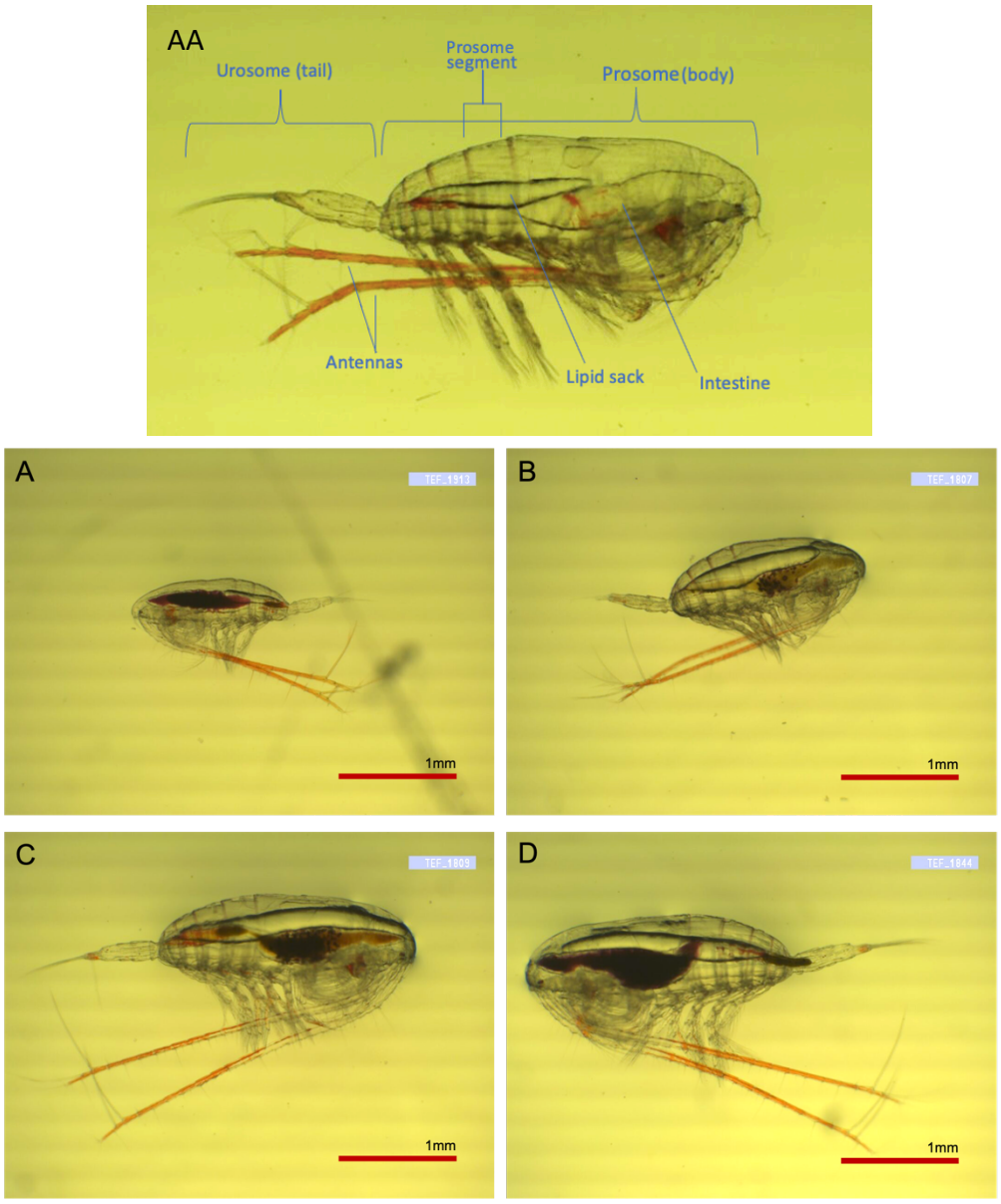

Figure 4: Panel AA: Imaged Calanus finmarchicus *(C3) from study. The main body (prosome) is divided between serval prosome segments. The tail (urosome) is also segmented with a tail-whisker at the end of the tail. The intestine and lipid sac makes up a major part of the prosome volume. Panel A-D illustrate the different life stages of* C. finmarchicus. *A= C2, B= C3, C= C4 and D=C5. All images were taken during sampling of copepods with a 3.6X magnification. All photos: Celine Våga.*

Surprisingly, despite its high ecological relevance and importance in the arctic and northern marine ecosystem, by knowledge there are currently no studies on the exposure effects of any CSI on *C. finmarchicus.* Thus, there is little experience and or guides that describe the susceptibility of *C. finmarchicus* to CSIs such as teflubenzuron. Exploring and linking molecular effects from CSI exposure to phenotypic alterations and adverse effects is necessary to broaden our understanding of the complex effects anthropogenic pollution has on the environment and the species within it. Hopefully, this expansion of knowledge of CSI exposure in marine arctic and boreal copepods will also be helpful in a regulatory setting or in future hazard and risk assessments.

1.4 Linkage of mechanistic information to regulatory relevant endpoints; Adverse Outcome Pathways

An AOP is defined as a "conceptual construct that portrays existing knowledge concerning the linkage between a direct molecular initiating event (MIE) and an adverse outcome (AO) at a biological level of organization relevant to risk assessment" (Ankley et al., 2010). Practically, this is done by identifying the cascade of events starting with the molecular initiating event (MIE), the first molecular interaction between a stressor and its biological target, to a sequence of intermediate causal key events (KEs) that ultimately lead to an adverse outcome (AO) of regulatory relevance (figure 5). The key event relationships (KER) are important to link similar, or completely different, AOPs together based on a common relationship to the KE and are fundamental in AOP network organizations.

The confidence behind each AOP and its content is evaluated by utilizing tailored Bradford-Hill weight-of-evidence considerations (Becker et al., 2015). By this approach, the mechanistic relation between KE's is assessed by the biological plausibility and the biological understanding of the process in question, resulting in a rating of either high, moderate, or low confidence. AOP Wiki (https://aopwiki.org) is a collaborative online database of AOP's hosted by the Society for the Advancement of Adverse Outcome Pathways (SAAOP). The AOP Wiki serves as one of several larger OECD-sponsored AOP Knowledgebase (AOP-KB) efforts . Within the AOP Wiki database, AOPs are connected by relevant KE and KER to create a network between AOPs. Such AOP networks help organize knowledge of effects from prototypical stressors to adverse outcomes that could be used in everything from academia to environmental risk management.

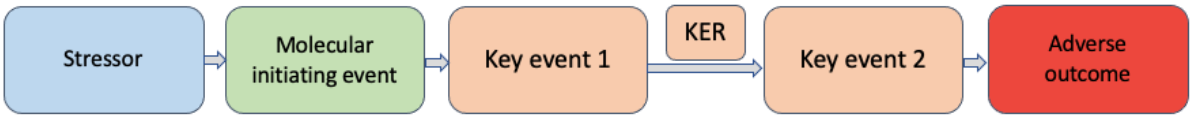

Figure 5: Schematic of a typical linear AOP. The AOP describes the causality and relationship between the stressor (blue), the molecular initiating event (MIE, green), and the following key events (KE, orange) at different orders of biological levels (e.g., cell, tissue, organ). Eventually, the KEs lead to adverse outcomes (AO, red).

To gain insight into the mechanistic effects of CSI on the molting process of *C. finmarchicus*, methods capable of detecting changes at distinct levels of biological organization are needed. Quantitative PCR (qPCR) is one tool suited for analysis of the genetic expression, where measurement of the fold genetic change can capture the molecular effects from CSI exposure. Additionally, microscopy paired with polymer-specific fluorescence probes allows for insight into the physiological structures and potential alterations in the composition of the cuticle (e.g., chitin content) from exposure to CSI. Connecting the molecular changes with changes at higher orders of biological level (e.g., physiological and developmental) allows for a deeper understanding of the relationship between distinct biological components and the biological system.

1.4.1 Relevant AOPs for molting inhibition in *C. finmarchicus*

There are currently five relevant AOPs available at AOPWiki describing molting inhibition in arthropods leading to an increase in mortality (Table 1 and Figure 6). The term 'premature molting' is used to describe the disruption and inhibition of molting in reference to the chitin synthesis machinery (Schmid et al., 2021) .However, as molting in crustaceans, and hence,

copepods, is a dynamic balance between synthesis and degradation, understanding the relationship and effect of inhibition of key points in the chitin metabolism and regulation becomes crucial.

Table 1: Overview of available AOPs of relevance to molting inhibition in arthropods

#	*AOP short name*
361	SUR binding leading to mortality
360	Chitin synthase 1 inhibition leading to mortality
359	Chitiobiase inhibition lading to mortality
358	Chitinase inhibition leading to mortality
4	EcR agonism leading to incomplete ecdysis associated mortality

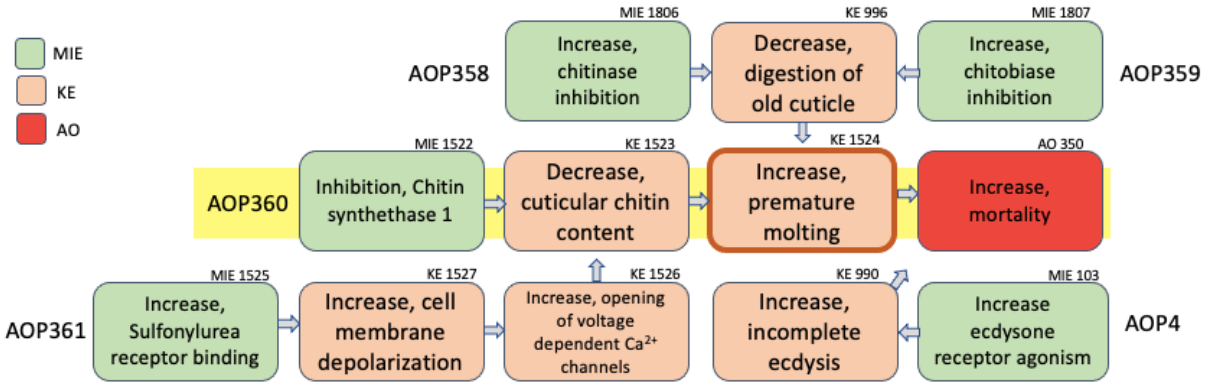

Figure 6: Overview of AOPs relevant for molting inhibition and molting associated mortality in crustaceans organized in a AOP network. Molecular initiating events (MIE, green), key events (KE, orange) are organized in adjacent key event relationships (KER) leading towards the common adverse outcome AO 350 "Increase, mortality" (red). A simplified version of AOP4 has been modified for graphical purposes and added to illustrate the extent of an AOP network. The main AOP of interest, AOP 360, is highlighted in yellow.

In brief, AOP 360 describes the increase in mortality in arthropods by premature molting caused by the inhibition of chitin synthase 1 (CHS1) and corresponding loss of cuticular chitin. Meanwhile, both AOP 359 and AOP 358 describe the same route to mortality by premature molting, but from the increased inhibition of chitinases and chitobiases. Additionally, AOP 361 describes the increase in premature molting by increased sulfonylurea receptor binding. To add on, AOP 4 describes increased mortality by incomplete ecdysis caused by the inhibition of the ecdysone receptor-mediated disruption of endocrine regulation of ecdysis. All the AOPs (except AOP 4) share the KE, "increase, premature molting", suggesting that inhibition of key proteins and or receptor agonism in chitin synthesis and chitin degradation has vital implications for molting and mortality in arthropods. All the listed AOPs have been evaluated as taxonomically relevant for the general phyla of arthropods due to the similar dependency and specificity of chitin synthesis. The mentioned AOPs can, by this assumption, also be relevant for molting inhibition in copepods.

Of the available AOPs, AOP 360 "Chitin synthase 1 inhibition leading to mortality" is the main AOP of relevance for molting inhibition in small crustaceans from teflubenzuron exposure (Schmid et al., 2022). The current prototypical stressors listed in AOP 360 are all members of the chemical group of pyrimidine nucleotide peptides. Pyrimidine nucleotide peptides are a group of IGR used in a similar matter as teflubenzuron on nuisance pests in agriculture.

Teflubenzuron is currently not listed as a stressor for molting-associated mortality in AOP 360. Interestingly, there is recent evidence of inhibited and altered chitin metabolism from teflubenzuron exposure in *Daphnia magna*, linking teflubenzuron to the mechanisms behind AOP 360 (Schmid et al., 2022).

1.5 Objective

The main objective of this study is to expand the current knowledge on the effects of CSI in the environment, using teflubenzuron as a prototypical stressor and *C. finmarchicus* as a non-target crustacean model species. Additionally, as sub-goals, this study seeks to, firstly, determine whether teflubenzuron may adversely affect *C. finmarchicus*. Secondly, to evaluate the molting disruption by teflubenzuron exposure at different levels of biological organization. Finally, this study will also try to provide and characterize a link between the molecular MoA and adverse effects using existing AOPs for molting disruption.

These goals will be achieved through the development of an effects toolbox for *C. finmarchicus* to characterize MoAs and adverse effects. By analyzing the molecular, physiological, and morphological changes and adverse effects from exposure to teflubenzuron at distinct levels of biological organization, this study hopes to provide new insight of the effect of the CSI teflubenzuron on *C. finmarchicus.*

2 Material and methods

2.1 Project overview

The main part of this study has been a joint project between NIVA Oslo and SINTEF Ocean in Trondheim. Cultivation of *C. finmarchicus* was done at the EMBRC-ERIC node at NTNU Sea Lab in Trondheim. Chemical prework and ecotoxicological acute testing were performed at the SINTEF Ocean analytical laboratory in Trondheim. Bioassays and results interpretation was mainly done at the NIVA Bioassay lab in Oslo. Trial of chitin content determination by fluorescent whole-body imaging were performed at the Norwegian Institute of Public Health (FHI). An overview of the main events and order of events is described in figure 7:

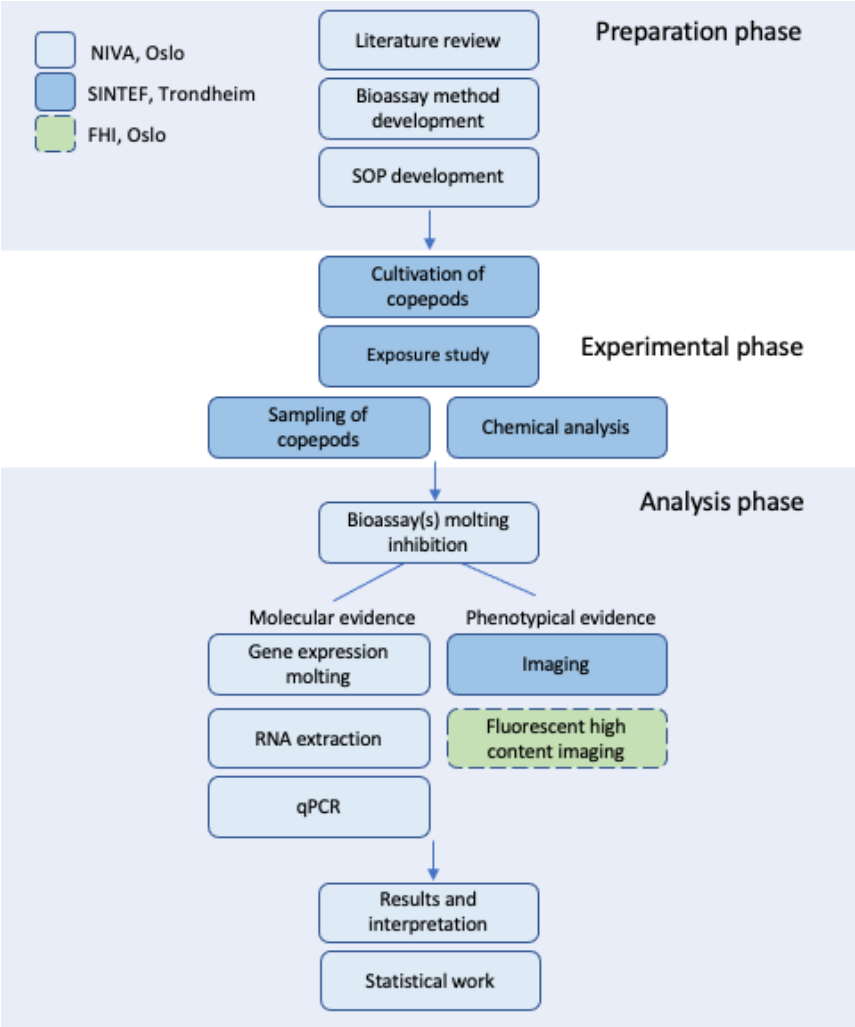

Figure 7: Overview of major events in this study and order during the project. This study can be divided into the preparations phase, the experimental phase, and the final analysis phase.

2.2 Sub-acute toxicity test of teflubenzuron on developing life stage *C. finmarchicus* copepods

2.2.1 Preparation phase

In preparation for the experimental phase, method selection, development, and optimization were performed by literature review and evaluation of different methodologies by trial. Methods initially proposed, such as enzyme-linked lectin assay (ELLA) and scanning electron imaging (SEM), were subsequently substituted with alternative methods more aligned with

the feasibility constraints of our study within the designated timeframe and level of complexity. The main study was designed and organized in collaboration with SINTEF Ocean to be executed at their location in Trondheim.

2.2.2 Culture conditions of *C. finmarchicus*

An overview of the general culture history and conditions is described by Hansen (2007). In brief, the culture of copepodite *C. finmarchicus* used in this study was raised in a temperature-controlled room at an ambient temperature of 10°C in natural running seawater prefiltered to 20µm at 9°C -10°C. The culture was established from eggs produced over 48 hours by 750 ovulating females randomly chosen from the running culture. The cultures were fed an approximate 60:40 mixture based on carbon of the unicellular algae *Rhodomonas baltica* and *Dunaliella tertiolecta* by tubing pump ad libitum to ensure normal growth and development. When the majority of the animals in the culture had developed into the stage copepodite 3 (C3), animals were collected in a bucket and transferred to the climate room at SINTEF Ocean for the experimental phase.

2.2.3 Experimental phase

A seven-day sub-acute to acute exposure study was performed using *C. finmarchicus* as the model species and teflubenzuron as the prototypical stressor based on internally designed procedures. Eight exposure concentrations covering the range of 0.001 µg/L – 3.0 µg/L teflubenzuron were chosen to encompass environmentally and regulatory-relevant concentrations. To accommodate studying the effects of teflubenzuron on at least one molting event, copepods of the developmental stage C3 were chosen as the starting point of this study. Based on Campbell et.al. 2001 expected mean developmental time of C3 copepods into C4 life stages takes between 3-5 days at a temperature of 8°C under non-limiting feeding conditions (Campbell et al., 2001), (Table 1 and Figure 2, Appendix II).

An overview of the treatment and workflow of the experimental period is provided in Figure 8. The copepods were left under exposure for seven days before termination and sampling. Due to the development of excess mortality in the highest exposure treatment (3.0 µg/L), this group was terminated and removed on day 6 and omitted from the main experiment.

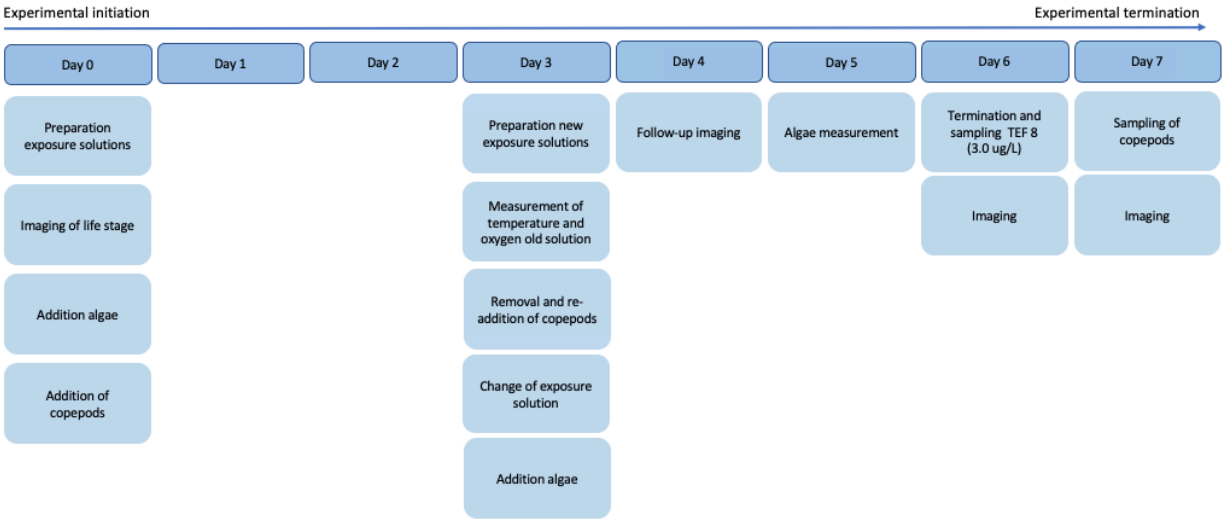

Figure 8: Overview of the experimental timeline and events/handling of the exposure flasks each day.

2.2.3.1 Test chemicals and stock solutions

Teflubenzuron (cat. nr. 45756; purity: 100. PESTANAL®, Merch/Supelco, Darmstadt, Germany) was used as prototypical CSI, and dimethyl sulfoxide (DMSO, cat. nr. 472301, Sigma-Aldrich, Darmstadt, Germany) was used as solubilizing agent. Preparation of stock solution was done by weighing and diluting 3.01mg teflubenzuron to a total volume of 10 ml with 100% DMSO (stock I). From this stock solution, 0.5ml was transferred to a 5ml beaker and diluted with DMSO (100%) (stock II). Each exposure treatment was prepared individually by diluting the given amount of stock solution of teflubenzuron (Table 12, appendix II) into the appropriate concentrations in a 10L flask with filtered seawater and DMSO. For each exposure treatment, a total of 8L exposure solution was made in the 10L flasks and evenly distributed into 2L flasks serving as exposure vessels. To verify the exposure concentrations of teflubenzuron during the experimental phase water samples were collected for analysis at the onset of the experiment and from the exposure flask on the day of solution renewal (day 3). Extraction and chemical analyses were performed at the analytical laboratory at SINTEF Ocean in Trondheim. The analysis was performed using an Agilent 6470 triple quadrupole analyzer coupled to an Infinity 1260 Infinity II liquid chromatography unit.

2.2.3.2 Experimental design

The experiment was performed in a temperature-controlled room at an ambient temperature of 10°C. Lights were turned on each morning at 8 am and turned off in the evening at 4 pm. To keep the algal feed in suspension during exposure, the exposure vessels were mounted on a plankton carousel with continuous cycling at approximately two rpm. For each of the exposure treatments, a total of 20 copepods at stage C3 were gently transferred into pre-prepared 2L glass flasks accompanied with 20ml algae (*Rhodomonas baltica*) to a total concentration of 9000 cells/ml (figure 9).

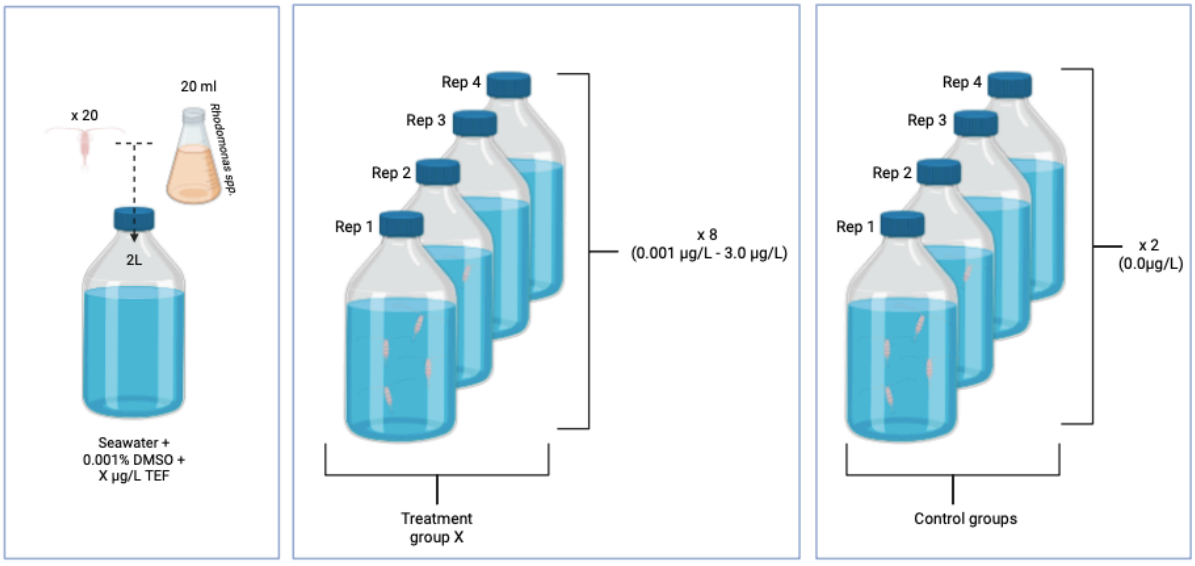

Figure 9: Schematic overview of main experimental design. Each treatment consists of 20 Calanus finmarchicus *copepods and 20ml of Rhodomonas baltica algae in a 2L solution of seawater, teflubenzuron (eight treatment concentrations, two control treatments) and DMSO (0.0001%). Each treatment group consists of four replicates. In total forty exposure flasks were prepared.*

Repletion of algae in the exposure flasks on days 3 and 5 was done by removing the exposure flasks from the rotating carousel, extracting a 20ml water sample while ensuring no animals

were lost, and measuring the current algal concentration with a Beckman Multisizer4 particle analyzer (Beckman, Coulter Life Sciences, Indianapolis, IN, US). Based on the current algae count, fresh algae and water were added to maintain the set algae density of 9000 cells/ml. The exposure solution was changed once during the experiment, where copepods were removed and temporarily stored in glass bowls while the exposure solution was changed. During solution change oxygen and temperature were measured using an optical oxygen sensor with a temperature probe (NeoFox with a FOSPOR-R sensor probe and TP thermistor, all from Ocean Insight, Orlando, FL, US). Determination of the developmental life stage and measurement of prosome lengths was done by camera imaging utilizing a Leica macroscope (Leica Z6 APO with a Leica MC170HD camera, both Leica Microsystems, Wetzlar, Germany) at a magnification of 3.6X.

2.2.3.3 Sampling of copepods

Sampling of copepods at the termination of the experiment was done by removing the experimental flasks from the plankton carousel, measuring oxygen and temperature, and straining the copepods out. The animals were gently strained through a partly submerged plankton mesh cup lined with a 150 µm plankton mesh disc (approx. 4cm diameter). Any copepods remaining in the exposure vessle were flushed off the sides with a squeeze bottle and poured into the plankton strainer cup. The plankton mesh disc was then gently removed from the strainer, placed upside down in a small glass petri dish filled with seawater, and flushed from the backside to collect the copepods. For copepods that escaped initial filtration (e.g., were stuck to the disc or were left in the exposure flask) an additional round of filtering was done by gently collecting them in a small cup before transferring them over into a 50ml Falcon tube (figure 10). A smaller plankton mesh disc (150 µm, 3cm diameter) was placed on top and secured with a modified cap for the tube. The Falcon tube was then flipped, water removed, and the plankton disc removed.

Copepods collected in the Petri dish were then individually imaged under the macroscope and mortality was assessed. The copepods were then individually picked and sampled for downstream analysis. Copepods for gene expression were sampled in 2.0 ml cryotubes for gene expression by the removal of water and the addition of 1.5 ml of DNA/RNA Shield (R1100-50, Zymo Research Corp., Irvine, CA, US). Copepods for trial fluorescent imaging, mainly dead and supplemented by live ones when needed, were sampled in 1.5ml Eppendorf tubes, water was removed, and snap-frozen in liquid nitrogen. Transport of samples from Trondheim to Oslo was done over dry ice in a Styrofoam-insulated travel box. Copepods for gene expression were stored at 4°C before extraction of RNA. Snap-frozen copepods for fluorescent imaging were stored in a -80°C freezer until use.

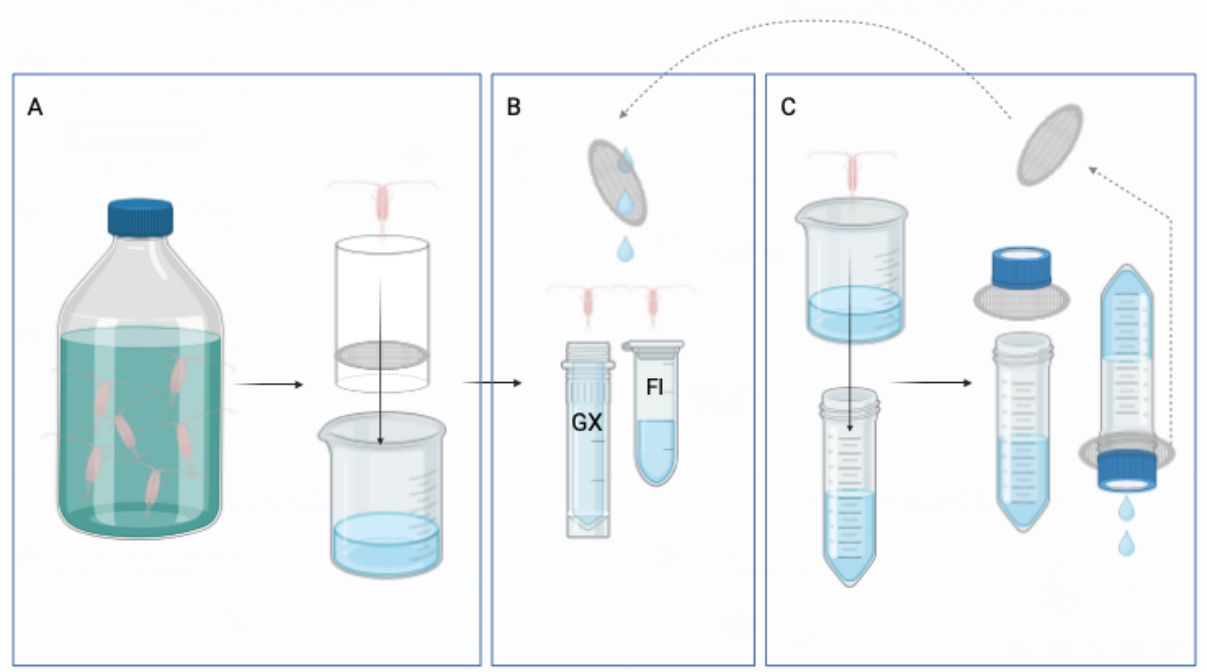

Figure 10: Schematic illustrating the sampling strategy. Panel A: The copepods were strained from the 2L exposure flasks through a partly submerged plankton mesh strainer cup lined with a plankton mesh disc (4cm diameter, 150 µm). The disc collects the animals, facilitating easy sampling into smaller collection tubes. Panel B: The copepods were flushed off the plankton mesh disk and sampled in 2ml cryotubes for gene expression analysis (GX). Copepods for trial-fluorescent imaging (FI) were sampled in 1.5ml Eppendorf tubes. Panel C: Alternatively, if straining proved difficult or the animals escaped straining, another round of filtration was done by pouring the animals over into a 50ml Falcon tube lined with a smaller plankton mesh disc (3cm diameter, 150 µm). The cap of the Falcon tube was modified with a large hole, allowing water to escape when flipped. The copepods collected on the plankton mesh disk were then flushed off and sampled as previously described.

2.2.4 Analysis phase

2.2.4.1 Adverse effects: Mortality

Mortality was assessed during the sampling based on the following chosen criteria: necrosis, disintegrated lipid sack, lack of movement in the intestine, immobilization and or lack of response to tactile stimuli. Mortality was measured as percent (%) dead copepods of the total number of copepods in each exposure treatment at the end of the exposure period.

2.2.4.2 Molecular effects: Gene expression

RNA extraction

RNA Shield was removed, and the samples were gently washed once with MilliQ water. Each sample was homogenized for RNA extraction using 2mm ceramic beads with a Precellys Evolution homogenizer (Bertin Technologies, Montigny-le-Bretonneux, France) at 6800 rpm with a cycle of 30 seconds of homogenization and a 45-second pause for four minutes twice. To prevent overheating of the samples during homogenization a two-minute pause was applied between the two rounds of homogenization. The following RNA extraction was done using the Quick-RNA™ Tissue/Insect MicroPrep kit (R2030, Zymo Research Corp., California, CA, US) according to the manufacturer's protocol. DNAse treatment was performed following the manufacturer's protocol. Extracted RNA was spectrophotometrically quantified using a Nanodrop Spectrophotometer (Nanodrop® ND-1000, Nano Drop Technologies, Wilmington, DE, US). An additional quality check of the extracted RNA's integrity was done using an Aligent RNA 6000 Nano kit (Aligent Technologies, Sante Clara, CA, US) with RNA Nano Lab Chips in

Bioanalyzer. An applied quality limit of 3000 ng/µl RNA was set for the total RNA yield based on requirements for gene expression by qPCR.

Gene expression by qPCR

A quantitative real-time reverse-transcriptional polymerase-chain reaction (qPCR) was performed based on extracted RNA with a 260/280 ratio of >1.8, and sufficient RNA integrity (table x, appendix). Primer design was done by Prime3Plus from a library of 26 selected genes relevant to chitin synthesis, chitin degradation as well as molting regulation (Table 1, Appendix III). Wherever possible, genes with expressed sequence tags from *C. finmarchicus* were prioritized in the primer design, as a secondary priority were genes found in copepods or other crustaceans, and the third priority was genes found in arthropods. Primer optimization of qPCR settings and temperatures was performed prior to the main analysis and resulted in a grouping of six temperatures and eight plates for all genes (Table 3, Appendix III).

cDNA hybridization was performed by mixing extracted RNA with qScript™ cDNA Supermix (Quantabio, Beverly, MA, US), and nuclease-free water to a total volume of 30µl and a total yield of 1500ng, with two technical replicates. The cDNA mix was distributed in duplicates into 96-well PCR plates and incubated for three minutes at 25°C, followed by 30 minutes at 42°C, and then five minutes at 85°C. The plate was finally held at 4°C to cool down before further usage or storage at -20°C (Eppendorf Mastercycler Thermal Cycler 5331, Eppendorf, Hamburg, Germany). Mastermix was prepared by mixing PerfeCTa SYBR® Green FastMix (Quantabio, Beverly, MA, US), forward and reverse primer of specific gene, and nuclease-free water to a final volume of 600µl with a ratio of respectively 5:1:1:2. A Biomek 3000 Laboratory Automation Workstation (Beckman Coulter Life Sciences, Indianapolis, IN, US) was utilized to arrange and fill a 384-well qPCR plate with cDNA and Mastermix. The qPCR was performed and analyzed using the BioRad CFX 384 system (Bio-Rad Laboratories, Hercules, CA, US). The generated counts were adjusted to the threshold of the standard curve with an efficiency (E) between 90% and 110%. Calculation of the mean normalized expression (MNE) was done following the 2-ΔΔCt- method utilizing a normalization factor based on three housekeeping genes (act, 16s, and ef1-a). The gene expression data was graphically presented as mean fold gene change measured. The statistical analysis of significant differences in expression was calculated and presented by the individual fold changes measures.

2.2.4.3 Physiological effects: Molting and development

Capture of molting inhibition and physiological deformities

Capture of visual morphological evidence of molting inhibition and physiological deformities was done by individual imaging of copepods from every exposure treatment using the Leica macroscope with a Leica MC170HD camera and 3.6X magnification as a part of the sampling procedure.

Life stage characterization and prosome length measurement

Characterization of the life stage was done by visual analysis of the individual images of copepods taken during sampling. Determination of the developmental stage was done by counting the number of prosome and urosome segments on the copepods, as well as measuring the length of the prosome, based on the morphological criteria following Mauchline et al., (Mauchline et al., 1998). All images of copepods were taken at the same

magnification (3.6X) and compared against a stage micrometer for measurement of prosome length. Calculation of life stage ratio was done based on counts of registered life stages in both live and dead copepods.

2.3 Calculation of ecotoxicologically relevant threshold levels

The calculation of relevant ecotoxicological endpoints was done using the drc package in R (Ritz, 2016). Calculated endpoints are presented as concentrations of teflubenzuron at the different calculated endpoints.

2.4 Statistical analysis of data

Statistical analysis of the generated data was statistically analyzed using R Studio (Core Team, 2024). The following packages were utilized in the data organization and statistical analysis of the data: “dplyr” (Wickham et al., 2023), “pheatmap” (Kolde, 2019), “drc” (Ritz, 2016), and “lm test” (Hothorn et al., 2022). All endpoints were tested for normality. Non-parametric data was tested for significance by inferential tests such as the Kruskal-Willis test, and linear regression (robust, simple, and multiple linear regression) in addition to correlation testing by Spearman’s r-test. Parametric data was tested by ANOVA, followed by Tukey test, simple linear regression, and correlation test by Pearson’s r-test. All statistical analyses utilized a significant level of 0.05 unless otherwise stated.

3 Results

3.1 Test Chemicals and chemical analysis

Results from the chemical analysis of teflubenzuron concentrations in the exposure treatments were delivered late and thus the nominal values of teflubenzuron were used throughout the thesis. For transparency purposes, the nominal values registered are listed in Table 2:

Table 2: Chemical analysis results from water samples taken from each exposure treatment at the start of the experimental period and at day 3 during solution change. Water samples were analyzed by LCMS at and by the SINTEF Ocean analytical lab.

Sample	*Nominal (µg/L)*	*Start (µg/L)*	*End (µg/L)*	*Average (µg/L)*	*% Nominal*
Control (C, 0.0 µg/L)	0.0	0.0	0.00035	0.00017	-
Solvent control (SC, 0.0 µg/L)	0.0	0.0	0.00043	0.00022	-
0.001 µg/L	0.001	0.0013	0.00084	0.0010	108
0.003 µg/L	0.003	0.0014	0.00169	0.0015	53
0.01 µg/L	0.01	0.0038	0.0065	0.0052	52
0.03 µg/L	0.03	0.0131	0.012	0.012	43
0.1 µg/L	0.1	0.0954	0.037	0.066	66
0.3 µg/L	0.3	0.220	0.229	0.225	75
1.0 µg/L	1.0	0.604	0.812	0.708	71
3.0 µg/L	3.0	1.462	0.334	0.898	30

3.2 Acute toxicity test of teflubenzuron exposure

3.2.1 Mortality

No mortality was observed in two of the low-exposure treatments (0.001 µg/L and 0.01 µg/L), while low mortality (<10% mortality) was found in both negative control and solvent control, as well as in one of the low-exposure treatments (0.003 µg/L), (Figure 11, and Table 3, Appendix II). Comparative Kruskal's Willis test ruled out any significant differences in mean mortality between the control treatments and the no-mortality treatments (0.001 µg/L and 0.01 µg/L treatments) (*p*-value, 0.1535). A robust linear regression model indicated a significant relationship between teflubenzuron concentration and mortality to only be present in the high-exposure treatments (0.03 µg/L – 1.0 µg/L), with an establishment of this relationship at 0.03 µg/L teflubenzuron (*t*-value= 6.372) (Table 4, Appendix II). By Spearman's correlation test, this relationship between exposure treatment and mortality in the high-exposure treatments was found to have a strong positive correlation (*rho*= 0.7948). Maximum mean mortality only reached 46.47% ±0.1% at the highest exposure concentration of 1.0 µg/L teflubenzuron. The NOEC in our study was registered at 0.01 µg/L teflubenzuron, and the LOEC value was registered at 0.003 µg/L teflubenzuron.

A five-parameter model with no constraints was applied to the mean mortality data and a dose-response curve was plotted (Figure 11). A benchmark dose for mean mortality (BMD) based on a 10% threshold level was calculated at 0.0400 µg/L teflubenzuron (Table 3).

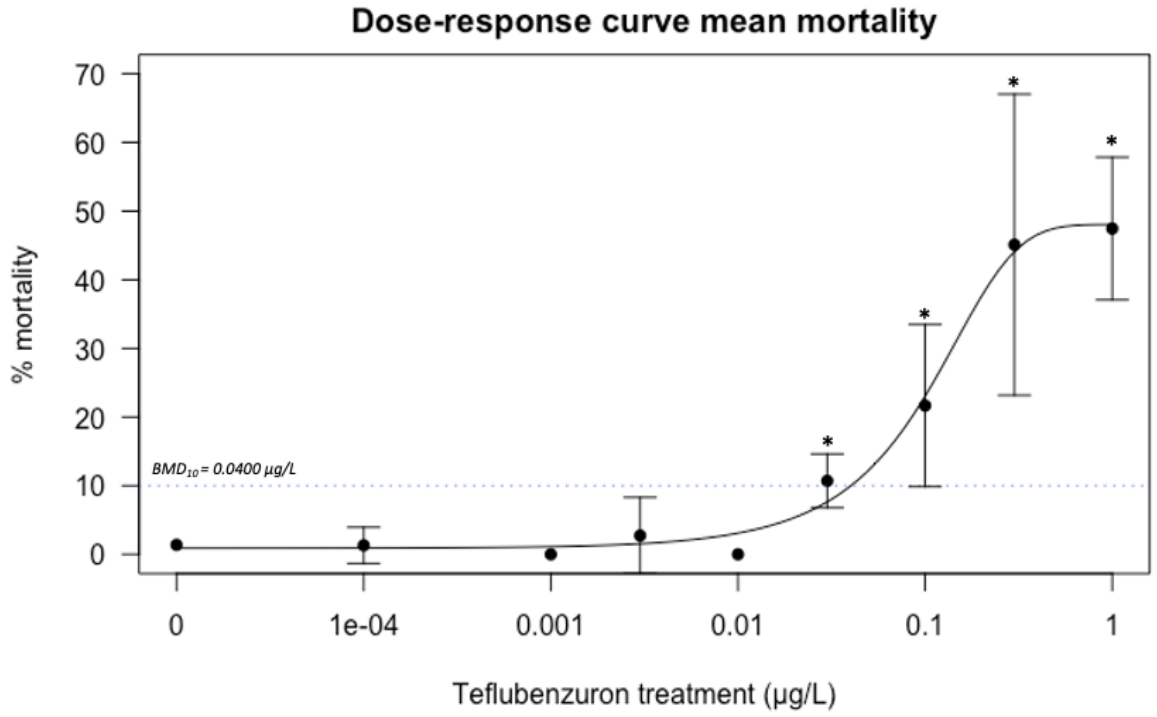

*Figure 11: Dose-response curve plotted against percent (%) mean mortality (x-axis) and log teflubenzuron concentration (y-axis). The whisker at each point indicates error bars calculated from the standard error mean (SEM). BMD10 is illustrated by the blue dotted line. *Significant mortality (p>0.05).*

3.2.2 RNA extraction

RNA extraction from low-exposure treatment samples (≥0.01 µg/L teflubenzuron) yielded sufficient RNA for downstream gene expression assays, with 3000 ng/µl or more RNA per sample (Table 11, Appendix II). Higher exposure treatment samples (<0.01 µg/L teflubenzuron) all had a total RNA yield of less than 3000 ng/µl. Of all samples, eight samples had a moderate RNA yield and 11 had a poor RNA yield. All poor RNA yield samples were found in treatments of teflubenzuron concentration above 0.01 µg/L. All samples had a high 260/280 ratio of 1.8 or above. The RNA integrity was sufficient for all samples, with only smaller impurities found within two of the solvent control samples (solvent control 1 and 2). A summary of data regarding RNA extraction can be found in Table in Appendix II.

3.2.3 Gene expression by qPCR

Due to low RNA yield in high-concentration treatment samples (<0.01 µg/L teflubenzuron), a conservative qPCR design approach was utilized by dividing the gene expression analysis between prioritized core genes, intermediate-priority genes, and low-priority genes (Table 2, Appendix III). The full library of genes (core, intermediate, and low) was analyzed in the control and low-concentration exposure treatments (0 µg/L – 0.01 µg/L treatments). The 0.03 µg/L treatments were only analyzed against core and intermediate genes. The final exposure treatments (0.1 µg/L – 1.0 µg/L) were not analyzed against any genes.

For both core genes, *chs2* and *cht3*, the mean fold expression increased with treatment concentration from 0 µg/L – 0.01 µg/L (Figure 12). *Chs2* was found to be less expressed at 0.03 µg/L teflubenzuron while the mean fold expression of *cth3* continues to increase at 0.03 µg/L.

All three intermediate priority genes related to the chitin synthesis pathway (*gfat, NAGase, pagm*) had an increasing expression with increasing exposure concentration, apart from g*fat* where a reduction in expression compared to the control groups was found at the 0.03 µg/L treatment (Figure 13 and 14). Both intermediate-priority chitin degradation genes, *ech* and *cda*, had an increasing expression until the 0.03 µg/L treatment where the expression was reduced (Figure 13 and 14). Of the two intermediate priority molting regulating genes *ethr* showed increasing expression at increasing treatment concentration, while *20e* only had increasing expression at increasing exposure concentration until the 0.03 µg/L treatment concentration. All low-priority genes (0.0 µg/L – 0.01 µg/L) had a similar expression trend across all functional gene groups with increasing expression at increasing exposure concentration (Figure 13 and 14). A heat map describing the mean fold change for all genes and a compilation of calculated individual dose-response curves for each gene are presented in the supplemented appendix (Figure 4 and 5, Appendix II).

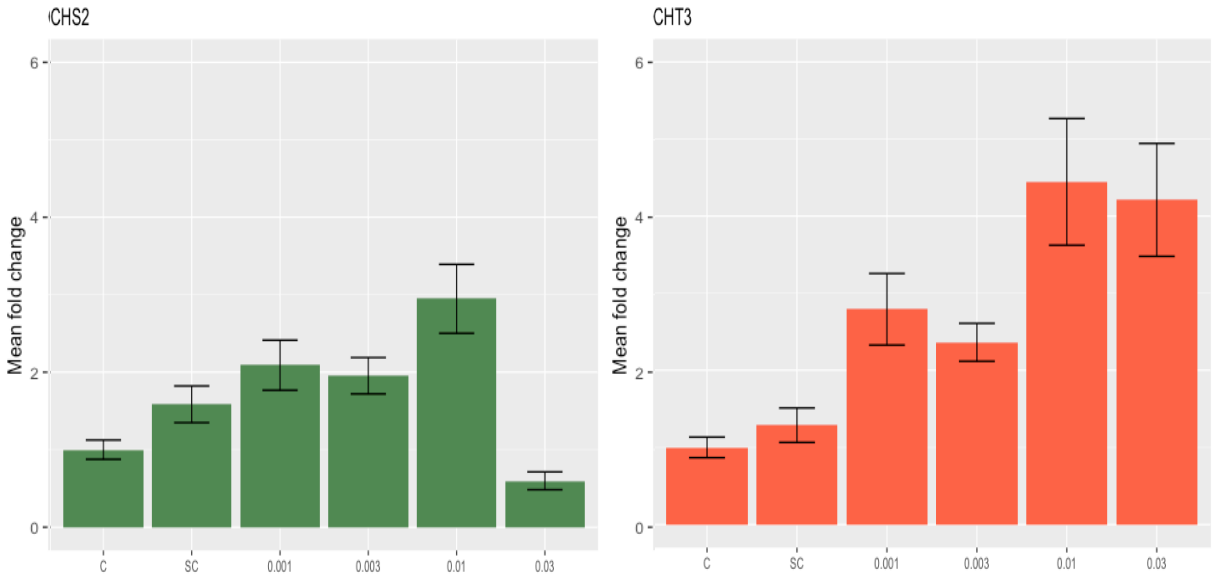

Figure 12: Comparison of mean fold change in the core genes chitin synthase 2 (chs2, green) and chitinase 3 (cht3, red). Each bar represents the mean fold change at each treatment and error bars were added to illustrate the standard error for each mean. C= negative control, SC= solvent control.

One-way ANOVA was applied for all genes across all treatments and found significant differences in mean fold change at different treatments (p-value, 9.23×10^{-15}). Calculations of significantly differentiated expression of each gene were done by simple linear regression using the solvent control as an interceptor. Based on the linear model no significant difference in fold change was found between the control treatments or between the low-exposure treatments. Significant change was only found in the expressions for *pagm* and *ech* measured in the 0.03 µg/L treatment (Figure 13 and Table 6 Appendix II). The correlation test by Parson's r-test indicated a weak positive correlation between the expression of molting relevant genes and all measured treatment concentration (r= 0.0780).

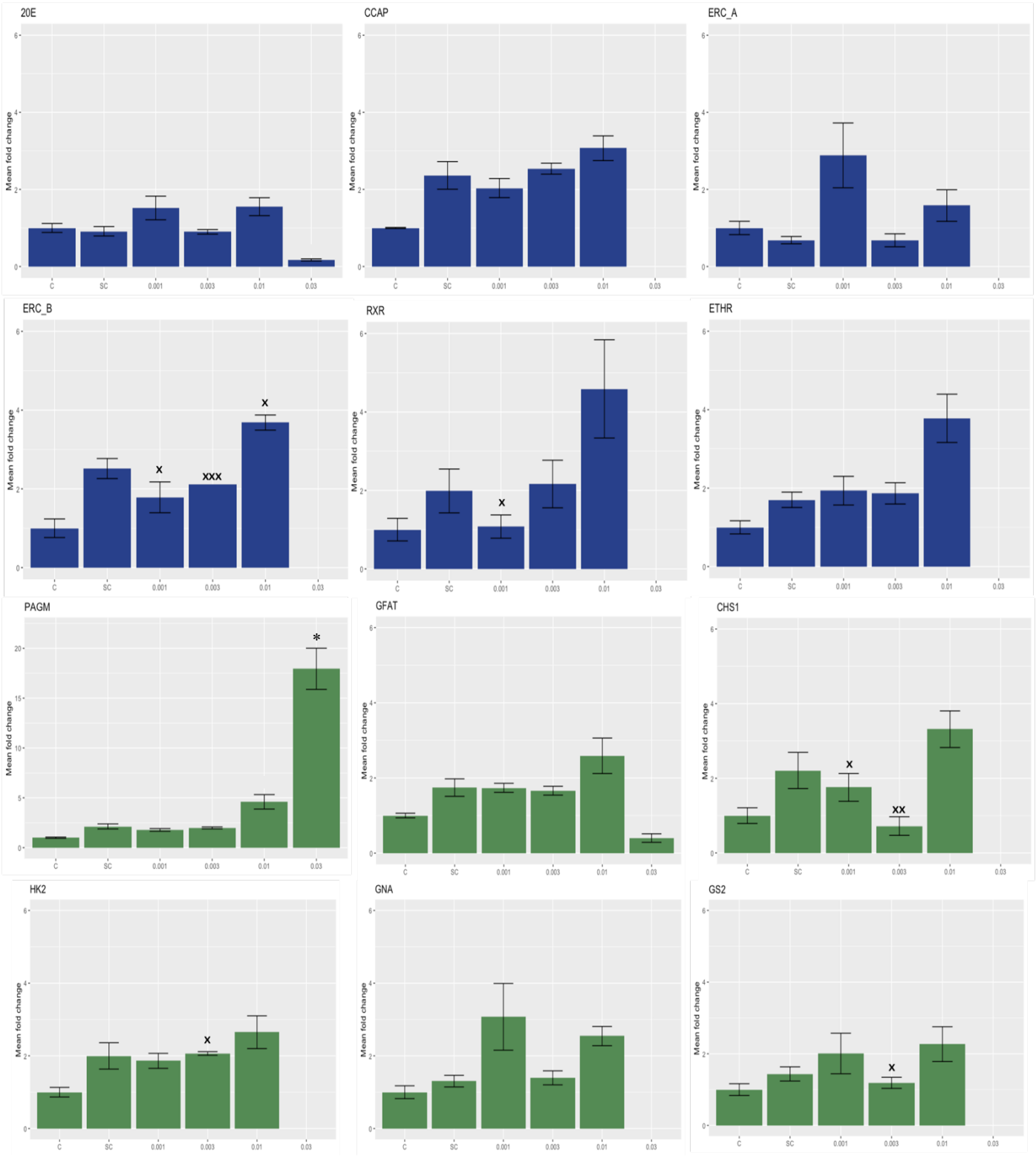

Figure 13: Mean fold change(x-axis) for molting relevant genes (dark blue) and chitin synthesis relevant genes (green). The whiskers indicate standard error mean (SEM) plotted for each treatment group (y-axis). On the treatment axis, C= Negative control, SC = Solvent control. All plots are scaled from 0 to 6-fold, except for the PAGM plot, where a scale of 0 to 20-fold is used.

**Significant mean fold change (p-value<0.05). X: The mean value could not be calculated for one of the replicates. Xx: The mean value could not be calculated for two of the replicates. Xxx: The mean value could not be calculated for three of technical the replicates.*

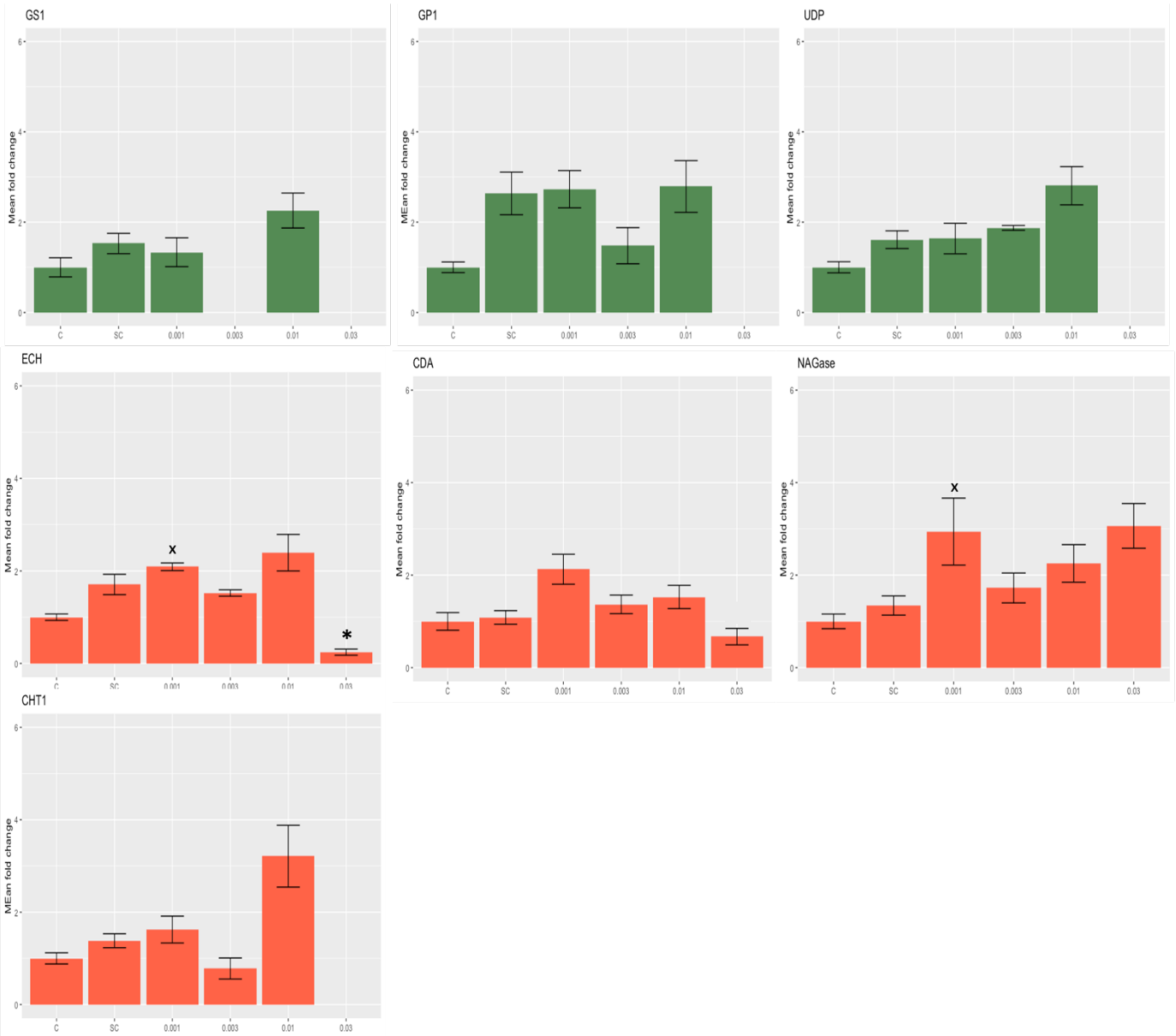

Figure 14: Mean fold change(x-axis) for chitin synthesis relevant genes (green) and chitin degradation relevant genes (red). The whiskers indicate the standard error mean (SEM) plotted for each treatment group (y-axis). On the treatment axis, C= Negative control, SC = Solvent control. All plots are scaled from 0 to 6-fold.

**Significant mean fold change (p-value<0.05). X: The mean value could not be calculated for one of the replicates. Xx: The mean value could not be calculated for two of the replicates. Xxx: The mean value could not be calculated for three of the technical replicates*

3.2.4 Developmental stage distribution

The developmental stage distribution was found to be heterogenous within each treatment replicate, treatment group as well as between treatment groups (Figure 15). In all treatments, there were a minimum of three distinct life stages. The life stage with the highest ratio (most common life stage) was the C3 life stage, followed by C4. The C3 and C4 life stages were the only life stages that were common for all treatments. The least common life stages registered were the smallest life stage, C2, and the largest life stage C5. The highest-developed life stage (C5) was only found in the negative control and solvent control, while C2-copepods were found in all treatments except the two control treatments (Figure 16).

A higher ratio of C4 and C5 life stages was registered in all experimental treatment groups compared to the pre-experiment group. Additionally, there was a lower ratio of C2 life stages in low-exposure treatments (0.0 µg/L – 0.01 µg/L) and a ratio of C2 in high-exposure treatments more in line with the ratio found in the pre-treatment group. Statistically, there were only significant differences in the ratio of C4 copepods in the experimental treatments and controls compared to the ratio in the pre-experimental group (chi-test, *p*-value>*a,* Table 8 Appendix II). No significant difference in ratios was found for the C2 or C3 groups between the pre-experiment and experimental treatments.

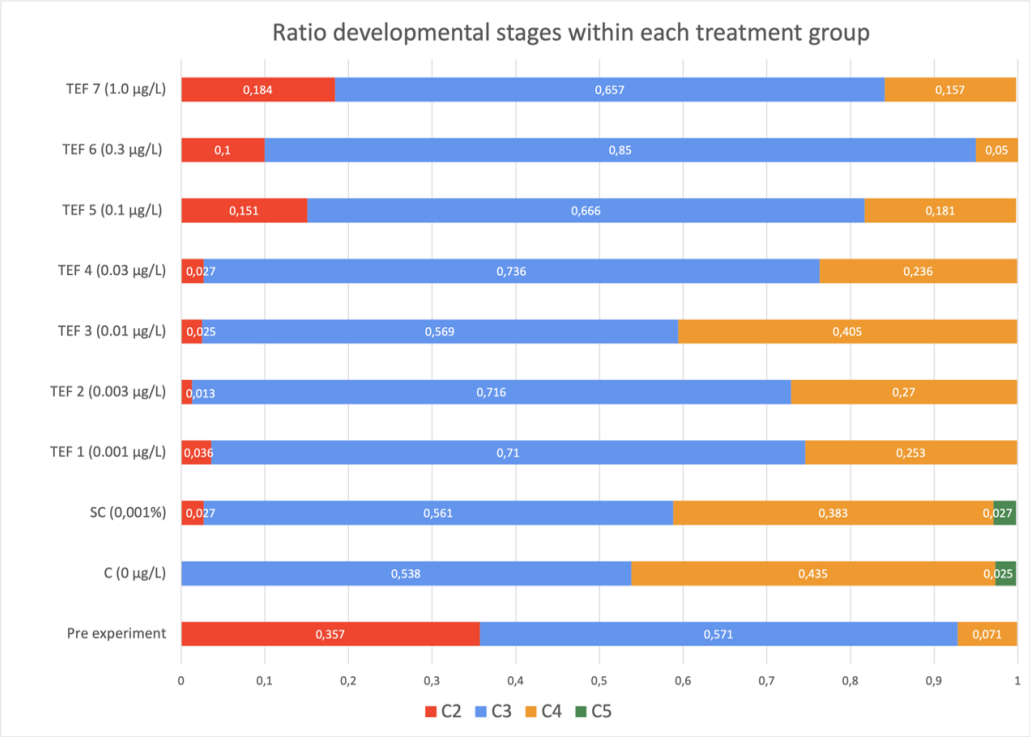

Figure 16: Life stage distribution of copepods as a ratio of the total number of copepods within one exposure group, colored by the life stage registered (C2= red, C3= blue, C4= orange and C5=green). For comparison, the ratio of life stages in the pre-experimental batch of animals is provided as the ratio bar on the bottom of the plot.

3.2.5 Prosome length

The mean prosome lengths of the copepods increased at higher developmental stages for all treatments in a stepwise trend as a consequence of molting (Figure 17 and Figure 7, Appendix II); with C3 being larger than C2, C4 larger than C3, and C5 larger than C4. Copepods in the higher exposure treatments (0.3 µg/L – 1.0 µg/L) had a smaller mean prosome size at every developmental life stage, compared to the copepods in the negative control and low exposure treatments (0.0 µg/L– 0.03 µg/L). For example, within the 1.0 µg/L exposure group, the C4 copepods have a mean prosome length of 1.68 mm, while the C3 copepods of the solvent control groups have a mean prosome length of 1.73 mm (Table 9, Appendix II). Furthermore, a 0.3 mm- 0.4 mm reduction in mean prosome length was measured at every developmental life stage from 0.1 µg/L- 1.0 µg/L, compared to the same endpoints measured in the 0.03 µg/L exposure treatment (Table 9, Appendix II).

One-way ANOVA of mean prosome length against all treatment groups indicated a significant difference in at least one of the treatment groups and determined that both life stage and treatment were exerting significant influences on prosome length (p-value, $<2 \times 10^{-16}$) (Table 10, Appendix II). A posthoc Tukey test further indicated significant differences in the mean prosome lengths between the low exposure treatments (0.0 µg/L – 0.03 µg/L) and the high exposure treatments (0.1 µg/L - 1.0 µg/L), with no significant differences within these two groups. Additionally, single linear regression tests on the relationship between promosome length and teflubenzuron treatment were also found to be significant for all high-exposure treatments (0.03 µg/L - 1.0 µg/L) and the 0.003 µg/L treatment (Table 10, Appendix II). A Pearson's correlation test proved a moderate negative correlation between exposure treatment and prosome lengths (*p*-value, 2.2×10^{-16}, r= -0.489), indicating a correlation between an increase in exposure concentration and the decrease in mean prosome length.

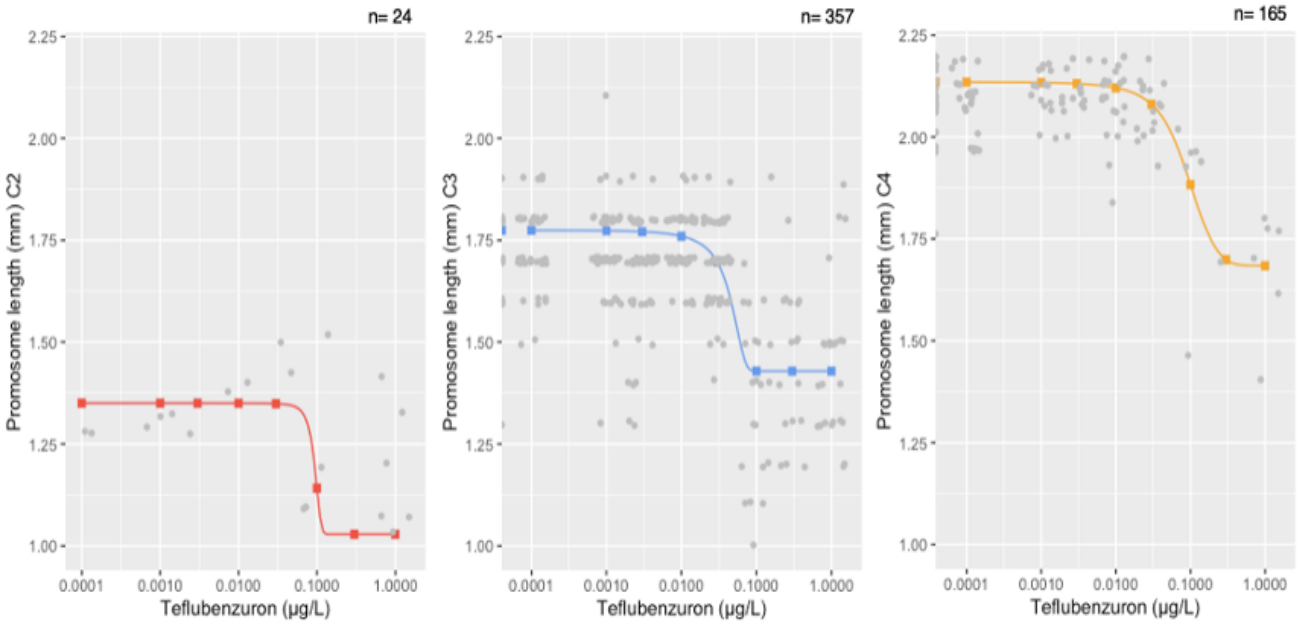

Figure 17: Illustrative dose-response curves of mean prosome lengths (y-axis) at C2 (red), C3 (blue) and C4 (orange) life stages across all experimental exposure treatments (x-axis). Every registered prosome measurement was plotted in grey for each life stage. Total number of registered prosome lengths (n) are given in the top right corner of each panel.

For illustrative purposes, three dose-response curves were fitted to the mean prosome lengths at C2, C3, and C4 against all treatments to illustrate the negative dose-dependent trend observed (Figure 17). A decrease in mean prosome lengths is present at the 0.03 µg/L exposure treatment for C2, C3, and C4 life stages, although this could not be proven statistically significant.

3.2.6 Morphological deformities

Several morphologically deformed copepods were observed and captured by imaging. The observed deformities were most extensive in the highest exposure treatments, and initially appeared in the 0.03 µg/L teflubenzuron treatments. Some of the most common morphological deformities found were deformed heads, antennas, tails and prosomes, as well as hunched backs and brokens exoskeleton segments (Figure 18). A larger compilation of images showing the morphological damages is found in Appendix IV.

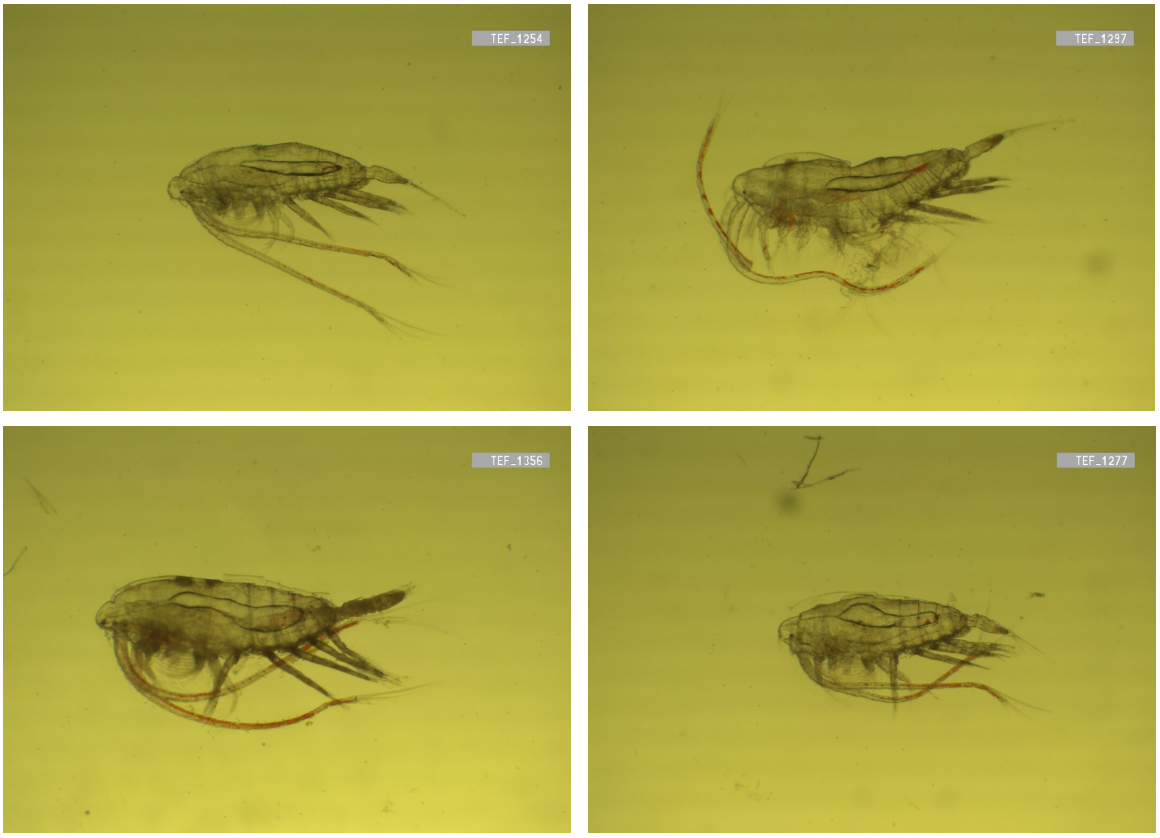

Figure 18: Compilation of images from Appendix IV showing morphological deformities in copepods form the high-exposure treatments (0.03 µg/L – 1.0 µg/L)

3.3 Summary toxicological dose descriptors

A summary of all ecotoxicological endpoints in this study such as NOEC, LOEC and BMD_{10} was gathered and presented in Table 3:

Tabell 3: Overview of ecotoxicological endpoints from the study.

Endpoint	*Biological organization*	*Toxicological dose descriptors*	*Nominal teflubenzuron []*
Mortality	Individual/ population	NOEC	0.01 µg/L
		LOEC	0.003 µg/L
		BMD_{10}	0.0400 µg/L
Prosome length	Tissue/ individual	$NOEC_{C2}$	0.01 µg/L
		$LOEC_{C2}$	0.1 µg/L
		$NOEC_{C3}$	0.01 µg/L
		$LOEC_{C3}$	0.03 µg/L
		$NOEC_{C4}$	0.01 µg/L
		$LOEC_{C4}$	0.03 µg/L

4 Discussion

4.1 Ecotoxicological effects from teflubenzuron exposure on developmental stages of *C .finmarchicus*; main findings from this study

There is a wide gap in knowledge on the ecotoxicological effects of teflubenzuron on marine species that needs to be filled. The available data is mostly oriented toward terrestrial species or bottom-feeding economically important marine species such as crabs and lobsters. This study however represents one of few studies on the ecotoxicological effects of CSI on a key pelagic micro-crustacean. The findings from this study also provide new supplementary insight into the effects of teflubenzuron on molting at distinct biological levels of organization in the novel model species *C. finmarchicus*. This insight will help expand the current knowledge and propose future recommendations for safe chemical levels in the marine environment. From our study, teflubenzuron is shown to cause adverse effects in the developmental life stages of *C. finmarchicus* at environmentally relevant concentrations, and at multiple levels of biological organizations. Adverse effects initially appear in our study within the 0.01 µg/L – 0.1 µg/L exposure range. Adjusting these concentrations from nominal to measured, this effect window is lowered to 0.005 µg/L - 0.066 µg/L, suggesting that the effects from teflubenzuron might be substantially more potent than previously anticipated. Within this concentration range, this study found effects on mortality, prosome length, morphological deformities, development, and indications of altered expression of molting relevant genes.

4.1.1 Apical endpoints: Mortality

From our study, mortality in exposed *C. finmarchicus* increases in a dose-dependent manner at increasing concentrations of teflubenzuron. Teflubenzuron starts to have a significant effect on mortality at 0.03 µg/L (*t*-value, 6.372), where a mean mortality of 10.71%±0.03 was registered. Correcting this concentration from nominal to measured, the significant concentration of teflubenzuron affecting molting is reduced to almost half at 0.0127 µg/L. Compared to recent studies on the effect of teflubenzuron on other marine crustacea, there is evidence that *C. finmarchicus* is potentially far more sensitive to teflubenzuron under experimental conditions similar to ours. The most comparable study of the acute effects of teflubenzuron on marine copepods was performed by Macken et al. in 2015 on the epibenthic copepod *Tisbe battagliai,* where NOEC and LOEC were measured at 0.0032 µg/L and 0.01 µg/L, respectively (Macken et al., 2015). These findings are in line with our own results, where the measured NOEC and LOEC were found to be 0.0050 µg/L and 0.0016 µg/L, respectively. By comparing these endpoints, the sensitivity of both copepods seems to be within the same order of magnitude, with a slightly higher sensitivity in the benthic copepod than the pelagic copepod. This conclusion is also in line with the expected higher bioavailability of teflubenzuron in the benthic zone and marine sediments, but also proposes that pelagic copepods might be just as vulnerable to teflubenzuron exposure as benthic and bottom-feeding organisms near marine sediments

Although our study only managed to uncover a maximum mortality endpoint of 47.46% mean mortality at the highest exposure treatment (1.0 µg/L), the physiological and morphological evidence captured by imaging points toward a more substantial degree of mortality from an ecological perspective (Appendix IV). The mortality criteria used in this study could be described as criteria for lethal immobilization, characterizing the animals as ‘absolute’ dead when endpoints such as necrosis, disintegration of the lipid sac, no intestinal movements or immobility were present. In comparison to the criteria for mortality set by the International

Organization for Standardization in ISO 14669:1999, "*Water quality — Determination of acute lethal toxicity to marine copepods (Copepoda, Crustacea)",* mortality is only defined as an absence in swimming activity for 10 seconds (ISO, 1999). This definition of mortality provided by ISO:14699 describes mortality more mechanically and could be a better description of molting-associated mortality than the 'absolute' lethal mortality definition, in addition to also providing the ecological perspectives on mortality. Application of a mechanical mortality definition/criteria would have substantially altered the mortality results in our study, as near total immobilization was present for all copepods, visually vital copepods included, in the highest exposure treatments of 0.1 µg/L - 1.0 µg/L teflubenzuron.

4.1.2 Molecular endpoints: Expression of molting relevant genes in response to teflubenzuron exposure

The main results from the gene expression study generally indicate an increase in the genetic expression across all analyzed genes (Figure 12-13, and Figure 4-5, Appendix II). However, the expanded analysis of gene expression from the 0.03 µg/L treatment on the set of core and intermediate priority genes uncovered some interesting deviations in the expression seen in the low-exposure treatments. For example, a reduced mean fold expression was found in genes such as *gfat, ech, cda,* and *20e* at 0.03 µg/L teflubenzuron. In comparison, the mean fold expression in genes such as *pagm, NAGase,* and *cht3* continued to increase at the 0.03 µg/L treatment. Of these genes, the expression of *pagm* and *ech* in response to 0.03 µg/L teflubenzuron was the only genes where expression was found to be significant (p-value< 0.05, Table 6 Appendix II); also revealing that none of the other expressions was found to have any statistical strength behind them. However, based on the calculated estimates (Table 6, Appendix II) and the "trend" seen in the distribution of mean fold change for each gene, there are some suggestions of interesting interactions between increasing teflubenzuron concentration and expression on molting relevant genes. The calculated R^2 values for each gene (Table 6, Appendix II) suggest that, on average, only 33% of the variation in the gene expression can be connected to the teflubenzuron treatment alone. This suggests that other variables, e.g., such as life stage and molt progression, have substantial influence on the expression results. A future expansion of data at higher exposure concentrations or more observations would be of great benefit to this study, and future ones.

The most suggested MoA of benzoylphenylurea chemicals is through inhibition of chitin synthetases (CHS) and the subsequent inhibition of chitin synthesis, eventually resulting in abortive or premature molting (Douris et al., 2016; IRAC, 2024; Schmid et al., 2023; Sun et al., 2015). Based on this, an altered expression of the chitin synthetase genes *chs1* and *chs2* are of special interest in this study as a possible link between molecular effects from teflubenzuron exposure and molting inhibition. The data generated on the expression of *chs1* was in this study rather inconclusive and has some major 'holes' likely related to the execution of the qPCR (Figure 13). The dose-response curve calculated for *chs1* based on predicted fold change suggests an increasing trend of expression at increasing exposure concentrations (Figure 4, Appendix II). However, additional analysis would be necessary to confirm or discard this suggested trend. Assuming that decreased expression of *chs1* causes reduced activity of CHS1 and inhibition in chitin synthesis, with further adverse implications for molting, an increased expression of *chs1* in our study seems counterintuitive with the adverse effects in mortality and morphology found. However, there are similar studies that have encountered

the same puzzling trend. To exemplify, *chs1* was found to be increasingly expressed at increasing treatments of diflubenzuron in the citrus red mite (*Panonychus citri)* and the red spider mite (*Tetranychus cinnabarinus*) (Xia et al., 2014; Xin et al., 2021). These studies concluded that diflubenzuron might inhibit chitin synthesis by upregulation of *chs1* rather than the more intuitive assumption of an inhibitory effect by reduced expression. Moreover, this trend was also found in the European lobster (*H. gammarus)* from exposure to sub-lethal concentrations of teflubenzuron in Olsvik's study from 2015, indicating that the expression patterns found in our study might harbor potential insight despite initially unexpected results (Olsvik et al., 2015). Nevertheless, it is important to point out that the missing data on molecular effects at exposure concentrations above 0.01 µg/L in this study inhibits any conclusions on the overall transcriptional effects of teflubenzuron on *chs1* in *C. finmarchicus.* From these preliminary results, there is no significant evidence linking *chs1* expression to the inhibition of CHS1 or molting inhibition.

Although the altered expression of *chs1* is mainly associated with chitin synthesis in the exoskeleton and molting inhibition, interestingly, Chen et al found evidence that inhibition of *chs2* also causes abnormal growth and development, as well as higher mortality, in the moth *Heorita vitessoides* (Chen et al., 2023). By RNA interference (RNAi) treatment with dsCHS2, the expression of *chs2* was reduced by a magnitude of 0.3-0.5, with increasing effect with time. Although CHS2 is linked to the chitin synthesis in the midgut and integument of insects (Arakane et al., 2005), Chen's study also describes the connection between CHS2 and the activity and feeding level of the insect. With reduced expression of *chs2,* the level of activity and feeding was subsequently reduced, suggesting that the adverse effects such as growth inhibition and increased mortality could be linked to the downregulation of *chs2,* and not only by the reduced expression of *chs1* alone (Chen et al., 2023). Thus, the effects of teflubenzuron on *chs1* and *chs2* may be confounding or even add to the effects of each other in regards to molting inhibition. From our study, the developmental inhibition, morphological deformities, and increased mortality could be aligned with the 0.4-fold reduction in the expression of *chs2* as seen in the highest analyzed exposure treatment. (Figure 12) Additionally, the measured filtration rate of the animals on day 5 is surprisingly consistent with the expression pattern of *chs2* (Figure 8, Appendix II). Although reduced feeding rate in response to reduced expression level of *chs2* was not an initial objective or point of interest, it could be an interesting endpoint to link towards the effect of CSI such as teflubenzuron and molting inhibition in future research.

Exposure to CSI has been shown to significantly impact chitin content and molting success in arthropods by the increased expression of chitinase (CHT) genes. From the study of chitinase knockdown and diflubenzuron exposure in the citrus red mite (*Panonychus citri),* Xia et al found a significant increase in the expression of *cht1* in addition to the reduction in chitin content (Xia et al., 2016). The study also reported inhibited molting where the animals were stuck within the old exoskeleton in a similar matter as reported in crustacea (Schmid et al., 2023). These findings in the literature are supported by the gene expression findings in our study where a 3.2 - 4.2-fold increase in the expression of both *cht1* and *cht3 w*as found compared to the negative control. The reduction in chitinase expression can, based on these findings, suggest that a decrease in the chitin degradation activity, both inhibits the normal detachment between the cuticle layers during molting, as well as the recycling activity by reduced cleavage of chitin into recyclable oligomers of NAcGlc (Rocha et al., 2012). Thus,

inhibition in the activity of chitinases, by reduced transcription, could have downstream effects on molting.

4.1.2.1 Temporal and developmental dependent changes in expression of molting relevant genes

Molting in copepods is a cyclical event organized through several steps/phases (molting, post-molt, pre-molt, and intermolt), each step with its distinct genetic expression pattern both spatial and temporal during molting (Christiane. Eichner et al., 2015; Knigge et al., 2021; Seear et al., 2010); (Schmid et al., 2023). For example, both Knigge et al and Seear et al found upregulation of genes related to glucosamine synthesis during the pre-molt phase, while Knigge et al also found that the expression of chitin synthases and chitinases to be upregulated later during ecdysis and the post-molt phase (Knigge et al., 2021; Seear et al., 2010). As suggested by these studies, the variations in the expression of molting-relevant genes could be a consequence of the cyclical nature of molting where the expression will be different based on the individual progression through the molting cycle. Moreover, several studies have demonstrated how the gene expression pattern of key chitin synthesis and degradation genes is expressed differentially between developmental stages (Christiane. Eichner et al., 2015; Christiane Eichner et al., 2015; Harðardóttir et al., 2019; Zhang et al., 2022). Zhang et al found a significant increase in the expression of *chs1* with increasing developmental life stage in pre-adult life stages of the Asian citrus psyllid (*Diaphorina citri*), a trend also found for the expression of chitinases by Eichner et al in *L. salmonis.* Additionally, the comprehensive study done by Harðardóttir et al in 2019 on chitin synthetases, chitin synthesis relevant genes and chitinases in *L. salmonis* all point to the same conclusion. Considering the heterogeneous life stage distribution found, one can also assume that different molting progressions were present. Both these factors could have had major implications for the expression of genes measured in our study.

Considering this, it is natural to comment on the implications the designed gene expression study could have had on the generated expression results. The genetic material used for qPCR is a composite of several copepods from the same exposure treatment group, with copepods at different degrees of progression through molting and different developmental life stages. The variance in measured fold change in gene expression in our study was found to be generally high for all treatments (Table 6, Appendix II) and could be a consequence of this differential expression at different life stages and progressions through molting. As a result, the qPCR is limited to describing the cumulated genetic expression of multiple *C. finmarchicus* copepods in response to teflubenzuron exposure. Hence, the overall value of the data generated from the gene expression study is low on an individual level. The data may however have higher value when considering the heterogeneity and diversity of a natural system in the open marine environment.

4.1.3 Physiological and morphological endpoints: Developmental inhibition and deformities

Based on the physiological findings of our study, teflubenzuron concentrations of 0.01 µg/L - 0.1 µg/L significantly reduce mean prosome length in *C. finmarchicus* under the experimental settings of our study. This reduction in mean prosome length was additionally also found across all life stages, suggesting that the effect on growth is indifferent to the life stage of the copepods. The reduction in prosome size found could be explained by several scenarios. Firstly, a scenario where the mechanical restraints on growth and development are a result

form stuck carapaces on the animals, preventing escape from the old exoskeleton and confinement at the animals 'old' size. This scenario would be facilitated by inhibitions of molting from e.g. inhibition of chitin synthesis. Secondly, as a secondary effect of mechanical restraints, reduced mobility affects the feeding activity of the animals, reducing nutritional uptake and further reducing the potential of normal growth and development.

Comparing the ratio of life stages found in the pre-experimental group with the highest exposure treated groups, our results indicate an arrest in development when exposed to 0.1 µg/L -1.0 µg/L teflubenzuron. The developmental arrest found in this exposure range suggests that the copepods have been 'stuck' and had to spend more time at a lower developmental stage compared to the control and low-exposure groups. Adding to the evidence, the ratio of life stages in these treatment groups was also more similar to that of the pre-experimental treatments, suggesting that nearly no development had occurred during the seven days of exposure at all. Alternatively, the findings of disintegrated carapaces by imaging in the high-exposure treatment groups (Appendix IV) might be evidence of molting-associated mortality for the copepods attempting to molt during the exposure period. Thus, the arrested development found in these treatments might falsely report no development or molting to have happened during the experiment, suggesting that there might have been normal development in these treatments after all, but that the ratio of larger life stages was reduced due to mortality.

High concentrations of teflubenzuron (<0.1 µg/L) also induced major morphological deformities and damages in the exposed copepods. During imaging, deformities such as deformed and smaller heads, abnormal antennas and tails, and deformed prosome segment was captured in a trend of increasing teflubenzuron concentration (Appendix IV). The extent of deformities and damages were most severe in the high-exposure treatments, with a near-instant reduction in adverse morphological effects at the 0.03 µg/L treated copepods. Although lack of current experience prevents confirmation, several of the copepods imaged show disruption and or inhibition of the molting process by the presence of double exoskeletons, breakage, and damage of the cuticle or even mortality associated with ecdysis. Samuelsen's chronic study of teflubenzuron exposure on juvenile *H. gammarus* describes and shows similar morphological damages as in this study, with deformities such as deformities on the carapace, walking legs, tail fan, abdomen, and antennas of the animals (Samuelsen et al., 2014). Additionally, Harðardóttir found severe morphological defects in *L. salmonis* with implications for survival more in line with the morphological defects observed in *C. finmarchicus* in this study (Harðardóttir et al., 2021). Although difficult to strengthen by statistical weight or evidence, the captured images are a visual link to the adverse effects of teflubenzuron in this study and should be taken into consideration, although no numbers are able to describe the effects seen.

4.2 Linking molecular effects to physiological deformities by AOP360; fitness of model

AOP 360 is considered to be taxonomically applicable for all arthropods undergoing continuous molting as the dependency of chitin, both qualitatively and quantitatively, is common within the whole phyla of arthropods. Thus, AOP 360 also applies to describe molting inhibition in *C. finmarchicus.* Currently, the prototypical stressors listed to cause inhibition of CHS1 in AOP 360 are pyrimidine nucleosides such as polymyxin D and B, and nikkomycins.

Teflubenzuron has been shown to have similar effects on arthropod CHS1 as pyrimidine nucleotides does and could be a potential candidate to incorporate as a prototypical stressor in AOP 360 (Sun et al., 2015).

However, the MIE of AOP 360 describes the initiation of the pathway by the inhibition of the activity level of CHS1, a definition that might be correct but not intuitive in regard to the expected molecular cause-and-effect relationship. The molecular activity of enzymes can be indirectly measured through the expression level of the gene from which the enzyme is transcribed. Thus, a reduced expression of *cht1* would signify a reduced activity or even inhibition of the enzyme. In this case, a reduced expression of *chs1* would entail less CHS1 activity and a reduction in chitin synthesis and chitin content with implications for molting. However, the expression level of genes alone does not necessarily explain or dictate the molecular cause-and-effect relationships observed in a biological system. Rather, an increased expression of *chs1* might be linked to feedback mechanisms upregulating chitin synthesis in the animal when inhibition of chitin synthesis occurs or if the accumulation of chitin is compromised. Hence, an increased expression of *chs1* might, although counterintuitive, be evidence of inhibition in the activity of CHS1. These assumptions lead to two different conclusions regarding the fitness of AOP 360 to describe the effects found in this study. Firstly, if a reduced expression of *cs1* signifies inhibition of CHS1 activity in *C. finmarchicus,* this study does not carry evidence to fall under the assumptions of the MIE in AOP 360. Secondly, if an increased expression of *chs1* signifies inhibition of CHS1 activity in *C. finmarchicus,* this study could carry evidence to characterize molting inhibition through AOP 360.

Additionally, AOP 360 suggests that inhibition or reduced activity in key enzymes in the upstream chitin synthesis pathway also reduces chitin content in the same manner as knockdown (and reduced expression) of *chs1* (Schmid et al., 2022), and thus could also be relevant evidence of support to AOP 360. In this study, such a reduction in the expression of chitin synthesis relevant genes was only found in *gfat* and *chs2* in the 0.03 µg/L treatment, although the reduction in fold change was not found statistically significant. In summary, AOP 360 had great potential to describe the molting inhibition in *C. finmarchicus* from teflubenzuron exposure. However, this study falls short of molecular evidence to link the adverse effects of teflubenzuron to an inhibition of CHS1. Expanding the data on the genetic expression of *chs1,* as well as other molting relevant genes, at higher exposure concentrations of teflubenzuron (>0.03 µg/L) would help determine the overall fitness of AOP 360 for *C. finmarchicus*.

4.3 Methods and study design; factors influencing results

4.3.1 Calanus finmarchicus as a study species; practical limitations of scale

One of the major issues with this study revolves around the practicality of *C. finmarchicus* as a study species and the experimental scale that is required. Despite the small size of *C. finmarchicus*, the required cultivation system to maintain the animals during an acute exposure study is quite extensive. To simulate a natural system, factors such as the ratio of biomass to water, water temperature and salinity, algae concentration, and water movement must be mimicked. Several of these factors and issues have already been solved at the SINTEF Ocean Sea Lab by utilizing temperature-regulated rooms and specially designed plankton carousels that allow continuous suspension of algae and movement of water. However, the

clever equipment design also provides some major limitations in this study. The plankton carousels are designed to hold a maximum capacity of 16 2L glass flasks and are quite large equipment requiring a decent amount of floor space. Thus, the size of the temperature-controlled experimental room, as well as the number of carousels available, dictates what experimental scale is practically feasible as well as experimental factors such as number of exposure concentrations or technical replicates.

Based on previous studies using plankton carousels and *C. finmarchicus* it was decided that 20 copepods per exposure vessel was practically feasible considering oxygen concentration and consumption rate of algae by the copepods. In short, more than 20 copepods require more frequent addition of algae and entail more disturbance during the exposure experiment. With 20 copepods per exposure flask, it was only necessary to replenish the algae twice during the exposure period (on day 4 and day 6). However, a limit of 20 copepods per treatment severely limits the available biomass to be distributed between downstream analyses and increases vulnerability should anything go wrong, or biomass be lost. Few biological replicates per exposure treatment also weakens the significant strength of the data generated. For future work, an upgrade in the experimental design regarding scale and number of animals in each exposure treatment replicate would be beneficial, although a larger scale would require significantly larger and more inputs on all levels.

4.3.2 Life stage heterogeneity and size bias during sampling

Assuming all the copepods were introduced to the experiment at the same developmental stage, there would ideally only have been one developmental stage present at the end of the experiment. However, we registered a range of life stages from C2 to C5 at the end of the experimental period, indicating that there must also have been a range of life stages at the initiation of the experiment. This assumption was also confirmed by the analysis of images taken of copepods in the pre-experimental group, where it was noted a heterogeneous distribution with a range of life stages from C2 to C4 (Figure 16). This suggests that heterogeneity was introduced at some point, either from external factors such as sampling bias or the addition of 'stowaways', or internal factors such as deviating developmental capacity or different feeding potential. Although a homogenous developmental stage distribution was not pivotal for the main results gathered in this study in regards to the objectives, synchronization in age/developmental stage does influence endpoints such as sensitivity to chemical exposure and expression of temporally regulated gene expression (Schmid et al., 2023).

4.3.3 Unexpected high mortality and implications for the gene expression study

Due to unexpected mortality in the high-exposure treatments (0.03 µg/L – 1.0 µg/L), the gene expression study lost much of its power of resolution at this exposure range, and hence, the potential to link these exposure concentrations to molecular effects during molting. In essence, this study was only able to analyze and describe the genetic expression in the sub-lethal window of exposure at the initial climb of the dose-response observed. Luckily, as the RNA yield of the 0.03 µg/L exposure treatments proved to be marginally sufficient to analyze against a handful of genes, the study was able to gather additional key data at an interesting exposure concentration. Based on the findings of the effect in the sub-studies on mortality and physiological/morphological defects, the 0.03 µg/L treatment marks a significant threshold for several of the adverse effects found. Following this opportunity, analysis of the

molecular effects at this treatment concentration was possible for a set of prioritized genes. This small window of opportunity yielded some interesting results that suggest a relationship between teflubenzuron and several genes of importance in the chitin metabolism and regulation of ecdysis. Based on the experience from this study, alternative study designs allowing for the detection of molecular evidence in an acute or lethal exposure range would be interesting and helpful to expand the knowledge of relevant effects in marine non-target organisms.

4.4 Environmental relevance

4.4.1 Bioavailability of teflubenzuron to *Calanus finmarchicus* in a laboratory setting and in the environment.

The bioavailability of teflubenzuron is influenced by several variables, such as environmental concentrations, physiochemical properties, persistence and removal from the environment, and biological exposure routes. As the environmental concentrations of teflubenzuron are low and the chemical is slightly hydrophobic, the bioavailability of teflubenzuron would practically be low to pelagic organisms. Regarding this study, the hydrophobicity of teflubenzuron would repulse the chemical toward the glass walls of the exposure flask, reducing the overall exposure and bioavailability of teflubenzuron to the copepods. A lack of significant effects on molting from teflubenzuron exposure could be explained by this physiochemical property as well as the experimental design. However, in the laboratory setting of this study, the bioavailability of teflubenzuron is apparently present and at a sufficient level to allow for an uptake resulting in the adverse effects observed. As a filter-feeding organism with a tough and hydrophobic exoskeleton, filtration of teflubenzuron from the water or bound to organic particles/algae would be the most probable route of uptake. Thus, the density of algae or organic particles could also be a factor influencing the bioavailability of teflubenzuron to *C. finmarchicus.*

Additionally, the timing of teflubenzuron usage and release into the open environment could be an important factor for the bioavailability of the chemical. The utilization of teflubenzuron in marine aquaculture facilities follows the development of salmon lice, with an optimal administration of teflubenzuron in the period before the ectoparasites reach adult life stages (Aldrin et al., 2023). Generally, *L. salmonis* starts to become an issue at around mid-May (week 20) and reaches a peak 'bloom' around the end of September (week 40), suggesting that an optimal application of in-feed teflubenzuron would be between late May and early June (Sommerset et al., 2024). This 'golden hour' of optimal treatment with teflubenzuron, unfortunately, coincides with the seasonal growth cycle of *C. finmarchicus*. The bloom of *C. finmarchicus* is at its highest (maximum biomass density) at the beginning of June, with a peak of new-generation juveniles found in August (Hansen et al., 2000; Madsen et al., 2001). Although the industry is advised against the application of in-feed CSI in the months of June-August, applications on either side of this restraint window still pose a potential risk of harm to non-target copepods such as *C. finmarchicus* (Nygaard et al., 2020). In Ritchie's study from 2002, high insecticidal efficacy post teflubenzuron treatment on parasitic *L. salmonis* was found 26 days post-treatment, indicating that teflubenzuron could still be excreted from the farmed fish long after the period of medication has ended. Combining this knowledge with the extensive findings of environmental persistence and distribution from farming sites e.g., Samuelsen's study from 2015, there is sufficient evidence to conclude that the overlap in the

seasonal growth pattern of *C. finmarchicus* and the period of chemotherapeutic treatment is a potential issue for non-target marine organisms (Samuelsen et al., 2015).

Based on the knowledge at hand, the most recent mapping of the environmental concentrations of teflubenzuron was published in 2014 by Langford et al (Langford et al., 2014). Based on Langford et al the environmental concentrations of teflubenzuron in close proximity to marine farming facilities were <0.01 µg/L -0.012 µg/L. In the ten-year period after the study was published, the utilization of chemical de-lousing strategies has drastically been reduced (Figure 1, Appendix II). Based on the lack of data and the strategic shifts within the aquaculture industry, the environmental concentrations of teflubenzuron could be considered low. Thus, the potential bioavailability can also be suggested to be reduced. Although, the number of new research on the effect of resuspension and distribution of teflubenzuron from marine sediments suggests that the issue might not entirely have been resolved by time (A. E. Parsons et al., 2021; Samuelsen, 2016; Samuelsen et al., 2015). Teflubenzuron could therefore still have impact on marine copepods such as *C. finmarchicus,* although the majority of research has by possible bias ruled out pelagic organisms as potential non-target organisms based on assumed low bioavailability. The findings from this study however suggest that the bioavailability of teflubenzuron to *C. finmarchicus* is relevant and that adverse effects at environmentally relevant concentrations is present.

4.4.2 Current environmental standards and relevance to this study

The Norwegian environmental quality standards (EQS) have evaluated the maximum acute concentration limit (MAC-EQS, quality class III) for teflubenzuron in coastal waters to be 0.012 µg/L, with a range of 0,0025 µg/L - 0,012 µg/L. Within this exposure range, it is expected to find "acute toxic effects at short time exposure" for marine organisms (Miljødirektoratet, 2020). This set MAC-EQS is based on ecotoxicological data of acute effects on the most sensitive organism found within the matrix in question; here coastal saltwater. In the case of teflubenzuron in the marine environment, the EQS is measured against *D. magna* (48h EC_{50}= 1.2 µg/L) with an assessment factor (AF) of 100 (Arp et al., 2014). Comparing the MAC-EQS threshold (0.0012 µg/L) with the measured acute effect threshold in this study (NOEC, 0.00127 µg/L) corresponding to the acute and adverse endpoints of mortality, physiology, morphology, and development found in this study, the safety threshold seems to be relevant and within the same order of magnitude. However, there could be value in arguing for revising the foundation of knowledge behind the EQS set for teflubenzuron. As the MAC-EQS is based on an freshwater crustacean species, considering utilizing recent acute toxicity data based on marine copepods would, in the case of *C. finmarchicus* and other marine species, be more suitable to describe sensitivity and to ensure a safe marine environment.

4.5 Future prospects and potentials

4.5.1 Optimization of study design based on experiences from this study

In hindsight, this study was not designed to capture gene expression data continuously, resulting in the loss of valuable information on the gene expression in response to teflubenzuron. For future work, more animals or a divided study between mortality and gene expression would be beneficial to observe and document both effects better. Alternatively, sampling of copepods at earlier and or several points of the exposure period would allow deeper insight into areas this study misses, as well as preserving biomass throughout the experiment for gene expression analysis. This strategy has had success in several other studies

and could have been implemented in this study to provide more information on endpoints at different levels simultaneously (Tollefsen et al., 2017)

4.5.2 The potential of fluorescent high-content imaging in chitin content determination

Chitin content determination in marine crustaceans using fluorescent probes is not an established method. Some studies have used chitin-specific fluorescent probes in studies on arthropods, but mainly for qualitative purposes such as visualization of chitin-rich structures (Chaudhari et al., 2011; Michels & Büntzow, 2010; Sugier et al., 2018). However, there are promising opportunities for the expansion of fluorescent imaging to also be utilized in a quantitative manner. Fluorescent chitin imaging utilizing the CellInsight instrument platform (Thermosphere Scientific, Waltham, US) proved to be a promising method of chitin content determination worthy of continued development. The sample preparation method is fairly straightforward and more robust regarding sample preservation and quality than anticipated. The benefit of this method is the degree of magnification and the quality of the generated images. As the measurement of chitin content is normalized against the fluorescence of nucleic material, the method also becomes applicable across all life stages and different sizes of copepods. In addition to having promising potential for fluorescent chitin content determination, the method is also an expansion of high-resolution structural imaging of larger organisms relative to the traditionally imaged eukaryote cells or organoids.

In association with the exploration of methods for chitin content measurement for this study, an opportunity to initiate a pilot collaboration between The Norwegian Institute of Public Health (FHI) and NIVA was taken. This thesis project has been a collaborator in this work, especially in the early method development phase. Future development of the method will continue beyond this study and be applied in future research and method development. To illustrate the possibilities of this method in future work, preliminary whole-body images of *C. finmarchicus are* supplied in Figure 8, Appendix II.

4.5.3 Future development of AOPs

Although this study was unable to link inhibition of CHS1 to molting inhibition in *C. finmarchicus* in line with AOP 360*,* other key areas of interest were explored and knowledge relevant to future AOP development was gathered. For example, this study was able to capture the effects of teflubenzuron exposure on physiological, morphological, and developmental levels, as well as mortality. All effects can additionally be linked to inhibition of molting, suggesting that AOPs describing molting inhibition or premature molting as a KE could be able to describe the effects found in our study. Additionally, based on the substantial effects of low concentrations in this study, teflubenzuron should be considered to be added to AOP 360 as a prototypical stressor.

Surprisingly, this study could be useful in linking teflubenzuron exposure to molting inhibition in *C. finmarchicus* through AOP 358 "*Chitinase inhibition leading to mortality".* Based on the findings from the gene expression study, there may be evidence of an increased trend in the expression of both *cht1* and *cht3* in *C. finmarchicus* at increasing exposure concentrations of teflubenzuron (Figure 12). These finding suggest an increase in chitinase activity, and possible disruption of normal molting, leading to premature molting. However, additional research on the relationship would probably be needed, but it could benefit substantially from the work

and data generated from this study. Additionally, the angle exploring the effect of *chs2* inhibition on molting could be interesting to pursue or incorporate into AOP 360.

4.6 Summary and conclusion

To conclude, this study was able to describe and measure multiple adverse effects at concentrations of 0.001 µg/L – 1.0 µg/L teflubenzuron in the marine key copepod *C. finmarchicus.* The effects were measured at several distinct levels of biological organizations associated with molting. A threshold of effects appears in the 0.03 µg/L -0.1 µg/L window of exposure for all endpoints measured. Due to the design of the exposure study high mortality had major implications for the resolution of the gene expression study, preventing linkage between molecular effects to the physiological effects and molting. Additionally, based on the limitations of the gene expression study, this study was unable to provide evidence that AOP 360 is applicable do describe molting associated mortality in *C. fimarchicus.* Future efforts to link teflubenzuron to the inhibition of *chs1,* as well as other molting relevant genes*, are* needed and the next step to further develop AOPs towards application in arctic and boreal species.

5 References

Aldrin, M., Huseby, R. B., Stige, L. C., & Helgesen, K. O. (2023). Estimated effectiveness of treatments against salmon lice in marine salmonid farming. *Aquaculture*, *575*, 739749. https://doi.org/https://doi.org/10.1016/j.aquaculture.2023.739749

Ankley, G. T., Bennett, R. S., Erickson, R. J., Hoff, D. J., Hornung, M. W., Johnson, R. D., Mount, D. R., Nichols, J. W., Russom, C. L., Schmieder, P. K., Serrrano, J. A., Tietge, J. E., & Villeneuve, D. L. (2010). Adverse outcome pathways: A conceptual framework to support ecotoxicology research and risk assessment. *Environmental Toxicology and Chemistry*, *29*(3), 730-741. https://doi.org/https://doi.org/10.1002/etc.34

Arakane, Y., Muthukrishnan, S., Kramer, K. J., Specht, C. A., Tomoyasu, Y., Lorenzen, M. D., Kanost, M., & Beeman, R. W. (2005). The Tribolium chitin synthase genes TcCHS1 and TcCHS2 are specialized for synthesis of epidermal cuticle and midgut peritrophic matrix. *Insect Molecular Biology*, *14*(5), 453-463. https://doi.org/https://doi.org/10.1111/j.1365-2583.2005.00576.x

Arp, H. P., Ruus, A., Macken, A., & Lillicrap, A. (2014). *Kvalitetssikring av miljøkvalitetsstandarder*. https://www.miljodirektoratet.no/globalassets/publikasjoner/M241/M241.pdf

Basedow, S. L., Renner, A., Espinasse, B., Falk-Petersen, S., Graeve, M., Bandara, K., Sørensen, K., Eiane, K., & Hagen, W. (2024). The impact of advection on a Subarctic fjord food web dominated by the copepod Calanus finmarchicus. *Progress in Oceanography*, 103268. https://doi.org/https://doi.org/10.1016/j.pocean.2024.103268

Becker, R. A., Ankley, G. T., Edwards, S. W., Kennedy, S. W., Linkov, I., Meek, B., Sachana, M., Segner, H., Van Der Burg, B., Villeneuve, D. L., Watanabe, H., & Barton-Maclaren, T. S. (2015). Increasing Scientific Confidence in Adverse Outcome Pathways: Application of Tailored Bradford-Hill Considerations for Evaluating Weight of Evidence. *Regulatory Toxicology and Pharmacology*, *72*(3), 514-537. https://doi.org/https://doi.org/10.1016/j.yrtph.2015.04.004

Burridge, L., Weis, J. S., Cabello, F., Pizarro, J., & Bostick, K. (2010). Chemical use in salmon aquaculture: A review of current practices and possible environmental effects. *Aquaculture*, *306*(1), 7-23. https://doi.org/https://doi.org/10.1016/j.aquaculture.2010.05.020

Campbell, R., G. , Wagner, M., M. , Teegarden, G., J. , Boudreau, C., A. , & Durbin, E., G. . (2001). Growth and development rates of the copepod Calanus finmarchicus reared in the laboratory. *Marine Ecology Progress Series*, *221*, 161-183. https://www.int-res.com/abstracts/meps/v221/p161-183/

Chang, E. S., & Mykles, D. L. (2011). Regulation of crustacean molting: A review and our perspectives. *General and Comparative Endocrinology*, *172*(3), 323-330. https://doi.org/https://doi.org/10.1016/j.ygcen.2011.04.003

Chaudhari, S. S., Arakane, Y., Specht, C. A., Moussian, B., Boyle, D. L., Park, Y., Kramer, K. J., Beeman, R. W., & Muthukrishnan, S. (2011). Knickkopf protein protects and organizes chitin in the newly synthesized insect exoskeleton. *Proceedings of the National Academy of Sciences*, *108*(41), 17028-17033. https://doi.org/doi:10.1073/pnas.1112288108

Chen, Q., Sun, M., Wang, H., Liang, X., Yin, M., & Lin, T. (2023). Characterization of Chitin Synthase B Gene (HvChsb) and the Effects on Feeding Behavior in Heortia vitessoides Moore. *Insects*, *14*(7), 608. https://www.mdpi.com/2075-4450/14/7/608

Core Team, R. (2024). *R: A language and environment for statistical
computing.* In (Version 1.3.1073) https://www.R-project.org/.
Cresci, A., Samuelsen, O. B., Durif, C. M. F., Bjelland, R. M., Skiftesvik, A. B., Browman, H. I., & Agnalt, A.-L. (2018). Exposure to teflubenzuron negatively impacts exploratory behavior, learning and activity of juvenile European lobster (Homarus gammarus). *Ecotoxicology and Environmental Safety*, *160*, 216-221. https://doi.org/https://doi.org/10.1016/j.ecoenv.2018.05.021
Douris, V., Steinbach, D., Panteleri, R., Livadaras, I., Pickett, J. A., Van Leeuwen, T., Nauen, R., & Vontas, J. (2016). Resistance mutation conserved between insects and mites unravels the benzoylurea insecticide mode of action on chitin biosynthesis. *Proceedings of the National Academy of Sciences*, *113*(51), 14692-14697. https://doi.org/doi:10.1073/pnas.1618258113
Eichner, C., Hamre, L. A., & Nilsen, F. (2015). Instar growth and molt increments in Lepeophtheirus salmonis (Copepoda: Caligidae) chalimus larvae. *Parasitology International*, *64*(1), 86-96. https://doi.org/https://doi.org/10.1016/j.parint.2014.10.006
Eichner, C., Harasimczuk, E., Nilsen, F., Grotmol, S., & Dalvin, S. (2015). Molecular characterisation and functional analysis of LsChi2, a chitinase found in the salmon louse (Lepeophtheirus salmonis salmonis, Krøyer 1838). *Experimental Parasitology*, *151-152*, 39-48. https://doi.org/https://doi.org/10.1016/j.exppara.2015.01.011
Felleskatalogen. (2018). Ektobann vet., Skretting A/S. In.
Folkehelseinstituttet. (2024). Bruk av legemidler i fiskeoppdrett i 2023 [Article]. Retrieved 15.04.2024, from https://www.fhi.no/he/legemiddelbruk/fisk/bruk-av-legemidler-i-fiskeoppdrett/
Grefsrud, E. S. (2024). *Risikorapport norsk fiskeoppdrett 2024- Produksjonsdødelighet hos oppdrettsfisk og miljøeffekter av norsk fiskeoppdrett*
(Rapport fra havforskningen Issue. https://www.hi.no/hi/nettrapporter/rapport-fra-havforskningen-2024-4
Grefsrud, E. S., Andersen, L. B., Grøsvik, B. E., Karlsen, Ø., Kvamme, B. O., Hansen, P. K., Husa, V., Sandlund, N., Stien, L. H., & Solberg, M. F. (2023). *Risikorapport norsk fiskeoppdrett 2023- Produksjonsdødelighet hos oppdrettsfisk og miljøeffekter av norsk fiskeoppdrett* [Risikorapport](Rapport fra havforskningen Issue.
Grefsrud, E. S., Bjørn, P. A., Grøsvik, B. E., Hansen, P. K., Husa, V., Karlsen, Ø., Kvamme, B. O., Samuelsen, O., Sandlund, N., Solberg, M. F., & Stien, L. H. (2022a). *Risikorapport norsk fiskeoppdrett 2022 - Kunnskapsstatus- Effekter på miljø og dyrevelferd i norsk fiskeoppdrett* [Risikorapport](Rapport fra havforskningen, Issue. Havforskningsinstituttet.
Grefsrud, E. S., Bjørn, P. A., Grøsvik, B. E., Hansen, P. K., Husa, V., Karlsen, Ø., Kvamme, B. O., Samuelsen, O. B., Sandlund, N., Solberg, M. F., & Stien, L. H. (2022b). *Risikorapport norsk fiskeoppdrett 2022 - kunnskapsstatus- Effekter på miljø og dyrevelferd i norsk fiskeoppdrett* [Risikorapport](Rapport fra havforskningen Issue.
Hansen, B. H., Altin, D., Hessen, K. M., Dahl, U., Breitholtz, M., Nordtug, T., & Olsen, A. J. (2008). Expression of ecdysteroids and cytochrome P450 enzymes during lipid turnover and reproduction in Calanus finmarchicus (Crustacea: Copepoda). *General and Comparative Endocrinology*, *158*(1), 115-121. https://doi.org/https://doi.org/10.1016/j.ygcen.2008.05.013

Hansen, B. W., Hygum, B. H., Brozek, M., Jensen, F., & Rey, C. (2000). Food web interactions in a Calanus finmarchicus dominated pelagic ecosystem—a mesocosm study. *Journal of Plankton Research*, *22*(3), 569-588. https://doi.org/10.1093/plankt/22.3.569

Harðardóttir, H. M., Male, R., Nilsen, F., & Dalvin, S. (2021). Chitin Synthases Are Critical for Reproduction, Molting, and Digestion in the Salmon Louse (Lepeophtheirus salmonis). *Life*, *11*(1). https://www.mdpi.com/2075-1729/11/1/47

Harðardóttir, H. M., Male, R., Nilsen, F., Eichner, C., Dondrup, M., & Dalvin, S. (2019). Chitin synthesis and degradation in Lepeophtheirus salmonis: Molecular characterization and gene expression profile during synthesis of a new exoskeleton. *Comparative Biochemistry and Physiology Part A: Molecular & Integrative Physiology*, *227*, 123-133. https://doi.org/https://doi.org/10.1016/j.cbpa.2018.10.008

Hothorn, T., Zeileis, A., Farebrother, R. W., Cummins, C., Millo, G., & Mitchell, D. (2022). *Testing Linear Regression Models*. In (Version 0.9-40) CRAN.

IRAC, I. M. W. G. (2024). *MODE OF ACTION CLASSIFICATION SCHEME* 11.1). https://irac-online.org/documents/moa-classification/

ISO. (1999). ISO 14669:1999. Water quality — Determination of acute lethal toxicity to marine copepods (Copepoda, Crustacea). In. International Organization for Standardization: International Organization for Standardization.

Jansson, R., Brown, R., Cartwright, B., Cox, D., Dunbar, D., Dybas, R., Eckel, C., Lasota, J., Mookerjee, P., Norton, J., Peterson, R., Starner, V., & S M, W. (1997). Emamectin benzoate: A novel avermectin derivative for control of lepidopterous pests.

Knigge, T., LeBlanc, G. A., & Ford, A. T. (2021). A Crab Is Not a Fish: Unique Aspects of the Crustacean Endocrine System and Considerations for Endocrine Toxicology [Review]. *Frontiers in Endocrinology*, *12*. https://doi.org/10.3389/fendo.2021.587608

Kolde, R. (2019). *pheatmap: Pretty Heatmaps*. In (Version 1.0.12) [Package]. CRAN. https://cran.r-project.org/web/packages/pheatmap/pheatmap.pdf

Langford, K. H., Øxnevad, S., Schøyen, M., & Thomas, K. V. (2014). Do Antiparasitic Medicines Used in Aquaculture Pose a Risk to the Norwegian Aquatic Environment? *Environmental Science & Technology*, *48*(14), 7774-7780. https://doi.org/10.1021/es5005329

Macken, A., Lillicrap, A., & Langford, K. (2015). Benzoylurea pesticides used as veterinary medicines in aquaculture: Risks and developmental effects on nontarget crustaceans. *Environmental Toxicology and Chemistry*, *34*(7), 1533-1542. https://doi.org/https://doi.org/10.1002/etc.2920

Madsen, S. D., Nielsen, T. G., & Hansen, B. W. (2001). Annual population development and production by Calanus finmarchicus, C. glacialis and C. hyperboreus in Disko Bay, western Greenland. *Marine Biology*, *139*(1), 75-93. https://doi.org/10.1007/s002270100552

Matsumura, F. (2010). Studies on the action mechanism of benzoylurea insecticides to inhibit the process of chitin synthesis in insects: A review on the status of research activities in the past, the present and the future prospects. *Pesticide Biochemistry and Physiology*, *97*(2), 133-139. https://doi.org/https://doi.org/10.1016/j.pestbp.2009.10.001

Mauchline, J., Blaxter, J. H. S., Douglas, B., & Tyler, P. A. (1998). *The Biology of Calanoid Copepods* (1 ed., Vol. 33). Academic Press.

Melle, W., Runge, J., Head, E., Plourde, S., Castellani, C., Licandro, P., Pierson, J., Jonasdottir, S., Johnson, C., Broms, C., Debes, H., Falkenhaug, T., Gaard, E., Gislason, A., Heath,

M., Niehoff, B., Nielsen, T. G., Pepin, P., Stenevik, E. K., & Chust, G. (2014). The North Atlantic Ocean as habitat for Calanus finmarchicus: Environmental factors and life history traits. *Progress in Oceanography*, *129*, 244-284. https://doi.org/https://doi.org/10.1016/j.pocean.2014.04.026

Merzendorfer, H. (2006). Insect chitin synthases: a review. *Journal of Comparative Physiology B*, *176*(1), 1-15. https://doi.org/10.1007/s00360-005-0005-3

Merzendorfer, H. (2013). Chitin synthesis inhibitors: old molecules and new developments. *Insect Science*, *20*(2), 121-138. https://doi.org/https://doi.org/10.1111/j.1744-7917.2012.01535.x

Michels, J., & Büntzow, M. (2010). Assessment of Congo red as a fluorescence marker for the exoskeleton of small crustaceans and the cuticle of polychaetes. *Journal of Microscopy*, *238*(2), 95-101. https://doi.org/https://doi.org/10.1111/j.1365-2818.2009.03360.x

Miljødirektoratet. (2020). *Grenseverdier for klassifisering av vann, sediment og biota – revidert 30.10.2020* [Guidance report](608). Miljødirektoratet. https://www.miljodirektoratet.no/globalassets/publikasjoner/M608/M608.pdf

Miljødirektoratet, V. (2010). Vannmiljø. In (pp. Søkeresultat vannregisteringer teflubenzuron i saltvann). Vannmiljø: Miljødirektoratet.

Myhre Jensen, E., Horsberg, T. E., Sevatdal, S., & Helgesen, K. O. (2020). Trends in de-lousing of Norwegian farmed salmon from 2000–2019—Consumption of medicines, salmon louse resistance and non-medicinal control methods. *PLOS ONE*, *15*(10), e0240894. https://doi.org/10.1371/journal.pone.0240894

Møller, E. F., Maar, M., Jónasdóttir, S. H., Nielsen, T. G., & Tönnesson, K. (2012). The effect of changes in temperature and food on the development ofCalanusfinmarchicusandCalanus helgolandicuspopulations. *Limnology and Oceanography*, *57*(1), 211-220. https://doi.org/https://doi.org/10.4319/lo.2012.57.1.0211

Nygaard, S., Klakegg, B., Markussen, Ø., Horsberg, T. E., Hamadi, M., & Persson, D. (2020). *TILTAKSVEILEDER KONTROLL MED LAKSELUS OG SKOTTELUS*. Lusedata.no. https://lusedata.no/wp-content/uploads/2022/03/2120.01.20-Tiltaksveileder-Lakselus-og-skottelus.pdf

Olsvik, P. A., Samuelsen, O. B., Agnalt, A.-L., & Lunestad, B. T. (2015). Transcriptional responses to teflubenzuron exposure in European lobster (Homarus gammarus). *Aquatic Toxicology*, *167*, 143-156. https://doi.org/https://doi.org/10.1016/j.aquatox.2015.07.008

Parsons, A., Samuelsen, O. B., Johnsen, I. A., Hannisdal, R., Tjensvoll, T., & Husa, V. (2021). Distribution and Persistence of Diflubenzuron and Teflubenzuron in the Marine Environment Around Salmonid Aquaculture Facilities [Original Research]. *Frontiers in Marine Science*, *8*. https://doi.org/10.3389/fmars.2021.694577

Parsons, A. E., Samuelsen, O. B., Johnsen, I. A., Hannisdal, R., Tjensvoll, T., & Husa, V. (2021). Distribution and Persistence of Diflubenzuron and Teflubenzuron in the Marine Environment Around Salmonid Aquaculture Facilities [Original Research]. *Frontiers in Marine Science*, *8*. https://doi.org/10.3389/fmars.2021.694577

Parsons, A. E., Samuelsen, O. B., Johnsen, I. A., R, H., Tjensvoll, T., & Husa, V. (2021). Distribution and Persistence of Diflubenzuron and Teflubenzuron in the Marine Environment Around Salmonid Aquaculture Facilities. . *Front. Mar. Sci.* , *8:694577*. https://doi.org/10.3389/fmars.2021.694577

Reygondeau, G., & Beaugrand, G. (2011). Future climate-driven shifts in distribution of Calanus finmarchicus. *Global Change Biology 17*(2), 756-766. https://doi.org/https://doi.org/10.1111/j.1365-2486.2010.02310.x

Ritz, C. (2016). *Analysis of Dose-Response Curves*. In (Version 3.0-1) [Package]. CRAN. http://www.r-project.org, http://www.bioassay.dk

Rocha, J., Garcia-Carreño, F. L., Muhlia-Almazán, A., Peregrino-Uriarte, A. B., Yépiz-Plascencia, G., & Córdova-Murueta, J. H. (2012). Cuticular chitin synthase and chitinase mRNA of whiteleg shrimp Litopenaeus vannamei during the molting cycle. *Aquaculture*, *330-333*, 111-115. https://doi.org/https://doi.org/10.1016/j.aquaculture.2011.12.024

Samuelsen, O. B. (2016). Persistence and Stability of Teflubenzuron and Diflubenzuron When Associated to Organic Particles in Marine Sediment. *Bulletin of Environmental Contamination and Toxicology*, *96*(2), 224-228. https://doi.org/10.1007/s00128-015-1707-1

Samuelsen, O. B., Lunestad, B. T., Farestveit, E., Grefsrud, E. S., Hannisdal, R., Holmelid, B., Tjensvoll, T., & Agnalt, A.-L. (2014). Mortality and deformities in European lobster (Homarus gammarus) juveniles exposed to the anti-parasitic drug teflubenzuron. *Aquatic Toxicology*, *149*, 8-15. https://doi.org/https://doi.org/10.1016/j.aquatox.2014.01.019

Samuelsen, O. B., Lunestad, B. T., Hannisdal, R., Bannister, R., Olsen, S., Tjensvoll, T., Farestveit, E., & Ervik, A. (2015). Distribution and persistence of the anti sea-lice drug teflubenzuron in wild fauna and sediments around a salmon farm, following a standard treatment. *Science of The Total Environment*, *508*, 115-121. https://doi.org/https://doi.org/10.1016/j.scitotenv.2014.11.082

Schmid, S., Ilyaskina, D., Lamoree, M., Laonards, P., & Tollefsen, K. E. (2021). *Linking disruption of chitin biosynthesis to molting-associated mortality in Daphnia magna exposed to teflubenzuron* [Paper].

Schmid, S., Rundberget, J. T., Song, Y., & Tollefsen, K. E. (2023). Age and Synchronization of Daphnia magna Affect Sensitivity to Teflubenzuron in Acute Standardized Toxicity Tests. *Environmental Toxicology and Chemistry*, *42*(8), 1806-1815. https://doi.org/https://doi.org/10.1002/etc.5688

Schmid, S., Song, Y., & Tollefsen, K. E. (2022). *Chitin synthase 1 inhibition leading to mortality*. https://doi.org/10.1787/35cd5862-en

Seear, P. J., Tarling, G. A., Burns, G., Goodall-Copestake, W. P., Gaten, E., Özkaya, Ö., & Rosato, E. (2010). Differential gene expression during the moult cycle of Antarctic krill (Euphausia superba). *BMC Genomics*, *11*(1), 582. https://doi.org/10.1186/1471-2164-11-582

Skinner, D. M. (1962). *THE STRUCTURE AND METABOLISM OF A CRUSTACEAN INTEGUMENTARY TISSUE DURING A MOLT CYCLE'*

Sommerset, I., Wiik-Nielsen, J., Moldal, T., Oliveira, V. H. S. d., Svendsen, J. C., Haukaas, A., & Brun, E. (2024). *Fiskehelserapporten 2023*. Veterinærinstituttet. https://www.vetinst.no/rapporter-og-publikasjoner/rapporter/2024/fiskehelserapporten-2023

Song, Y., Rundberget, J. T., Evenseth, L. M., Xie, L., Gomes, T., Høgåsen, T., Iguchi, T., & Tollefsen, K. E. (2016). Whole-Organism Transcriptomic Analysis Provides Mechanistic Insight into the Acute Toxicity of Emamectin Benzoate in Daphnia

magna. *Environmental Science & Technology*, *50*(21), 11994-12003. https://doi.org/10.1021/acs.est.6b03456

Song, Y., Villeneuve, D. L., Toyota, K., Iguchi, T., & Tollefsen, K. E. (2017). Ecdysone Receptor Agonism Leading to Lethal Molting Disruption in Arthropods: Review and Adverse Outcome Pathway Development. *Environmental Science & Technology*, *51*(8), 4142-4157. https://doi.org/https://doi.org/10.1021/acs.est.7b00480

Strachan, F., & Kennedy, C. J. (2021). The environmental fate and effects of anti-sea lice chemotherapeutants used in salmon aquaculture. *Aquaculture*, *544*, 737079. https://doi.org/https://doi.org/10.1016/j.aquaculture.2021.737079

Sugier, K., Vacherie, B., Cornils, A., Wincker, P., Jamet, J.-L., & Madoui, M.-A. (2018). Chitin distribution in the Oithona digestive and reproductive systems revealed by fluorescence microscopy. *PeerJ*, *6*, e4685. https://doi.org/10.7717/peerj.4685

Sun, R., Liu, C., Zhang, H., & Wang, Q. (2015). Benzoylurea Chitin Synthesis Inhibitors. *Journal of Agricultural and Food Chemistry*, *63*(31), 6847-6865. https://doi.org/10.1021/acs.jafc.5b02460

Tollefsen, K. E., Song, Y., Høgåsen, T., Øverjordet, I. B., Altin, D., & Hansen, B. H. (2017). Mortality and transcriptional effects of inorganic mercury in the marine copepod Calanus finmarchicus. *Journal of Toxicology and Environmental Health, Part A*, *80*(16-18), 845-861. https://doi.org/10.1080/15287394.2017.1352198

Wickham, H., François, R., Henry, L., Müller, K., & Vaughan, D. (2023). *dplyr: A Grammar of Data Manipulation*. In (Version 1.1.4) https://cran.r-project.org/web/packages/dplyr/index.html

Willis, K. J., & Ling, N. (2003). The toxicity of emamectin benzoate, an aquaculture pesticide, to planktonic marine copepods. *Aquaculture*, *221*(1), 289-297. https://doi.org/https://doi.org/10.1016/S0044-8486(03)00066-8

Wright, D. A., Savitz, J. D., Dawson, R., Magee, J., & Smucker, R. A. (1996). Effect of diflubenzuron on the maturation and reproductive success of the copepod Eurytemora affinis. *Ecotoxicology*, *5*(1), 47-58. https://doi.org/10.1007/BF00116323

Xia, W.-K., Ding, T.-B., Niu, J.-Z., Liao, C.-Y., Zhong, R., Yang, W.-J., Liu, B., Dou, W., & Wang, J.-J. (2014). Exposure to Diflubenzuron Results in an Up-Regulation of a Chitin Synthase 1 Gene in Citrus Red Mite, Panonychus citri (Acari: Tetranychidae). *International Journal of Molecular Sciences*, *15*(3), 3711-3728. https://www.mdpi.com/1422-0067/15/3/3711

Xia, W.-K., Shen, X.-M., Ding, T.-B., Niu, J.-Z., Zhong, R., Liao, C.-Y., Feng, Y.-C., Dou, W., & Wang, J.-J. (2016). Functional analysis of a chitinase gene during the larval-nymph transition in Panonychus citri by RNA interference. *Experimental and Applied Acarology*, *70*(1), 1-15. https://doi.org/10.1007/s10493-016-0063-0

Xin, T., Li, Z., Chen, J., Wang, J., Zou, Z., & Xia, B. (2021). Molecular Characterization of Chitin Synthase Gene in Tetranychus cinnabarinus (Boisduval) and Its Response to Sublethal Concentrations of an Insecticide. *Insects*, *12*(6), 501. https://www.mdpi.com/2075-4450/12/6/501

Zhang, C., Hu, W., Yu, Z., Liu, X., Wang, J., Xin, T., Zou, Z., & Xia, B. (2022). Characterization of Chitin Synthase A cDNA from Diaphorina citri (Hemiptera: Liviidae) and Its Response to Diflubenzuron. *Insects*, *13*(8), 728. https://www.mdpi.com/2075-4450/13/8/728

Zhang, X., Yuan, J., Li, F., & Xiang, J. (2021). Chitin Synthesis and Degradation in Crustaceans: A Genomic View and Application. *Marine Drugs*, *19*(3), 153. https://www.mdpi.com/1660-3397/19/3/153

Zhu, K. Y., Merzendorfer, H., Zhang, W., Zhang, J., & Muthukrishnan, S. (2016). Biosynthesis, Turnover, and Functions of Chitin in Insects. *Annual Review of Entomology*, *61*(1), 177-196. https://doi.org/10.1146/annurev-ento-010715-023933

Aarflot, J. M., Skjoldal, H. R., Dalpadado, P., Skern-Mauritzen, M., & Fields, D. (2018). Contribution of Calanus species to the mesozooplankton biomass in the Barents Sea. *ICES Journal of Marine Science*, *75*(7), 2342-2354. https://doi.org/10.1093/icesjms/fsx221

Harðardóttir, H. M., Male, R., Nilsen, F., Eichner, C., Dondrup, M., & Dalvin, S. (2019). Chitin synthesis and degradation in Lepeophtheirus salmonis: Molecular characterization and gene expression profile during synthesis of a new exoskeleton. Comparative Biochemistry and Physiology Part A: Molecular & Integrative Physiology, 227, 123-133. https://doi.org/https://doi.org/10.1016/j.cbpa.2018.10.008

Hansen, B. H., Altin, D., Hessen, K. M., Dahl, U., Breitholtz, M., Nordtug, T., & Olsen, A. J. (2008). Expression of ecdysteroids and cytochrome P450 enzymes during lipid turnover and reproduction in Calanus finmarchicus (Crustacea: Copepoda). General and Comparative Endocrinology, 158(1), 115-121. https://doi.org/https://doi.org/10.1016/j.ygcen.2008.05.013

Appendix

I. Summary literature review

A

Event	Diflubenzuron	Teflubenzuron	Emamectin
Ecdysone receptor agonism	884	302	398
Ion channels	1840	610	998
Circulating ecdysis triggering hormone	213	65	50
Incomplete ecdysis	233	71	38
Abdominal muscle contraction	286	163	194
Digestion of old cuticle	902	225	303
Chitin synthase 1	1220	332	337
Cuticular chitin content	2280	505	421
Premature molting	2680	754	1160
Chitinase	791	230	271
Chitobiase	104	29	16
20-hydroxyecdysone	602	161	131
Chitin laminar organization	132	38	47
Prevent chitin degradation by chitinases	600	166	212
Procuticle protection	115	55	29
New cuticle secretion	1870	461	668
Cell injury/death	1270	324	1180

B

Event	Diflubenzuron	Teflubenzuron	Emamectin
Ecdysone receptor agonism	6	3	8
Ion channels	11	6	21
Circulating ecdysis triggering hormone	1	1	1
Incomplete ecdysis	2	1	1
Abdominal muscle contraction	0	0	1
Digestion of old cuticle	8	5	9
Chitin synthase 1	6	4	4
Cuticular chitin content	8	6	5
Premature molting	24	8	28
Chitinase	6	5	6
Chitobiase	2	1	2
20-hydroxyecdysone	6	3	3
Chitin laminar organization	1	0	1
Prevent chitin degradation by chitinases	6	5	4
Procuticle protection	0	0	1
New cuticle secretion	9	6	12
Cell injury/death	23	11	34

C

Event	Diflubenzuron	Teflubenzuron	Emamectin
Ecdysone receptor agonism	6	3	8
Ion channels	11	6	21
Circulating ecdysis triggering hormone	1	1	1
Incomplete ecdysis	2	1	1
Abdominal muscle contraction	0	0	1
Digestion of old cuticle	8	5	9
Chitin synthase 1	6	4	4
Cuticular chitin content	8	6	5
Premature molting	24	8	28
Chitinase	6	5	6
Chitobiase	2	1	2
20-hydroxyecdysone	6	3	3
Chitin laminar organization	1	0	1
Prevent chitin degradation by chitinases	6	5	4
Procuticle protection	0	0	1
New cuticle secretion	9	6	12
Cell injury/death	23	11	34

Figure X: Summary of literature review presented in heat maps. Of available literature that has researched the effects of chitin inhibition related to stressors such as diflubenzuron, teflubenzuron, and emamectin there are few that researches (or even mention) the key ecological species C. finmarchicus*. Figure A describes the number of literature hits on events relevant to chitin inhibition and stressors. Figure B illustrates the same literature hits as Figure A but is oriented toward hits that mention* C. finmarchicus*. The heat-map gradient of Figure B is linked to Figure A and represents the relative amount of* C. finmarchicus *hits of the total literature hits. Figure C describes the same as Figure B but is not linked to the total number of literature hits. Figure C represents the number of literature hits of events and stressors relevant to or mentioning* C. finmarchicus*. Based on the literature search following statements have been made: 1) There is generally much more research on diflubenzuron than teflubenzuron and emamectin, 2) Research on premature molting, changes in cuticle integrity and ion-channels have the most research, 3) There is little research that is oriented towards C. finmarchicus relative to other study species and 4) The main research on CSI effects on C. finmarchicus is related to premature molting, cell injury/death and ion channels.*

II. Figures and tables

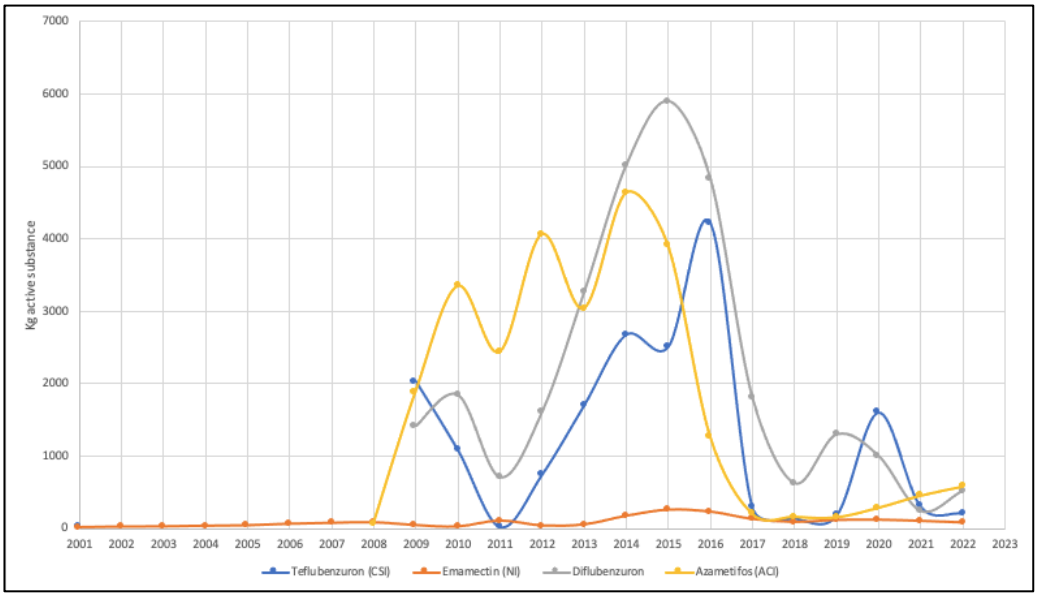

Figure 1: Historical overview of the usage of veterinary chitin synthesis inhibitors (CSI), neural inhibitors (NI) and acetylcholine inhibitors (ACI) in Norwegian aquaculture. Compounds (teflubenzuron (blue), emamectin (orange), diflubenzuron (grey) and azamethiphos (yellow), plotted against year (x-axis) and Kg active substance used (y-axis). The numbers are based on reported sales of substances against salmon lice feed companies and pharmaceutical wholesalers to the Norwegian Institute of Public Health (FHI, https://www.fhi.no/he/legemiddelbruk/fisk/bruk-av-legemidler-i-fiskeoppdrett/).The high peak of teflubenzuron usage in 2014-2016 reflects the increased resistance to the drugs by salmon louse. The following decrease in 2017 reflects the strict regulation in usage of CSI to halter resistance in salmon louse to CSI.

Table 1: Mean developmental stage durations in days(d) based on Campbell et.al.2001 and experimental experience at SINTEF with C. finmarchicus *as a study species.*

Stage	*Egg*	*N1*	*N2*	*N3*	*N4*	*N5*	*N6*	*C1*	*C2*	*C3*	*C4*	*C5*	*C6*
Development time (days)		1.4	2.3	3.7	7.0	8.8	10.5	12.4	14.7	17.4	20.8	25.9	35.6
Stage duration (SD, days)	1.4	0.9	1.4	3.3	1.8	1.7	2.0	2.3	2.7	3.4	5.1	9.6	
SINTEF SD (days)								3.1	3.7	4.6	7.0	13.2	

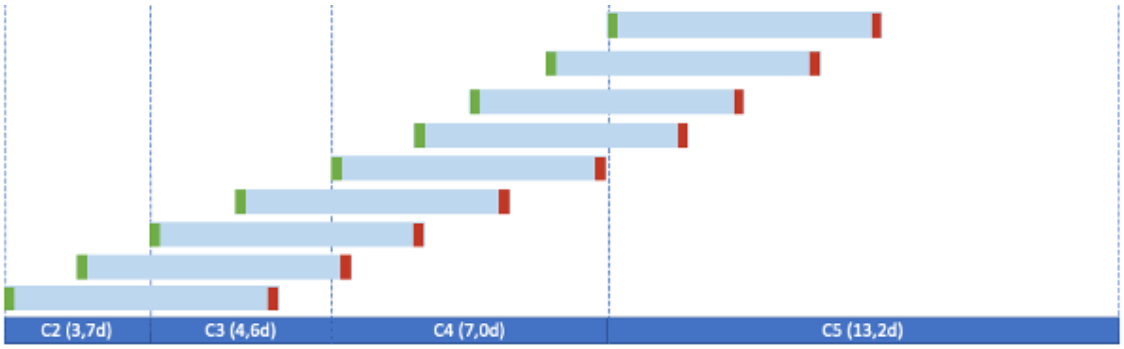

Figure 2: Illustration of theoretical developmental progression based on individual life stage development at different points of experimental initiation. The blue boxes represent one week (duration of experiment). The green tips indicate the progression point of the copepod at initiation of experiment, the red tips indicate the progression point at the end of the experimental period.

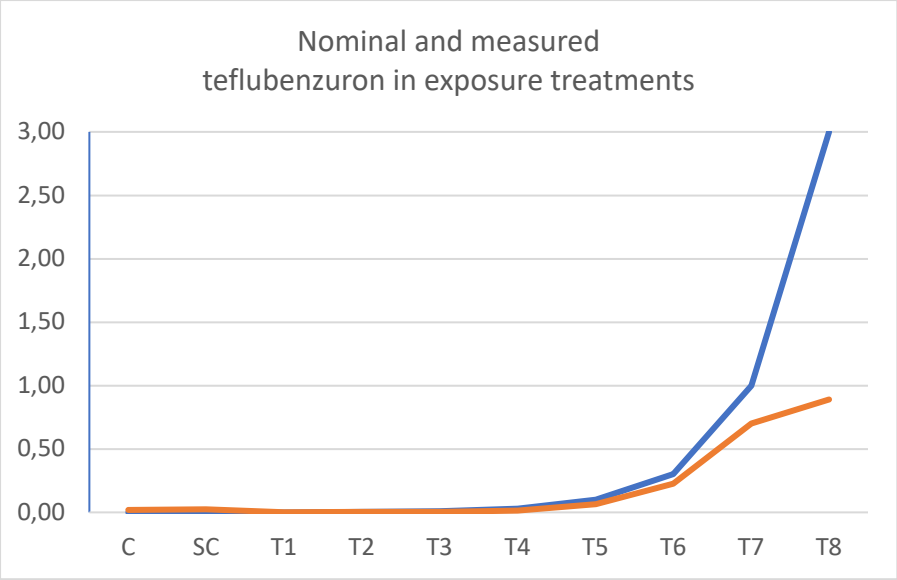

Figure 3: Visualization line plot describing the difference between the nominal concentrations of teflubenzuron (blue) and the measured concentrations (orange) plotted as µg/L /L teflubenzuron (x-axis) in each treatment group (y-axis)

Tabell 2: Difference in nominal and measured concentrations of teflubenzuron. The average measured concentration of teflubenzuron represents the concentration of teflubenzuron measured in each treatment towards the end of the experimental period. Chemical analysis was performed by the SINTEF Ocean analytical lab.

Treatment	*Nominal (µg/L)*	*Average measured (µg/L)*	*% Nominal*
3.0 µg/L	3.0	0.898	30
1.0 µg/L	1.0	0.708	71
0.3 µg/L	0.3	0.225	75
0.1 µg/L	0.1	0.066	66
0.03 µg/L	0.03	0.012	43
0.01 µg/L	0.01	0.0052	52
0.003 µg/L	0.003	0.0015	53
0.001 µg/L	0.001	0.0010	108
Solvent control (0.001%)	0.0	0.00022	-
Control (0.0 µg/L)	0.0	0.00017	-

*Table 3: Descriptive mortality statistics of percentage mortality in each replicate flask of each treatment group, standard deviation of mean mortality (SD), and coefficient of variance of mean mortality (CV). *Mortality based on 6 days of exposure before termination of the experiment and was omitted for the experiment. Data is presented for transparency.*

Treatment	TEF Control (0 µg/L)				Solvent control (0.001%)				TEF 1 (0.001 µg/L)			
Treatment replicate	1	2	3	4	1	2	3	4	1	2	3	4
Mortality (%)	5.55	0.00	0.00	0.00	5.26	0.00	0.00	0.00	0.00	0.00	0.00	0.00
Mean mortality	1.38				1.31				0.00			
SD	0.02				0.02				0.00			
CV	2.00				2.00				NA			

Treatment	TEF 2 (0.003 µg/L)				TEF 3 (0.01 µg/L)				TEF 4 (0.03 µg/L)			
Treatment replicate	1	2	3	4	1	2	3	4	1	2	3	4
Mortality (%)	0.00	0.00	0.00	11.00	0.00	0.00	0.00	0.00	15.00	10.52	5.55	11.76
Mean mortality	2.74				0.00				10.71			
SD	0.05				0.00				0.03			
CV	2.0				NA				0.39			

Treatment	TEF 5 (0.1 µg/L)				TEF 6 (0.3 µg/L)				TEF 7 (1.0 µg/L)			
Treatment replicate	1	2	3	4	1	2	3	4	1	2	3	4
Mortality (%)	9.09	33.33	14.28	30.00	16.66	40.00	57.14	66.66	40.00	58.33	54.54	37.50
Mean mortality	21.67				45.11				47.46			
SD	0.11				0.21				0.10			
CV	0.54				0.48				0.21			

Treatment	TEF 8* (0.1 µg/L)			
Treatment replicate	1	2	3	4
Mortality (%)	NA	23.00	38.46	50.00
*Mean mortality**	29.48			
SD	0.164			
CV	0.59			

Table 4: Collected results from statistical significance testing of non-parametric mortality data. A significance level of 0.05 was utilized for all listed significance test.

Treatment	*Spearman's r*		*Robust single linear regression (t<2)*
	p-value (Mean mortality) (p<0.05)	*Rho (Mean mortality) (<±0.06)*	
Control (0.0 µg/L)	0.866 (1.00)	-0.071 (-1.00)	NA
Solvent control (0.001%)			0.00
TEF 1 (0.001 µg/L)	1.00 (1.00)	0.00 (0.00)	-0.244
TEF 2 (0.003 µg/L)			0.00
TEF 3 (0.01 µg/L)			-0.244
TEF 4 (0.03 µg/L)	0.0002 (0.083)	0.794 (1.00)	6.372
TEF 5 (0.1 µg/L)			12.670
TEF 6 (0.3 µg/L)			26.670
TEF 7 (1.0 µg/L)			28.010

Tabell 5: Mean fold change gene expression for all genes and calculated standard error mean (SEM) based on double delta Ct-method and normalization against negative control (MFC control= 1). C= Negative control, SC= Solvent control.

	Mean fold change (±SEM)				
Gene	*SC*	*0.001 µg/L*	*0.003 µg/L*	*0.01 µg/L*	*0.03 µg/L*
chs2	1.586 (±0.236)	2.091 (±0.323)	1.954 (±0.234)	2.947 (±0.444)	0,598 (±0.115)
cht3	1.287 (±0.222)	2.792 (±0.464)	2.363 (±0.245)	4.445 (±0.821)	4.210 (±0.732)
gfat	1.744 (±0.232)	1.737 (±0.119)	1.661 (±0.117)	2.590 (±0.471)	0.400 (0.112)
NAGase	1.342 (±0.208)	2.941 (±0.724)	1.721 (±0.322)	2.252 (±0.405)	3.063 (±0.483)
pagm	2.131 (±0.254)	1.781 (±0.134)	1.985 (±0.099)	4.601 (±0.723)	17.94 (±2.066)
ech	1.707 (±0.219)	2.089 (±0.082)	1.522 (±0.068)	2.394 (±0.394)	0.244 (±0.066)
cda	1.085 (±0.146)	2.126 (±0.323)	1.368 (±0.200)	1.527 (±0.251)	0.669 (±0.177)
ethr	1.701 (±0.195)	1.934 (±0.365)	1.865 (±0.271)	3.779 (±0.615)	-
20e	0.914 (±0.121)	1.518 (±0.306)	0.899 (±0.059)	1.552 (±0.232)	0.171 (±0.027)
hk2	1.998 (±0.362)	1.862 (±0.206)	2.065 (±0.049)	2.650 (±0.405)	-
gs2	1.436 (±0.198)	2.007 (±0.566)	1.188 (±0.154)	2.268 (±0.485)	-
udp	1.611 (±0.196)	1.637 (±0.338)	1.873 (±0.052)	2.806 (±0.422)	-
gna	1.304 (±0.159)	3.073 (±0.918)	1.394 (±0.192)	2.543 (±0.264)	-
gp1	2.635 (±0.472)	2.729 (±0.413)	1.97 (±0.386)	2.789 (±0.572)	-
gs1	1.527 (±0.224)	1.333 (±0.318)	0.894 (±0.257)	2.257 (±0.387)	-
cht1	1.381 (±0.150)	1.623 (±0.290)	0.780 (±0.227)	3.211 (±0.668)	-
erc_a	0.683 (±0.094)	2.882 (±0.840)	0.680 (±0.168)	1.581 (±0.410)	-
erc_b	2.515 (±0.254)	1.784 (±0.391)	2.115 (NA)	3.683 (±0.191)	-
rxr	1.986 (±0.559)	1.078 (±0.296)	2.163 (±0.606)	4.589 (±1.252)	-
ccap	2.362 (±0.358)	2.034 (±0.247)	2.537 (±0.142)	3.068 (±0.326)	-

*Table 6: Overview of calculated estimates and standard errors for each gene and treatment based on results from linear regression test on individual fold change values against solvent control as interceptor. Tests where the response in individual fold change was found to be significant are highlighted by **bold** numbers. C= Negative control, SC= Solvent control.*

		Linear regression test (P<0.05)					Standard error	Multiple r-squared
Gene	*C*	*SC*	*0.001 µg/L*	*0.003 µg/L*	*0.01 µg/L*	*0.03 µg/L*	*SE*	R^2
chs2	-0.586	1.586	0.505	0.368	1.361	-0.987	0.767	0.396
cht3	-0.287	1.287	1.504	1.076	3.157	2.923	1.439	0.356
gfat	-0.7445	1.744	-0.007	-0.083	0.845	-1.343	0.653	0.419
NAGase	-0.342	1.342	1.598	0.379	0.910	1.72	1.309/1.212	0.222
pagm	-1.131	2.131	-0.350	1,985	2.470	**15.811**	15.811	0.782
ech	-0.707	1,707	0.382	-0.184	0.687	**-1.463**	0.606/0.561	0.529
cda	-0.085	1,085	1.041	0.282	0.442	-0.415	0.630	0.262
ethr	-0.701	1,701	0.232	0.163	3,779	2.077	1.021	0.352
20e	0.085	0,914	0.604	-0.015	0.638	-0.742	0.4902	0.371
hk2	-0.998	1,998	-0.135	0.0670	0.6522	-	0.823	0.228
gs2	-0.436	1,436	0.571	-0.248	0.831	-	1.016	0.130
udp	-0.611	1,611	0.0263	0.2618	1.195	-	0.773/0.835	0.291
gna	1.304	1,304	1.769	0.090	1.239	-	1.269	0.209
gp1	-1.635	2,635	0.093	-0.665	0.153	-	1.195/1.291	0.186
gs1	-0.527	1,527	-0.194	-0.633	0.729	-	0.837/ 1.025	0.184
cht1	-0.381	1,381	0.241	-0.601	1.829	-	0.996	0.330
ecr_a	0.316	0,683	2.198	-0.003	0.897	-	1.227	0.232
ecr_b	-1.515	2,515	-0.731	-0.399	1.167	-	0.832/1.218	0.527
rxr	-0.986	1,986	-0.908	0.176	2.602	-	1.968	0.225
ccap	-1.363	2,362	-0.328	0.174	0.705	-	0.707	0.386

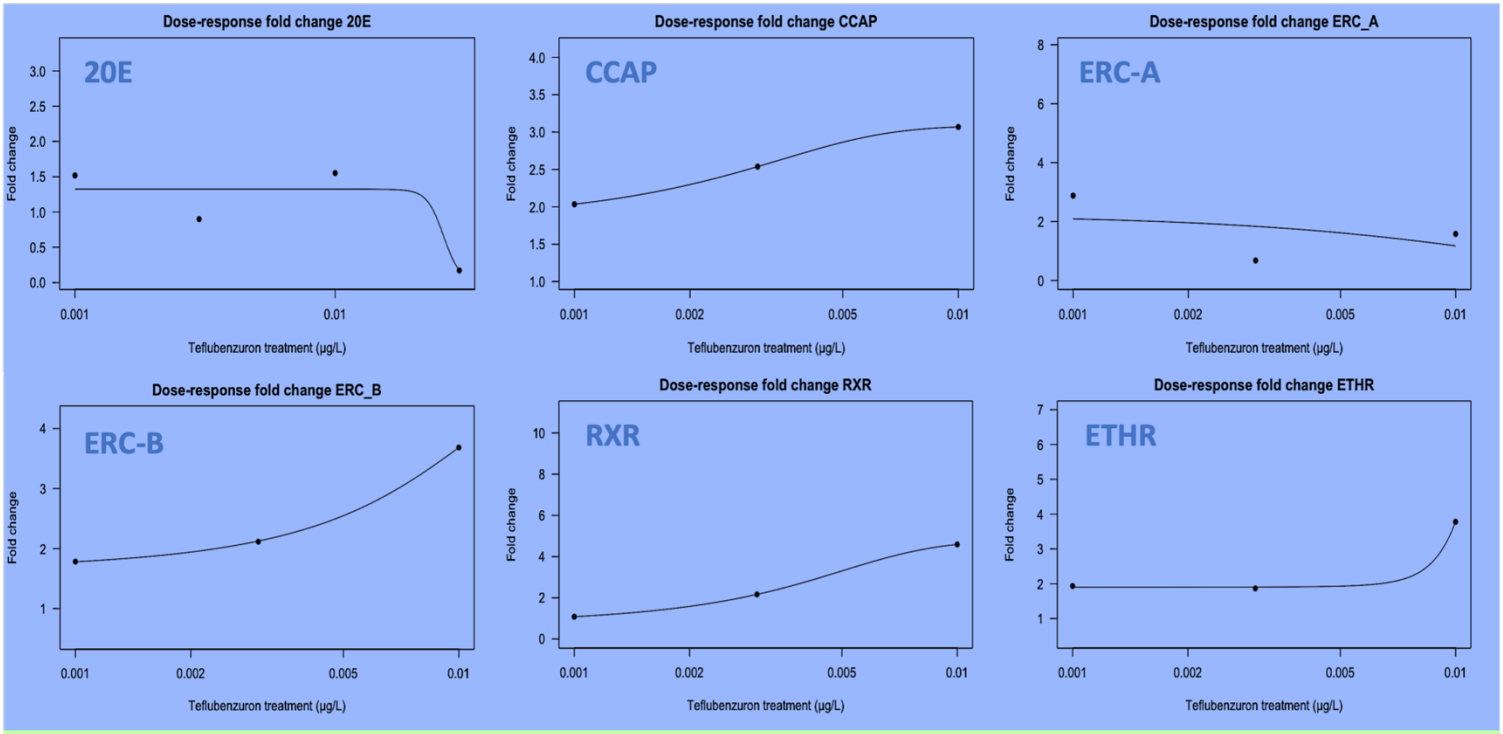
Dose-response fold change 20E
20E
Fold change
Teflubenzuron treatment (µg/L)
Dose-response fold change CCAP
CCAP
Fold change
Teflubenzuron treatment (µg/L)
Dose-response fold change ERC_A
ERC-A
Fold change
Teflubenzuron treatment (µg/L)
Dose-response fold change ERC_B
ERC-B
Fold change
Teflubenzuron treatment (µg/L)
Dose-response fold change RXR
RXR
Fold change
Teflubenzuron treatment (µg/L)
Dose-response fold change ETHR
ETHR
Fold change
Teflubenzuron treatment (µg/L)

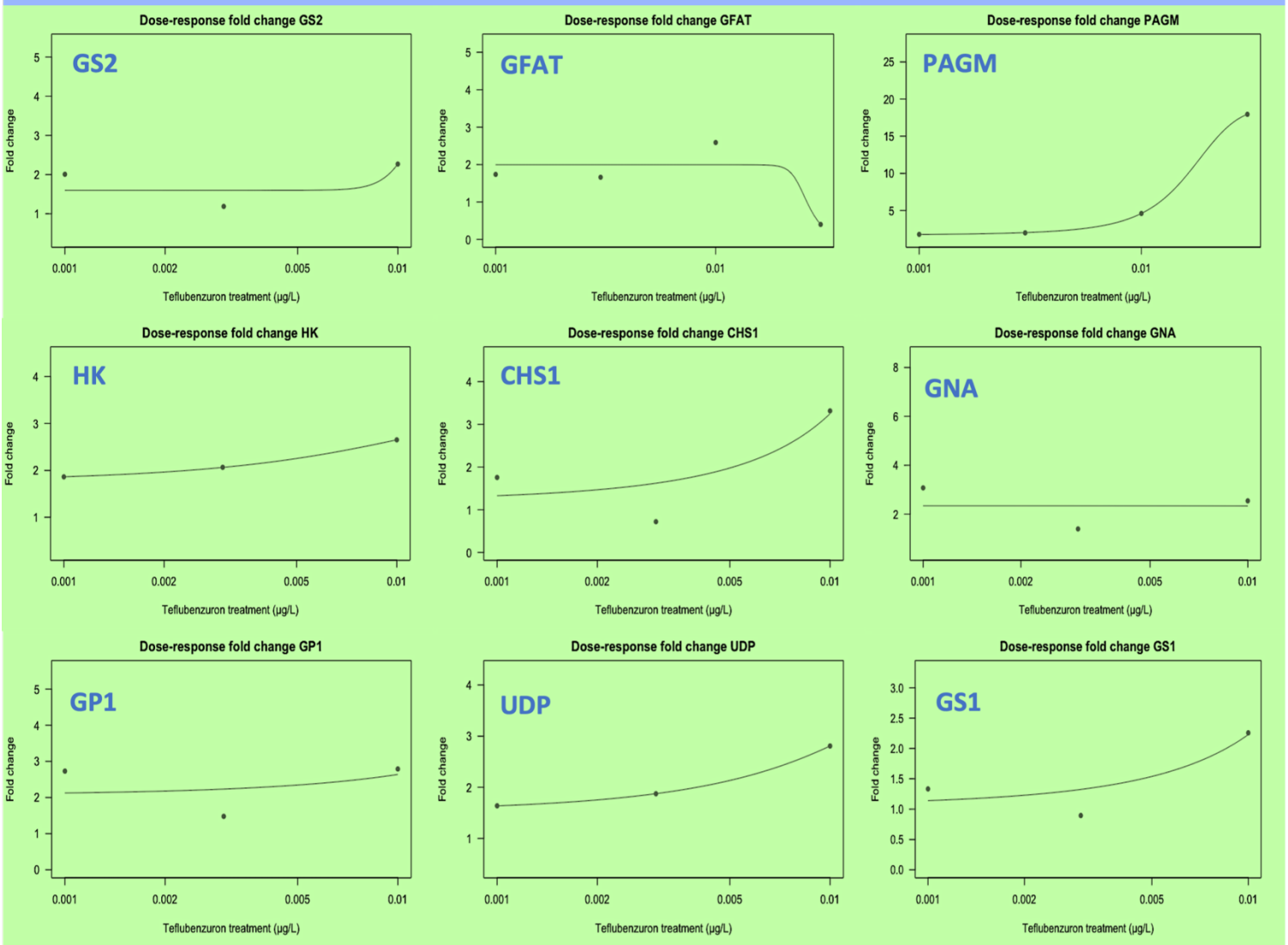
Dose-response fold change GS2
GS2
Fold change
Teflubenzuron treatment (µg/L)
Dose-response fold change GFAT
GFAT
Fold change
Teflubenzuron treatment (µg/L)
Dose-response fold change PAGM
PAGM
Fold change
Teflubenzuron treatment (µg/L)
Dose-response fold change HK
HK
Fold change
Teflubenzuron treatment (µg/L)
Dose-response fold change CHS1
CHS1
Fold change
Teflubenzuron treatment (µg/L)
Dose-response fold change GNA
GNA
Fold change
Teflubenzuron treatment (µg/L)
Dose-response fold change GP1
GP1
Fold change
Teflubenzuron treatment (µg/L)
Dose-response fold change UDP
UDP
Fold change
Teflubenzuron treatment (µg/L)
Dose-response fold change GS1
GS1
Fold change
Teflubenzuron treatment (µg/L)

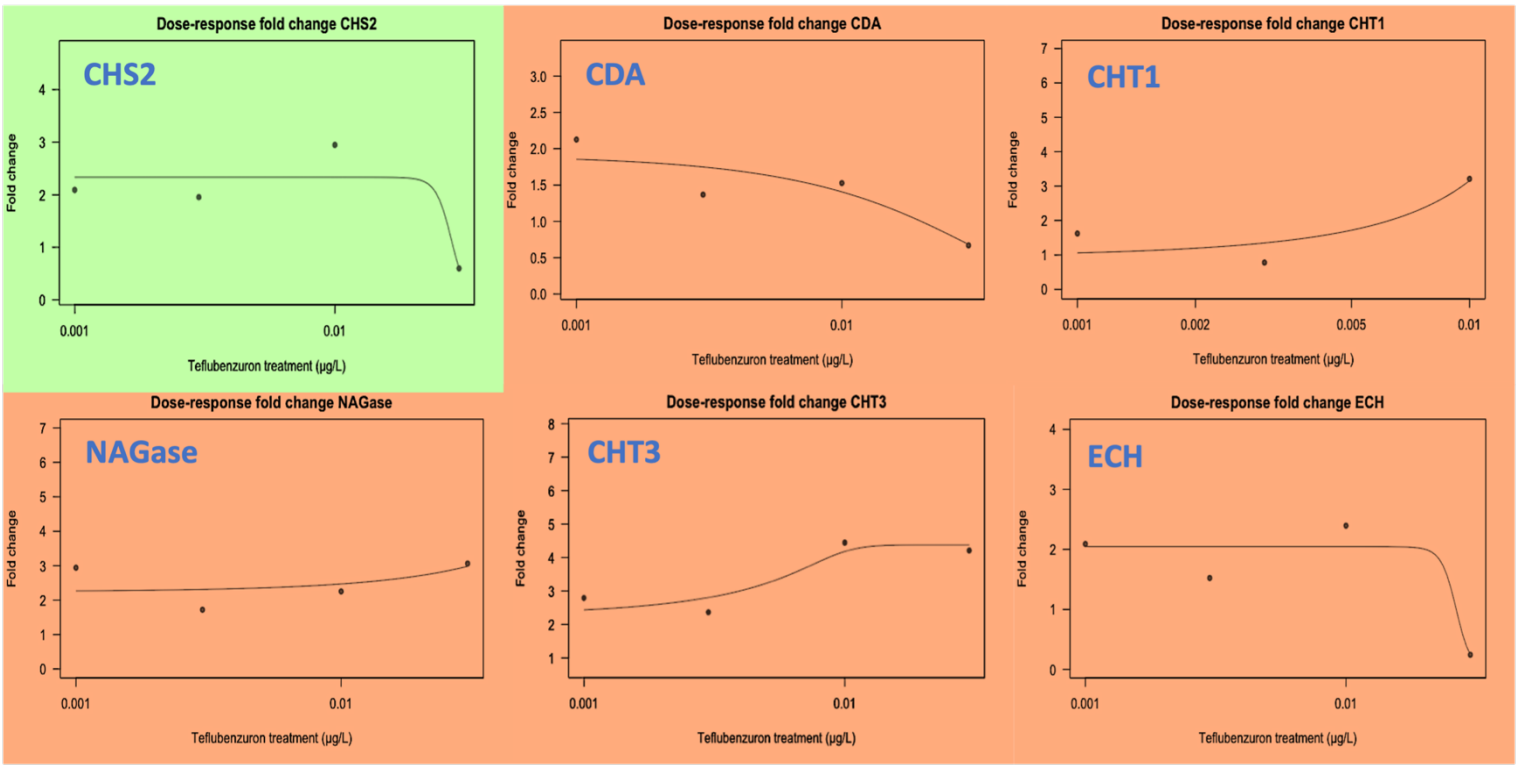

Figure 4: Compilation of predicted dose-response curve of mean fold gene expression at increasing teflubenzuron exposure (0.0 ug/L - 0.01 ug/L or 0.01 ug/L - 0.03 ug/L). Blue= ecdysis regulating genes, green= chitin synthesis genes, and red= chitin degradation genes.

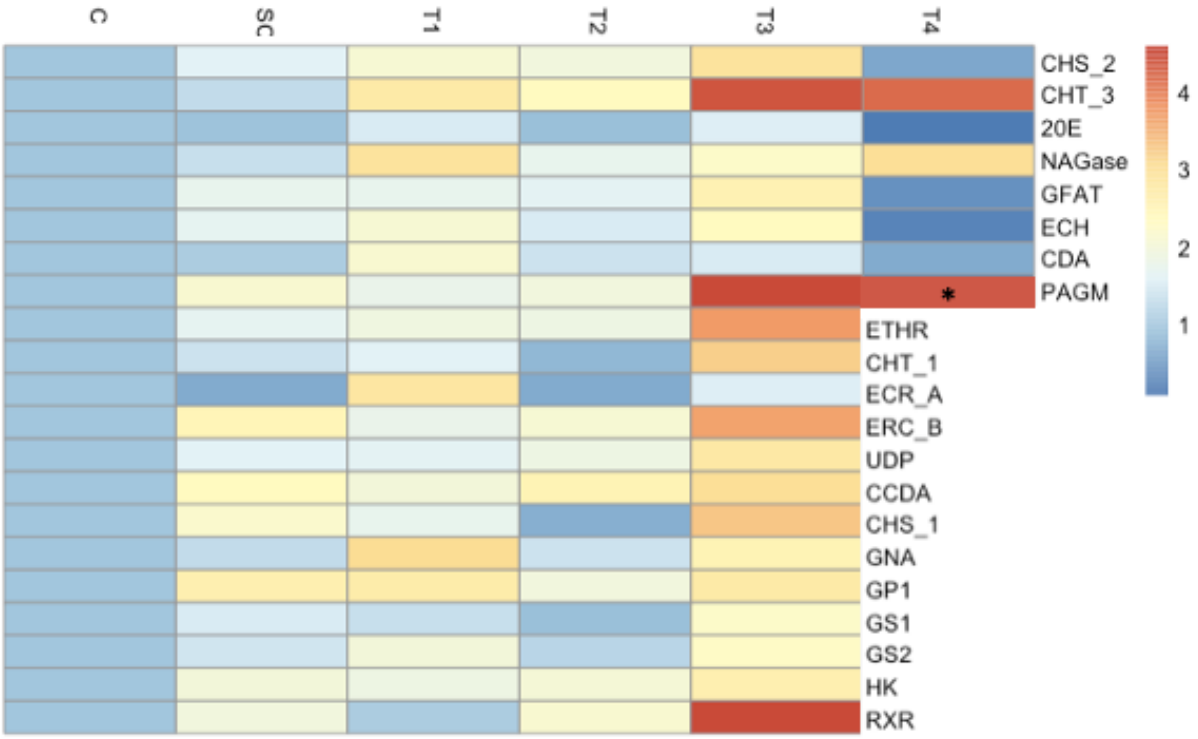

*Figure 5: Heat maps mapping the mean fold change of each treatment against the library of core and intermediate genes normalized against the control treatment. C= Negative control, SC =solvent control, T1= 0.001 ug/L, T2= 0.003 ug/L and T3= 0.01 ug/L. *Mean fold change PAGM at T4 = 17.94. To increase resolution of plot at lower mean fold changes, the T4 PAGM value was removed but is colored red to indicate the increase in expression measured.*

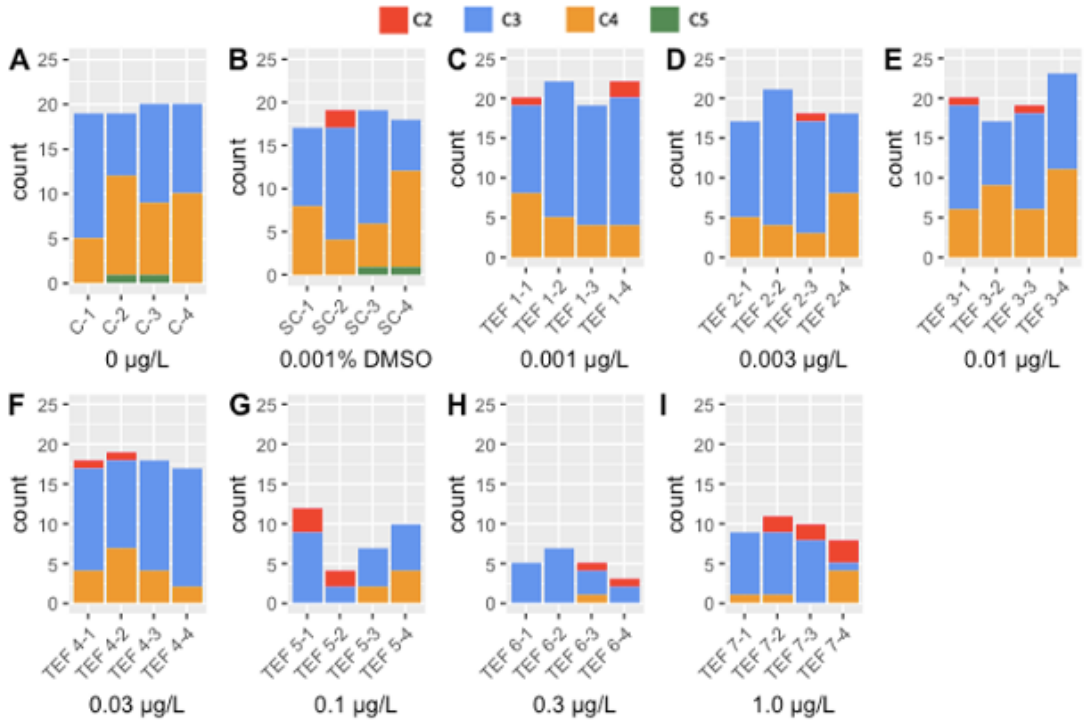

Figure 6: Registered copepods in all treatments grouped by exposure concentration and each individual exposure replicate. Each bar represents the total number of copepods within that exposure replicate (count), colored by category of life stages (C2= red, C= blue3, C4= orange or C5= green) registered.

Table 7: Life stage distribution of copepods by treatment group as a ratio of copepods at each life stage based on the total number of imaged animals in each exposure treatment. Treatment 8 (3.0 µg/) was omitted from the experiment but added to the dataset for transparency.

			Ratio life stage			
Treatment	*[teflubenzuron]*	*Total copepods imaged*	*C2*	*C3*	*C4*	*C5*
Pre experiment	0 µg/L	70	0.357	0.571	0.071	
Control	0 µg/L	78		0.583	0.435	0.025
Solvent control (0.001%)	0 µg/L	73	0.027	0.561	0.383	0.027
TEF 1	0.001 µg/L	83	0.036	0.710	0.253	
TEF 2	0.003 µg/L	74	0.013	0.716	0.270	
TEF 3	0.01 µg/L	79	0.025	0.569	0.405	
TEF 4	0.03 µg/L	72	0.027	0.736	0.236	
TEF 5	0.1 µg/L	33	0.151	0.666	0.181	
TEF 6	0.3 µg/L	20	0.100	0.850	0.050	
TEF 7	1.0 µg/L	38	0.184	0.657	0.157	
TEF 8*	3.0 µg/L	64	0.140	0.703	0.156	

Table 8: Overview of values from categorical Chi test of independence on life stage ratio data. Df= Degrees of freedom, CV= Critical value

			Chi X^2 (p>CV)			
Treatment	*Df*	*CV*	*C2*	*C3*	*C4*	*C5*
All treatments	27	40.113	10.30	12.23	132.62	0.0
Control treatments (Control + Solvent control)	3	7.82	0.02	1.43	58.89	0.0
Low exposure treatments (0.001 µg/L – 0.01 µg/L)	6	12.59	0.03	3.70	53.07	0.0
High exposure treatments (0.03 µg/L – 1.0 µg/L)	9	16.969	3.23	6.31	19.86	0.0

*Table 9: Mean prosome length (mm) at each life stage for all exposure treatments, standard deviations (SD) and calculated coefficient of variance (CV). *Omitted from experiment but supplied in the table for transparency.*

Treatment	TEF Control (0.0 µg/L)			TEF Solvent control (0.001%)				TEF 1 (0.001 µg/L)		
Life stage	C3	C4	C5	C2	C3	C4	C5	C2	C3	C4
Mean prosome length (mm)	1.702	2.135	2.200	1.300	1.729	2.110	2.250	1.300	1.727	2.142
SD	0.094	0.101	NA	NA	0.100	0.073	0.07	NA	0.109	0.074
CV	5.52	4.73	NA	NA	5.78	3.45	3.45	NA	6.31	3.45

Treatment	TEF 2 (0.003 µg/L)			TEF 3 (0.01 µg/L)			TEF 4 (0.03 µg/L)			TEF 5 (0.1 µg/L)		
Life stage	C2	C3	C4	C2	C3	C4	C2	C3	C4	C2	C3	C4
Mean prosome length (mm)	1.300	1.673	2.140	1.400	1.737	2.131	1.450	1.692	2.076	1.140	1.386	1.883
SD	NA	0.130	0.068	NA	0.077	0.106	0.070	0.103	0.083	0.250	0.225	0.194
CV	NA	7.78	3.17	NA	4.43	4.97	4.82	6.08	3.99	17.98	16.23	10.30

Treatment	TEF 6 (0.3 µg/L)			TEF 7 (1.0 µg/L)			TEF 8* (3.0 µg/L)		
Life stage	C2	C3	C4	C2	C3	C4	C2	C3	C4
Mean prosome length (mm)	0.900	1.447	1.700	1.157	1.453	1.683	0.988	1.375	1.620
SD	NA	0.177	NA	0.151	0.186	0.160	0.070	0.133	0.139
CV	NA	11.98	NA	12.90	12.80	9.50	7.08	9.67	8.58

Tabell 10: Collected results from statistical significance testing of parametric prosome length data. A significance level of 0.05 was utilized for all listed significance tests

Treatment	*Tukey test (p<0.05)*	*Single linear regression (p<0.05)*	*Pearson's r*	
			p-value (p<0.05)	*rho*
All treatments	NA	NA	$<2.2x10^{-16}$	$< 2 \times 10^{-16}$
Control (0.0 µg/L)	0.999	0.5033	0.504	0.478
Solvent control (0.001%)	-	-		
TEF 1 (0.001 µg/L)	0.796	0.1069	0.018	0.422
TEF 2 (0.003 µg/L)	0.445	0.0326		
TEF 3 (0.01 µg/L)	0.999	0.7838		
TEF 4 (0.03 µg/L)	0.192	0.0098	2.74×10^{-6}	0.0139
TEF 5 (0.1 µg/L)	0.000	< 2e-16		
TEF 6 (0.3 µg/L)	0.000	1.22e-14		
TEF 7 (1.0 µg/L)	0.000	< 2e-16		

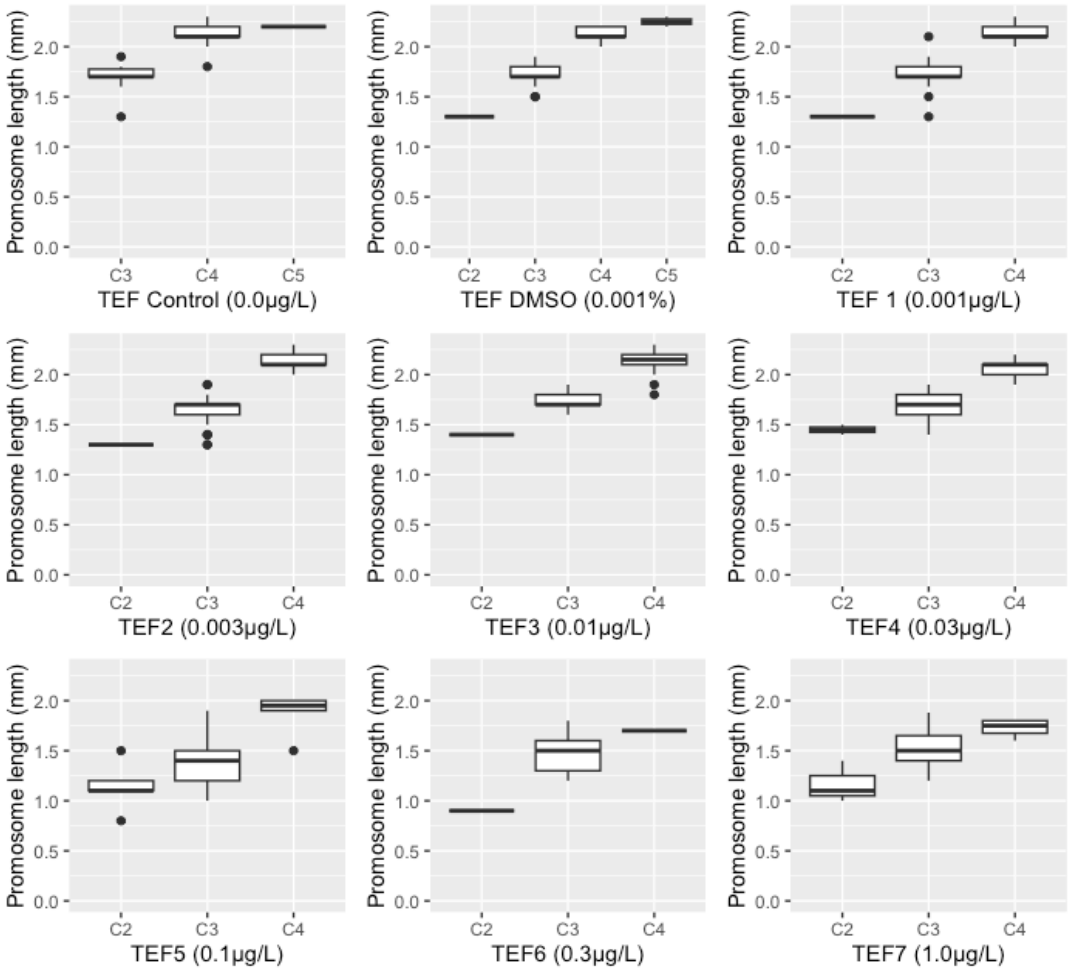

Figure 7: Boxplot of prosome lengths at different developmental stages (C2, C3, C4 and C5) grouped by exposure treatment groups. Each box represents the span of the first to third quadrantile values, the whiskers represent the distance between min and max values, dots represent the outliers, and the line within the box represents the median value.

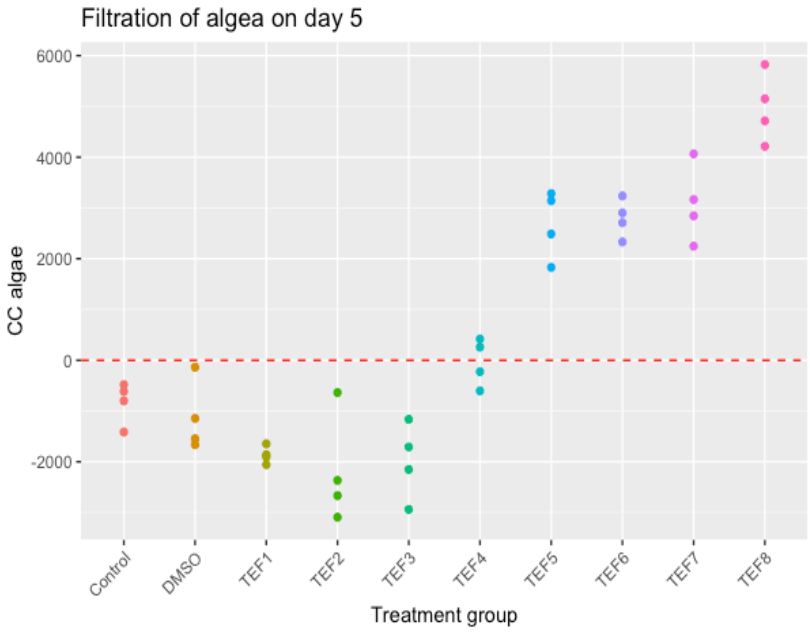

Figure 8: Removal of algae based on measured cell count (CC) (y-axis) in water samples taken from each treatment group (x-axis) compared to algae added on day 5. Negative algae count indicates removal of algae, while positive values indicate accumulation of algae.

Tabell 11: Total RNA extracted from each exposure treatment and replicate. The value for each measurement is categorized by a traffic-light color system according to quality criteria for the given measurement; green = sufficient/good quality, orange = moderate/intermediate quality, and red = low/poor quality. Yield RNA (ng/µl) from each sample is based on 15 µl eluate. The number of animals (#) is listed for each exposure treatment sample. TEF: teflubenzuron.

TEF treatment	#	*Total RNA yield (ng/µl)*	*260/280*	*RNA integrity*	*TEF treatment*	#	*Total RNA yield (ng/µl)*	*260/280*	*RNA integrity*
Control (0.0 µg/L)	16	13812.45	2.15		TEF 4 (0.03 µg/L)	17	3296.85	2.13	
	16	13602.45	2.14			17	3645.90	2.16	
	15	12478.20	2.14			17	3510.75	2.14	
	20	6647.70	2.11			15	6046.50	2.14	
Solvent control (0.00%)	15	10643.55	2.17		TEF 5 (0.1 µg/L)	10	1262.55	2.17	
	17	9738.45	2.14			4	642.00	2.06	
	16	6569.55	2.11			6	643.20	2.17	
	14	12058.50	2.14			7	1283.55	2.05	
TEF 1 (0.001 µg/L)	17	5335.80	2.13		TEF 6 (0.3 µg/L)	5	574.05	2.08	
	14	7905.75	2.14			3	267.45	1.80	
	16	5665.35	2.12			3	305.70	1.98	
	19	10375.05	2.13			1	202.20	2.08	
TEF 2 (0.003 µg/L)	14	10442.85	2.14		TEF 7 (0.1 µg/L)	6	644.85	2.08	
	17	7015.20	2.09			5	184.95	2.09	
	15	6666.30	2.11			5	190.80	1.82	
	16	3012.75	2.13			5	513.15	2.06	
TEF 3 (0.01 µg/L)	17	4457.85	2.09		TEF 8 (3.0 µg/L)		NA	NA	NA
	16	8993.10	2.14			10	1032.00	2.10	
	16	13544.25	2.14			8	523.65	2.04	
	18	9558.30	2.14			8	1224.45	2.06	

Tabell 12: Details of stock preparation of teflubenzuron treatments used in exposure

Treatment	*[]*µg/L	*Extracted from*	*Extracted volume (ml)*	*Total volume (ml)*	*% DMSO*
Stock 1	300 000	Weighed out	3 mg	10	100
Stock 2	30 000	Stock 1	0.5	5	100
TEF 8	3	Stock 1	0.1	10 000	0.001
TEF 7	1	Stock 1	0.33	10 000	0.0003
TEF 6	0.3	Stock 2	0.1	10 000	0.001
TEF 5	0.1	Stock 2	0.33	10 000	0.0003
TEF 4	0.03	TEF 8	100	10 000	0.00001
TEF 3	0.01	TEF 7	100	10 000	3.3×10^{-6}
TEF 2	0.003	TEF 6	100	10 000	0.00001
TEF 1	0.001	TEF 5	100	10 000	3.3×10^{-6}

Solution	*[] %*	*Extracted from*	*Extracted volume (ml)*	*Total volume (ml)*	-
DMSO blank	0.001%	100%	0.100	10 000	-

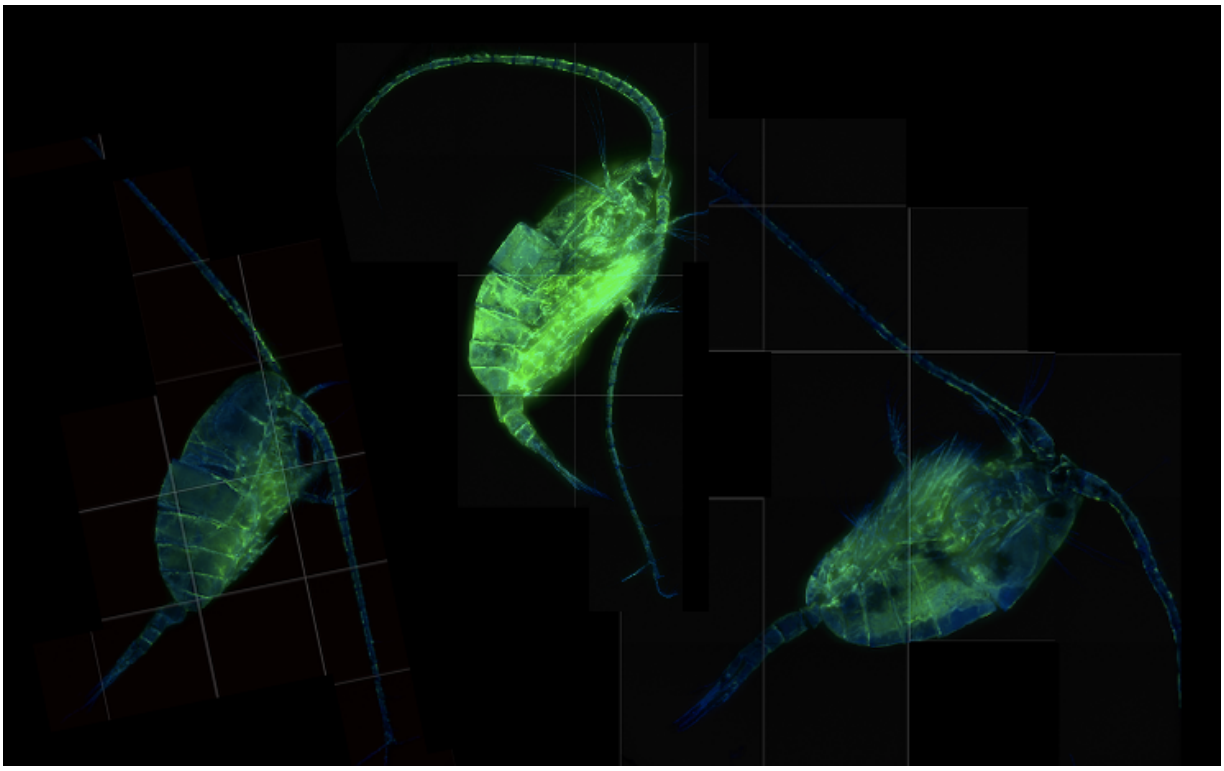

Figure 8: Preliminary fluorescent images by double staining with chitin specific probes, WGA (green light) and Calcofluor (blue light), and nucleic acid specific probes, DAPI (blue light) and Acridine Orange (green light). The pilot copepods imaged have not been exposed to any chemical stressors. Copepod to the left and right are stained by WGA-FICT and DAPI. Middle copepod is stained with Calcofluor and Acridine Orange. Laser scanning combined with stacking of images generates a composite image of fluorescence in the animals. Photos: Jarle Ballangby, FHI.

III. Genes, primers and priority list

Tabell 1: Library of genes and complementary primers for molting and molting regulation used in the gene expression study.

Flea Base ID/ Accession number	*Functional category*	*Gene name*	*Gene symbol*	*Type*	*Species*	*Forward primer*	*Reverse primer*
EU548071.1	Regulation of ecdysis	Crustacean cardioactive peptide	ccap	mRNA	*Daphnia pulex*	GTCGTGTTTGTGTTCTTTGCTTG	ATGGGATTGATGGCAGAGTTGAT
KJ361517.1	Regulation of ecdysis	Ecdysis triggering hormone receptor	ethr	mRNA	*Lepeophtheirus salmonis*	CATCATGTCCACAAAGTTCCGAG	TTTTCTTACTTCCATTCCCCCGG
GQ351503.1	Regulation of ecdysis	Ecdysone receptor a	ecr-a	mRNA	*Tigriopus japonicus*	AATAGCCTCGGGTTTACTCAAGG	ACCTGTCCCTTCTTTTTCCTCTC
AB274824.1	Regulation of ecdysis	Ecdysone receptor b	ecr-b	mRNA	*Daphnia magna*	CGAGCTTCCGGTTACCACTATAA	CGTTTCCGTATTTGCACTGGTAG
M55099.1	Regulation of ecdysis	20-hydroxyecdysone	20e	mRNA	*Drosophila melanogaster*	GGAATCCGATAATGAACTGCGTG	ACTGGATGATTCTGGACAGCATT
GDIQ01008023.1	Regulation of ecdysis	Retinoid-X-receptor	rxr	mRNA	*Daphnia magna*	GGGGTGTGTAGTGATAGAGCAAA	TTGGTTATGACACATGTTTGGCC
GR411056.1	Chitin synthesis	Chitin synthase 1	chs1	mRNA	*C. finmarchicus*	AGCGAAAGGGACCATGATGT	ATCCACGCAACCCTTTCTGT
EL696936.1	Chitin synthesis	Chitin synthase 2	chs2	mRNA	*C. finmarchicus*	ATCGCTGGCTCTGTACTCTAATG	AACAGTCTCACGGTCGGAAATAA
FF277206.1	Chitin synthesis	Glucose-6-phosphate isomerase	gpi	mRNA	*Homarus americanus*	AGAGCTCGCAACATAGATGGTTC	TCCAGTCTCCCGAAATAACCTTG
GDIQ01003928.1	Chitin synthesis	Glutamine:fructose-6-phosphate amidotransferase	gfat	TSA	*Daphnia magna*	CATCACTTGTACTTGCAGCATCC	CAGGGAAGTGCTTGGATTTGAAG
KX427139.1	Chitin synthesis	UDP-N-acetylglucosamine pyrophosphorylase	udp	mRNA	*Tigriopus japonicus*	TGGTATACTCAGCGGCCAATATC	GCTTGACCAATTCTCGTGTGTTC
EL965996.1	Chitin synthesis	Glutamine synthetase 2	gs2	mRNA	*C. finmarchicus*	CTTTCAAGTACAACAAGGAGCCC	ACAGTAGTAAGGTCCCTGAGGTC
M96798.1	Chitin synthesis	Glutamine synthetase	gs1	mRNA	*Panulirus argus*	ACCAGGACACTCAACTTTACTCC	AGGACCAGCTTATTGTTACCCAG
KX427137.1	Chitin synthesis	Glucosamine-6-phosphate-N-acetyltransferase	gna	mRNA	*Tigriopus japonicus*	GAATCTCATGGTGCGTTCTTTGG	TCTCATGGGTAGAAGTGTCCTCA
ES237348.1	Chitin synthesis	Hexokinase 2	Hk2	mRNA	*Macrobrachium nipponense*	ACCTATGTGTCTCAGTTACCCAC	GCCATGAAGTTGAAAAGGTCCTC
FG985878.1	Chitin synthesis	Phosphoacetylglucosamine mutase	pagm	mRNA	*C. finmarchicus*	CGGGTTTAGGACTAAGGCTGAG	GTCCACCAGCTTGATACCATTGT
MT081355.1	Chitin degradation	Chitinase1	cht1	mRNA	*Tityus serrulatus*	GAAAACCCCTCTTTGCTTCTGAC	GCTCCACGTTCCAGTATTTCATG
GBFB01079597.1	Chitin degradation	Chitinase2	cht2	mRNA	*C. finmarchicus*	TCACATTGATCCAGTCCAAGTCC	AGGAGGAGAATTACAGCGACAAG
GBFB01085236.1	Chitin degradation	Chitinase3	cht3	mRNA	*C. finmarchicus*	CCCTGGTCTTGAATTTCATGCTG	GTCCCACTTACAGTACACTCCAG
GBFB01069506.1	Chitin degradation	Chitin deactylase 1	cda	mRNA	*C. finmarchicus*	TTGTATGACTCCTCCATCACAGC	CTTCACGACGATCCAGTTCATTC
GBFB01151866.1	Chitin degradation	Endochitinase	ech	mRNA	*C. finmarchicus*	CACCCAGCCTCTCTCAAGTATAC	TGTATGCGACGACTACTCTGATG
DQ280379.1	Chitin degradation	Beta-N-acetylglucosaminidase	NAGase	mRNA	*Fenneropenaeus chinensis*	AGTCTTACTGTGTAGAGCCTCCT	GTGTTCCAGCAGTTGAGATTCAC
ES414812.1	Housekeeping genes	Elongation factor a	ef1α	mRNA	*C. finmarchicus*	ACAAGGGATGGGCTGTTGAG	TATGGGCGGTGTGACAATCC
Tarrant et.al 2008	Housekeeping genes	Glyceraldehyde-3-phosphate dehydrogenase	gadph		*C. finmarchicus*	CACCTGATGTGTCTGTGGTTG	CTTGAGCTTGGCACAGATTTC
	Housekeeping genes	16S ribosomal	16s		*C. finmarchicus*	AAGCTCCTCTAGGGATAACAGC	CGTCTCTTCTAAGCTCCTGCAC
	Housekeeping genes	Beta-actin	act		*C. finmarchicus*	CCATTGTCCGTCTTGATCTTG	AAAGAGTAGCCACGCTCAGTG

Tabell 2: Priority list of genes and primers for molting and molting relevant genes in Calanus finmarchicus.

Flea Base ID/ Accession number	*Functional category*	*Gene name*	*Gene symbol*	*Priority ranking*	*Priority type*	*AOP relevance*
EL696936.1	Chitin synthesis	Chitin synthase 2	*chs2*	1	Core	AOP360. AOP358
GBFB01085236.1	Chitin degradation	Chitinase3	*cht3*			
M55099.1	Regulation of ecdysis	20-hydroxyecdysone	*20e*	2	Inter-mediate	AOP360. AOP358. AOP359
DQ280379.1	Chitin degradation	Beta-N-acetylglucosaminidase	*NAGase*			
GDIQ01003928.1	Chitin synthesis	Glutamine: fructose-6-phosphate amidotransferase	*gfat*			
GBFB01151866.1	Chitin degradation	Endochitinase	*ech*			
GBFB01069506.1	Chitin degradation	Chitin deactylase 1	*cda*			
FG985878.1	Chitin synthesis	Phosphoacetylglucosamine mutase	*pagm*			
KJ361517.1	Regulation of ecdysis	Ecdysis triggering hormone receptor	*ethr*			
MT081355.1	Chitin degradation	Chitinase1	*cht1*			
GQ351503.1	Regulation of ecdysis	Ecdysone receptor a	*erc-a*			
AB274824.1	Regulation of ecdysis	Ecdysone receptor b	*erc-b*			
KX427139.1	Chitin synthesis	UDP-N-acetylglucosamine pyrophosphorylase	*udp*			
Tarrant et.al 2008	Housekeeping genes	16S ribosomal	*16s*			
	Housekeeping genes	Beta-actin	*act*			
ES414812.1	Housekeeping genes	Elongation factor a	*ef1α*			
EU548071.1	Regulation of ecdysis	Crustacean cardioactive peptide	*ccap*	3	Low	AOP360. AOP358. AOP359
KX427139.1	Chitin synthesis	UDP-N-acetylglucosamine pyrophosphorylase	*udp*			
GDIQ01008023.1	Regulation of ecdysis	Retinoid-X-receptor	*rxr*			
FF277206.1	Chitin synthesis	Glucose-6-phosphate isomerase	*gpi*			
M96798.1	Chitin synthesis	Glutamine synthetase	*gs1*			
ES237348.1	Chitin synthesis	Hexokinase 2	*hk2*			
EL965996.1	Chitin synthesis	Glutamine synthetase 2	*gs2*			
KX427137.1	Chitin synthesis	Glucosamine-6-phosphate-N-acetyltransferase	*gna*			
GBFB01079597.1	Chitin degradation	Chitinase2	*cht2*			
Tarrant et.al 2008	Housekeeping genes	Glyceraldehyde-3-phosphate dehydrogenase	*gapdh*			

Tabell 3: Optimal temperatures for qPCR for each gene primer set. Genes of similar optimal temperature grouped together to optimize qPCR runs and plate organization

*Temperature (*C)*	*Gene primer*					
64.2	*hk2*	*chs-1*				
62.5	*chs-1*	*pagm*	*20e*	*cht3*		
60.0	*ccap*	*NAGase*	*act*	*cda*	*g2s*	*gfat*
56.6	*16s*	*ethr*	*gna*	*erc-a*		
53.8	*gp1*	*cht1*	*rxr*	*cht2*	*udp*	*gapah*
51.6	*ech*	*erc-b*	*ef1-a*	*ss1*		

Tabell 4: Overview of genes analyzed by qPCR. The full library of genes was analyzed in the control treatments and 0.001 µg/L - 0.01 µg/L treatments. Additionally. core genes were analyzed from the 0.03 µg/L treatment. No genes were analyzed in the 0.1 µg/L - 1.0 µg/L treatments. Genes that were removed from the main analysis due to issues with primer optimization: gadph *and* cht2

Gene name	*Gene symbol*	*Functional category*	*Priority nr.*	*Control. Solvent control. TEF1-TEF3 (0.0-0.01)*	*TEF4 (0.03)*
Chitin synthase 2	*chs2*	Chitin synthesis	1	X	X
Chitinase3	*cht3*	Chitin degradation		X	X
Ecdysis triggering hormone receptor	*ethr*	Regulation of ecdysis	2	X	X
Chitinase1	*cht1*	Chitin degradation		X	
Ecdysone receptor a	*erc-a*	Regulation of ecdysis		X	X
Ecdysone receptor b	*erc-b*	Regulation of ecdysis		X	
20-hydroxyecdysone	*20e*	Regulation of ecdysis		X	X
Glutamine: fructose-6-phosphate amidotransferase	*gfat*	Chitin synthesis		X	X
Phosphoacetylglucosamine mutase	*pagm*	Chitin synthesis		X	X
Endochitinase	*ech*	Chitin degradation		X	X
Chitin deactylase 1	*cda*	Chitin degradation		X	X
Beta-N-acetylglucosaminidase	*NAGase*	Chitin degradation		X	X
16S ribosomal	*16s*	Housekeeping genes		X	X
Beta-actin	*act*	Housekeeping genes		X	X
Elongation factor a	*ef1α*	Housekeeping genes		X	X
Crustacean cardioactive peptide	*ccap*	Regulation of ecdysis	3	X	
UDP-N-acetylglucosamine pyrophosphorylase	*udp*	Chitin synthesis		X	
Retinoid-X-receptor	*rxr*	Regulation of ecdysis		X	
Glucose-6-phosphate isomerase	*gpi*	Chitin synthesis		X	
Glutamine synthetase	*gs1*	Chitin synthesis		X	
Hexokinase 2	*hk2*	Chitin synthesis		X	
Glutamine synthetase 2	*gs2*	Chitin synthesis		X	
Glucosamine-6-phosphate-N-acetyltransferase	*gna*	Chitin synthesis		X	
Glyceraldehyde-3-phosphate dehydrogenase	*gapdh*	Housekeeping genes		X	

IV. Image compilation: Dose-dependent morphological deformities in *Calanus finmarchicus* from teflubenzuron exposure

Description: A set of images from each exposure treatment has been selected and organized in this document to illustrate the extent of damage, deformities, molting inhibition, and mortality at different exposure concentrations. Some control images have been selected to highlight the difference between the visual effects and normal development within each treatment.

All images were taken with a Leica Macroscope (Leica Z6 APO with a Leica MC170HD camera, both Leica Microsystems, Wetzlar, Germany) with a magnification of 3,6X. All images were taken by Celine Våga as a part of the thesis. A scale bar of 1mm is supplemented for the first image in every image series and is applicable for the other images within the same exposure group.

Upon inquiry, access to the full folder of images could be arranged.

Exposure treatment TEF 8 (3.0 µg/L)

Figure 1: Images of copepods from the omitted exposure treatment TEF 8 (3.0ug/L). Image A: Normal C3 copepod with minor signs of necrosis. Image B: Abnormal alive copepod with serious deformities on both the prosome and the urosome. Image C: Dead copepod with extreme damage. Image D: Abnormal alive copepod with serious deformities on the prosome as well as antennas. Signs of necrosis ad additional exoskeleton stuck to the prosome. Image E: Abnormal copepod with deformities on the prosome and breakage of the exoskeleton, Image F: Dead copepod with complete necrosis and broken exoskeleton attached.

Exposure treatment TEF 7 (1.0 µg/L)

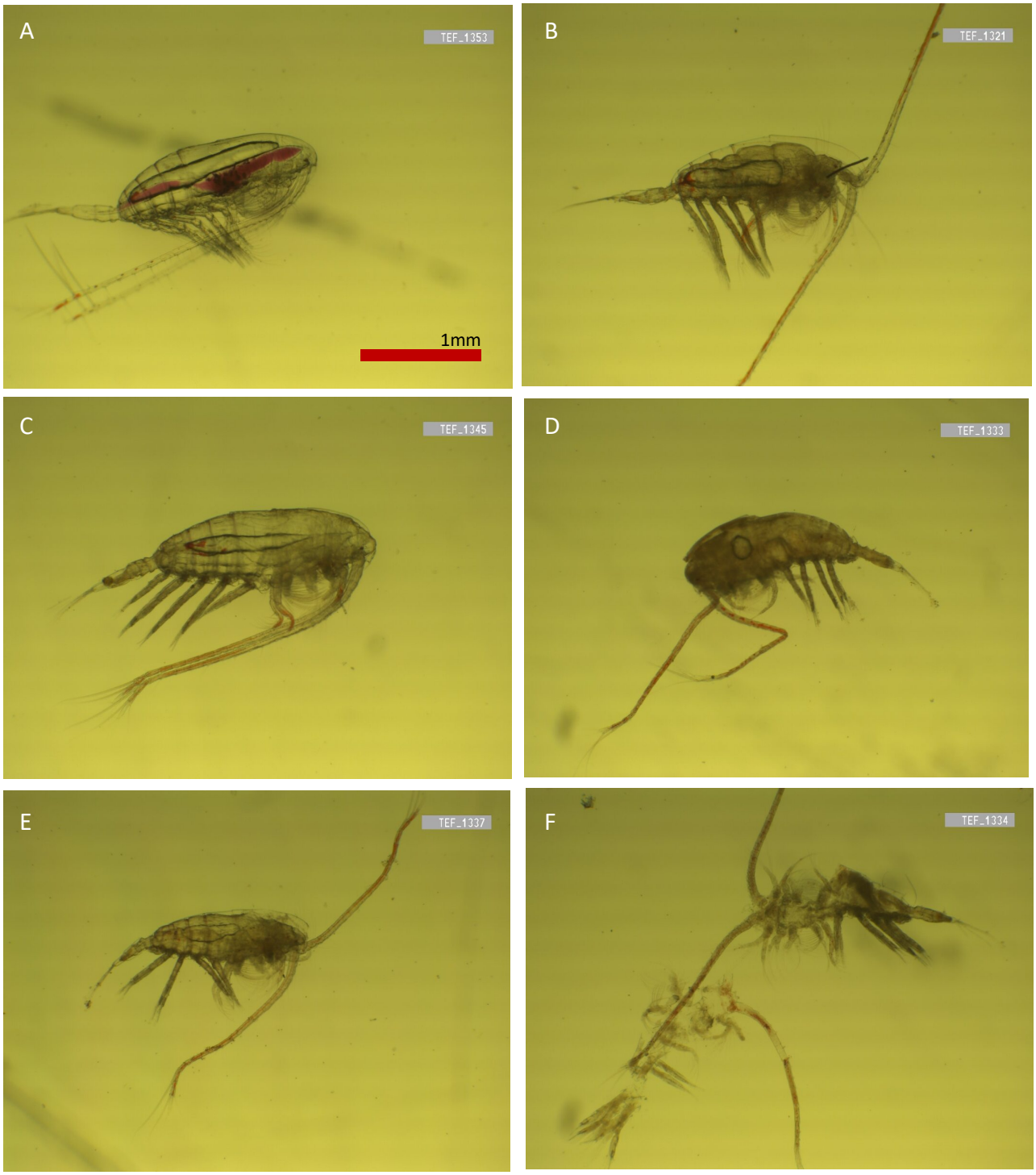

Figure 2: Images of copepods from exposure treatment TEF 7 (1.0 ug/L). Image A: The copepod is a C3 individual of normal health. Image B: The copepod is necrotic with intact lipid sack. The animal is stuck within a larger new exoskeleton and has deformities on the main body and tail appendages. Image C: Copepod on image C is a large C4 with small initial signs of necrosis and an intact lipid sack. Signs of a newly formed exoskeleton can be seen around the outer edges of the animal over the head and between the attachment points between the legs and the prosome, as well as at the tip of the tail. Image D: The copepod is completely dead with serious necrosis and disintegrated lipid sack. Image E: The copepod has an intact lipid sack but shows signs of necrosis, deformities of the prosome and an attached outer exoskeleton. Image F: Two disintegrated copepod remains. The leg appendages and the antennas are still attached to the remains.

Exposure treatment TEF 6 (0.3 µg/L)

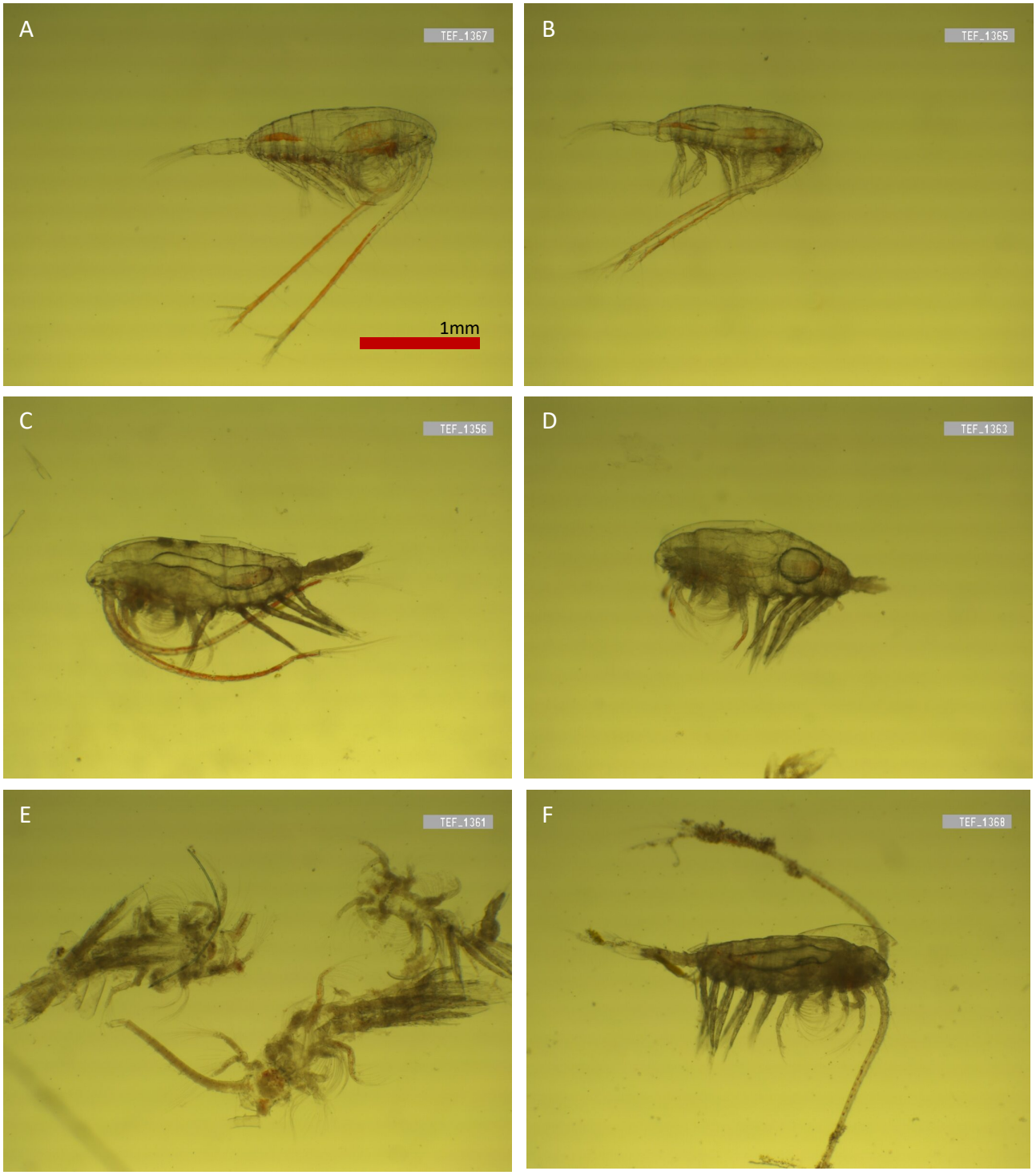

Figure 3: Captured images of TEF 6 (0.3 ug/L) exposed copepods. Image A: Normal and alive C3 copepod with no signs of molting inhibition or deformities. Image B: The copepod is a smaller C3 individual with signs of molting inhibition. Notice the stuck exoskeleton on above the head of the copepod. Image C: The copepod still has intact lipid sack, but show several clear signs of necrosis (darker areas on the posterial parts of the prosome (two distinct spots), the leg appendages and on the tail. The old exoskeleton is also visible on the posterior of the prosome with a clear breakage point above the two necrotic areas. Image D: The copepod is dead, with both clear necrosis and disintegrated circular lipid sack in the interior of the animal. Notice the remains of the new exoskeleton around the head of the copepod and the deformities of the body under/within the new exoskeleton. Image E: Three disintegrated copepods with necrotic legs and antennas still attached. Image F: The copepod has an intact lipid sack, but is completely necrotic with debris stuck to the antennas and tail segment. Notice remnants of exoskeleton still stuck on the head of the animal.

Exposure treatment TEF 5 (0.1 µg/L)

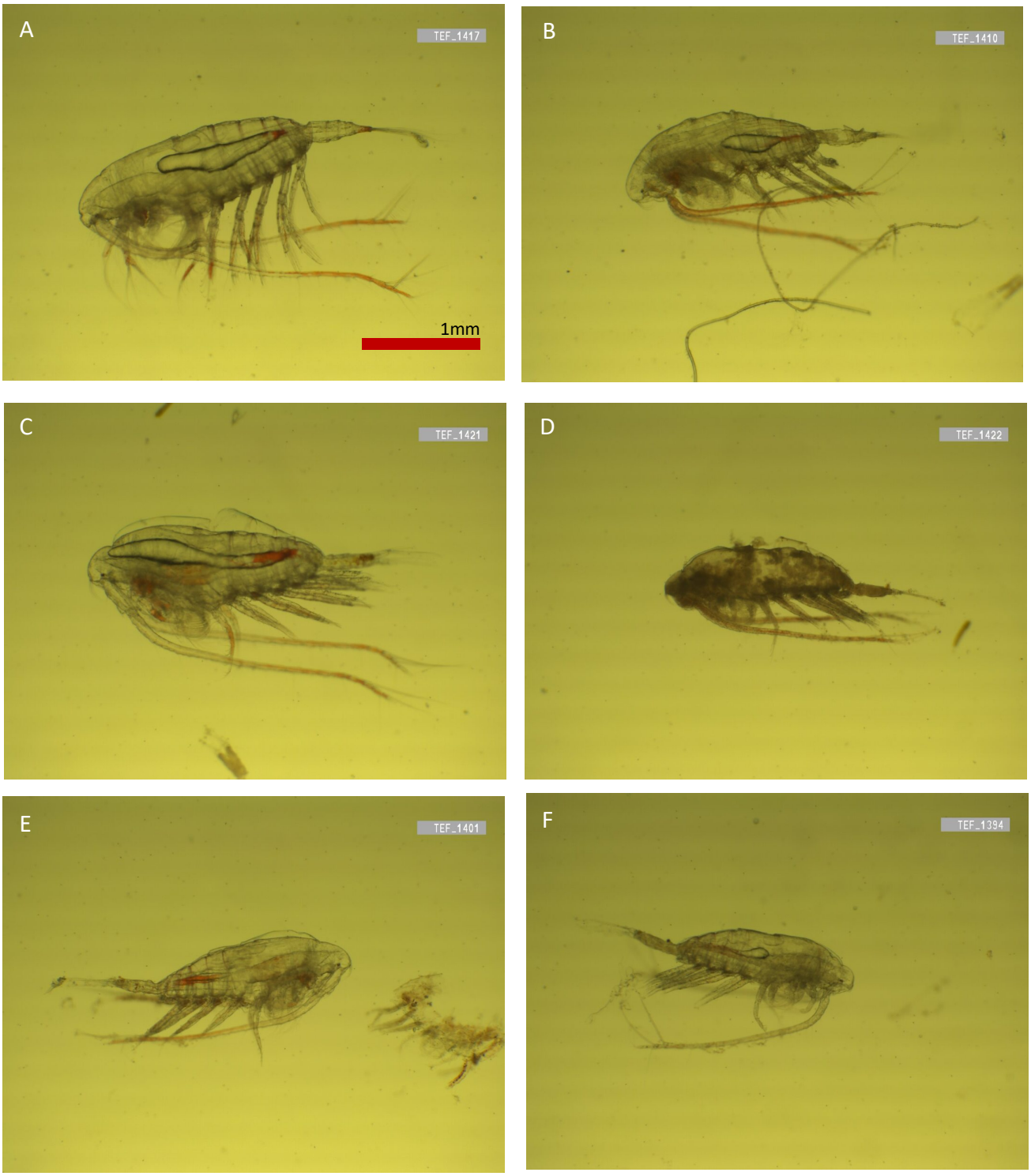

Figure 4: Captured images of TEF 5 (0.1 µg/L) copepods. Image A: Normal C4 individual with fine vital indicators. Image B: Abnormal copepod with breakages in the cuticle visible on the urosome with early signs of necrosis. Image C: Also abnormal copepod with a 'tight band' around the head. The copepod also has an extra skeleton stuck on the prosome. Image D: Copepod with complete necrosis and double exoskeleton in addition to the 'tight band' around the head similarly to the copepod on image C. Image E: Seemingly vital copepod with an additional exoskeleton on the prosome. Additionally, to the right of the animal is a disintegrated copepod. Image F: Also a seemingly vital copepod, but has a slightly deformed head, similarly to the copepods in image C and D.

Exposure treatment TEF 4 (0.03 µg/L)

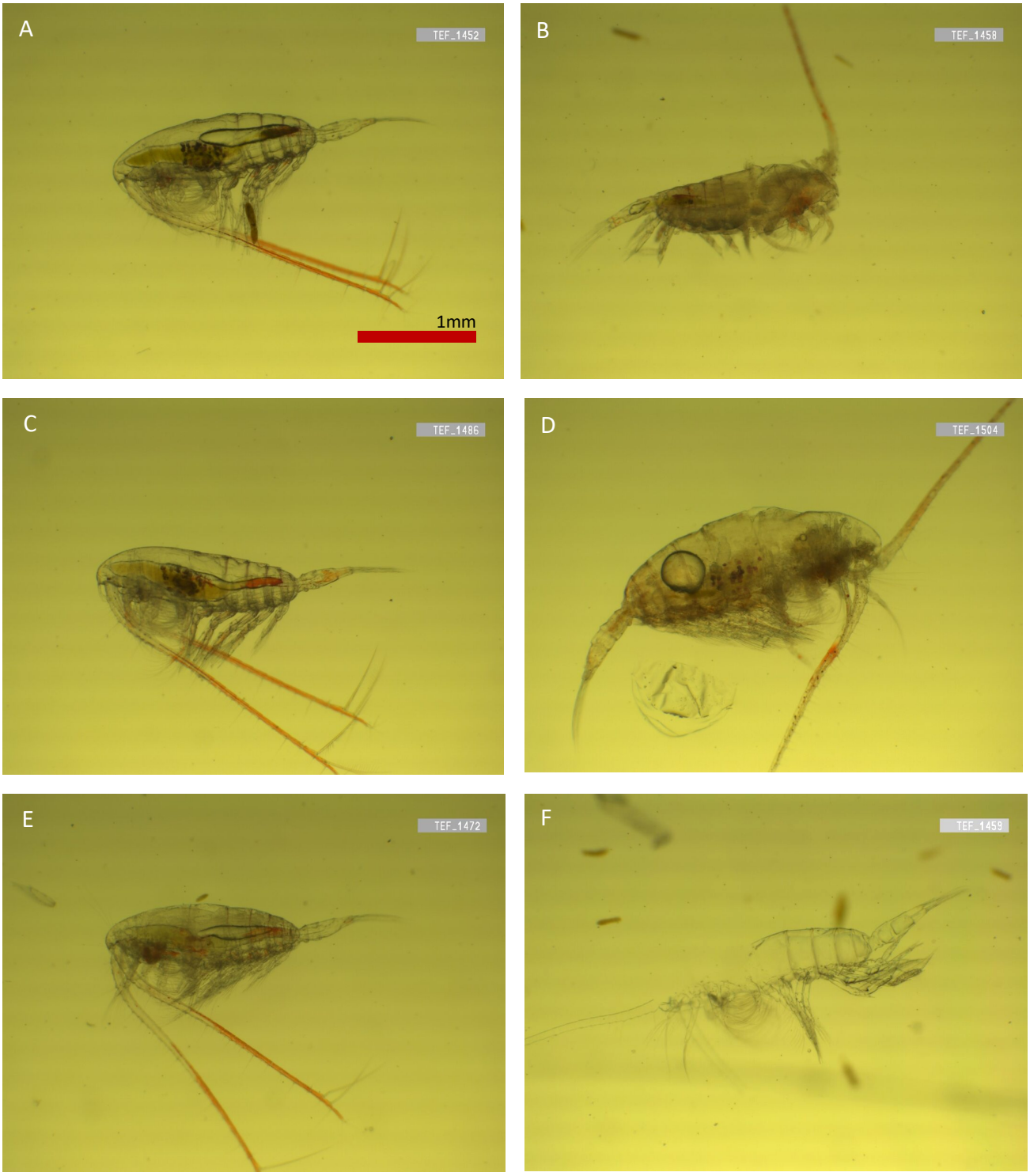

Figure 5: Captured images of TEF 4 (0.03 µg/L). Image A: Copepod on image A is a normal C3 copepod. Image B: Copepod on image B is dead with severe necrosis and has an abnormal prosome. Image C: Normal C3 copepod with indications of molting visible on the lower back of the animal. Image D: Dead copepod with disintegrated lipid sac and exoskeletal deformities and breakage around the head. Image E: Necrotic but viable copepod with intact lipid sac. Image F: Successfully molted carapace completely escaped leaving transparent 'ghost' of former inhabitant. Notice the clean retraction of apical appendages such as antennas and legs. Additionally, the point of escape from the carapace seems to be at the upper back of the animal.

Exposure treatment TEF 3 (0.01 µg/L)

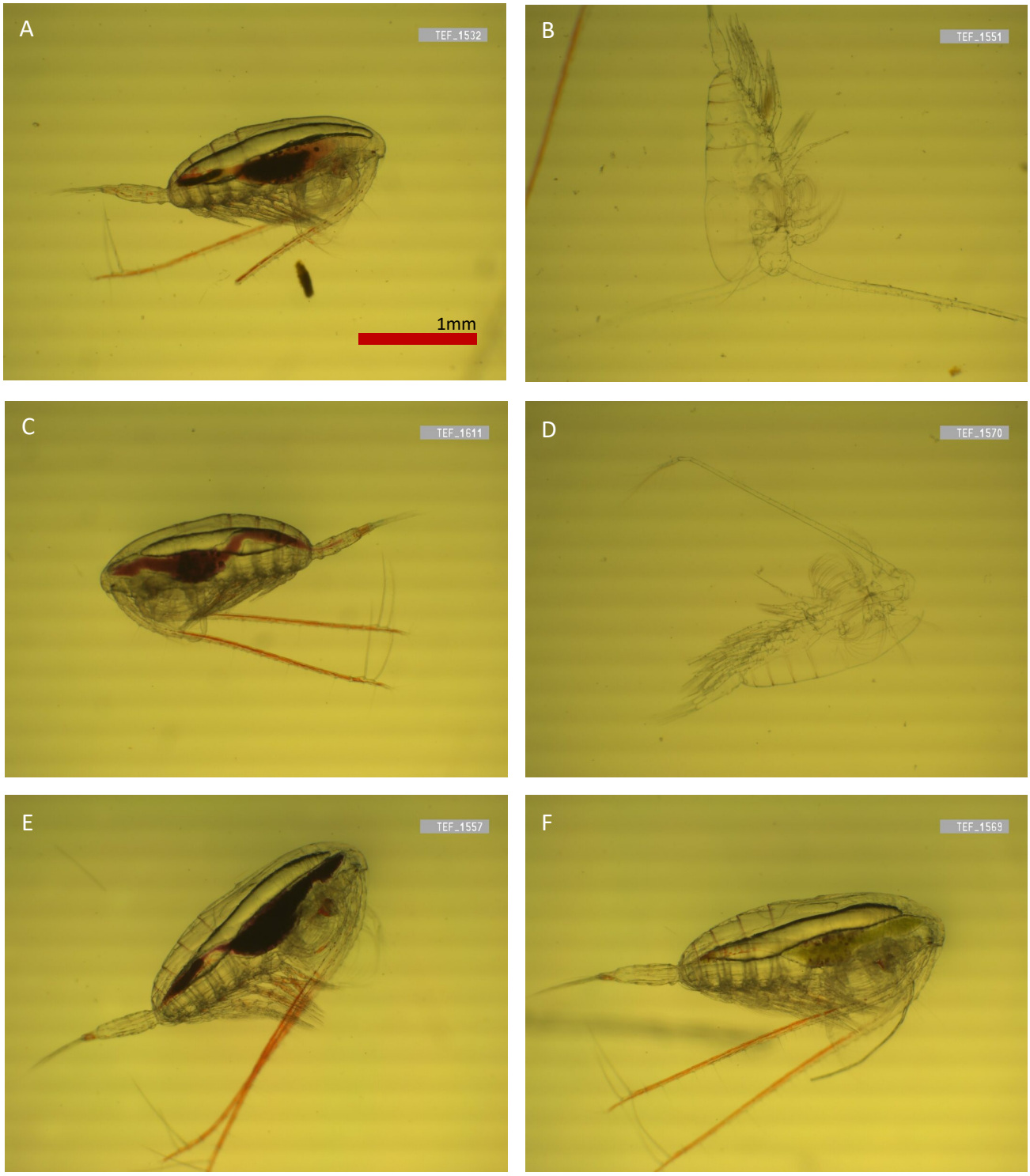

Figure 6: Captured images of TEF 3 (0.01 µg/L). Image A: Normal C3 copepod with one broken antenna. Image B: Successfully molted exoskeleton remnants of a former C3 copepod. Image C: Normal C3 copepod. Image D: Successfully molted exoskeleton. Note the breakage point of the carapace at the top of the carapace where the head of the animal would have been. Image E: Normal C4 copepod with indications of molting. Note the double layered exoskeleton on the prosome. Image F: Normal C4 copepod. Similar indications of molting like the copepod on image E.

Exposure treatment TEF 2 (0.003 µg/L)

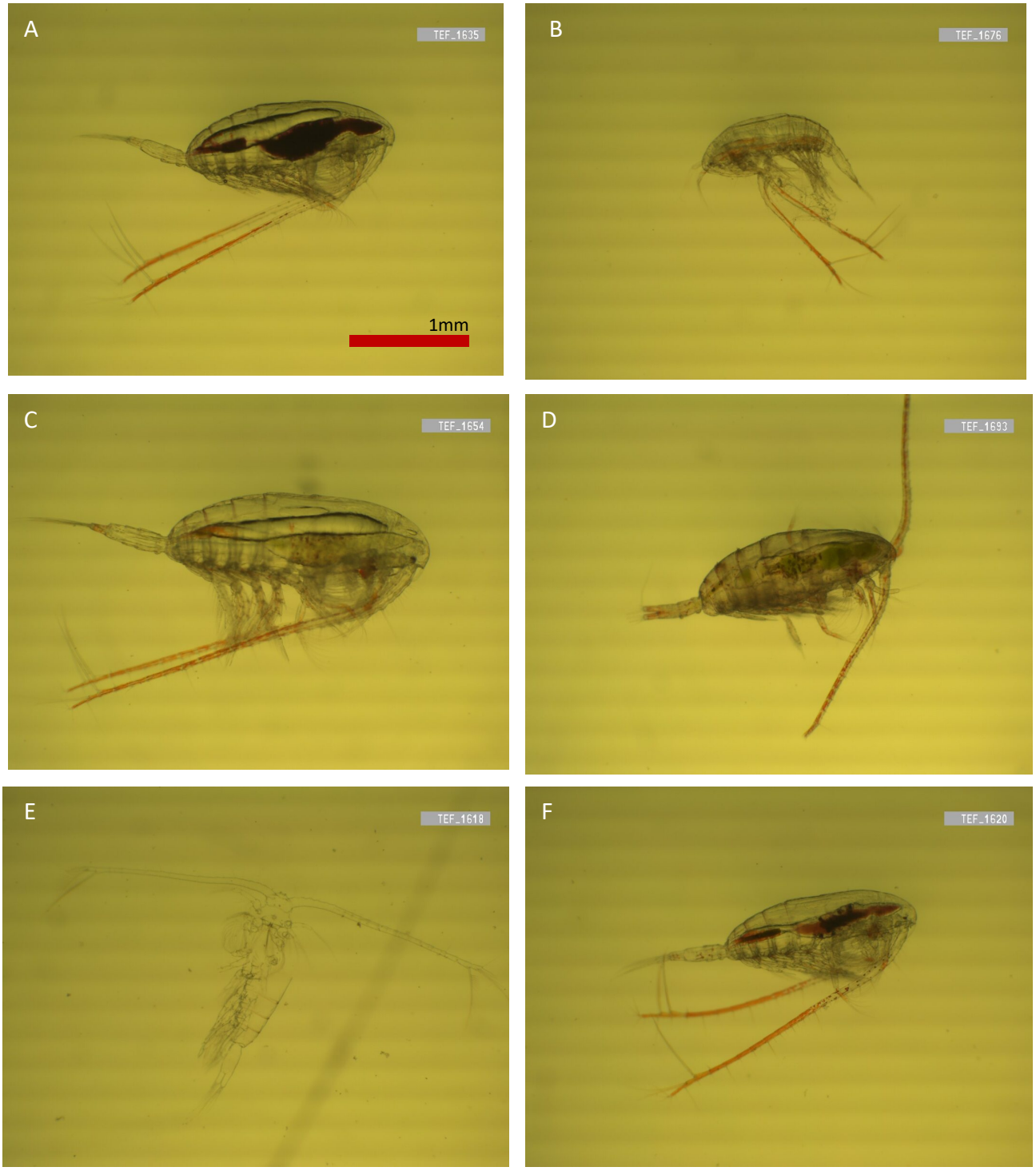

Figure 7: Captured images of TEF 2 (0.003 µg/L). Image A: Normal C3 copepod. Image B: Abnormal copepod with deformed prosome. Notice position of antennas and hunched back. Additionally, an extra exoskeleton is visible on the back of the animal. Image C: Normal C4 copepod. Possible signs of molting. Notice the extra cuticle layer on the prosome. Image D: Necrotic copepod with intact lipid sack. Image E: Successfully molted exoskeleton. Notice breakage point on the upper back where the head would have been positioned. Image F: Normal C3 copepod.

Exposure treatment TEF 1 (0.001 µg/L)

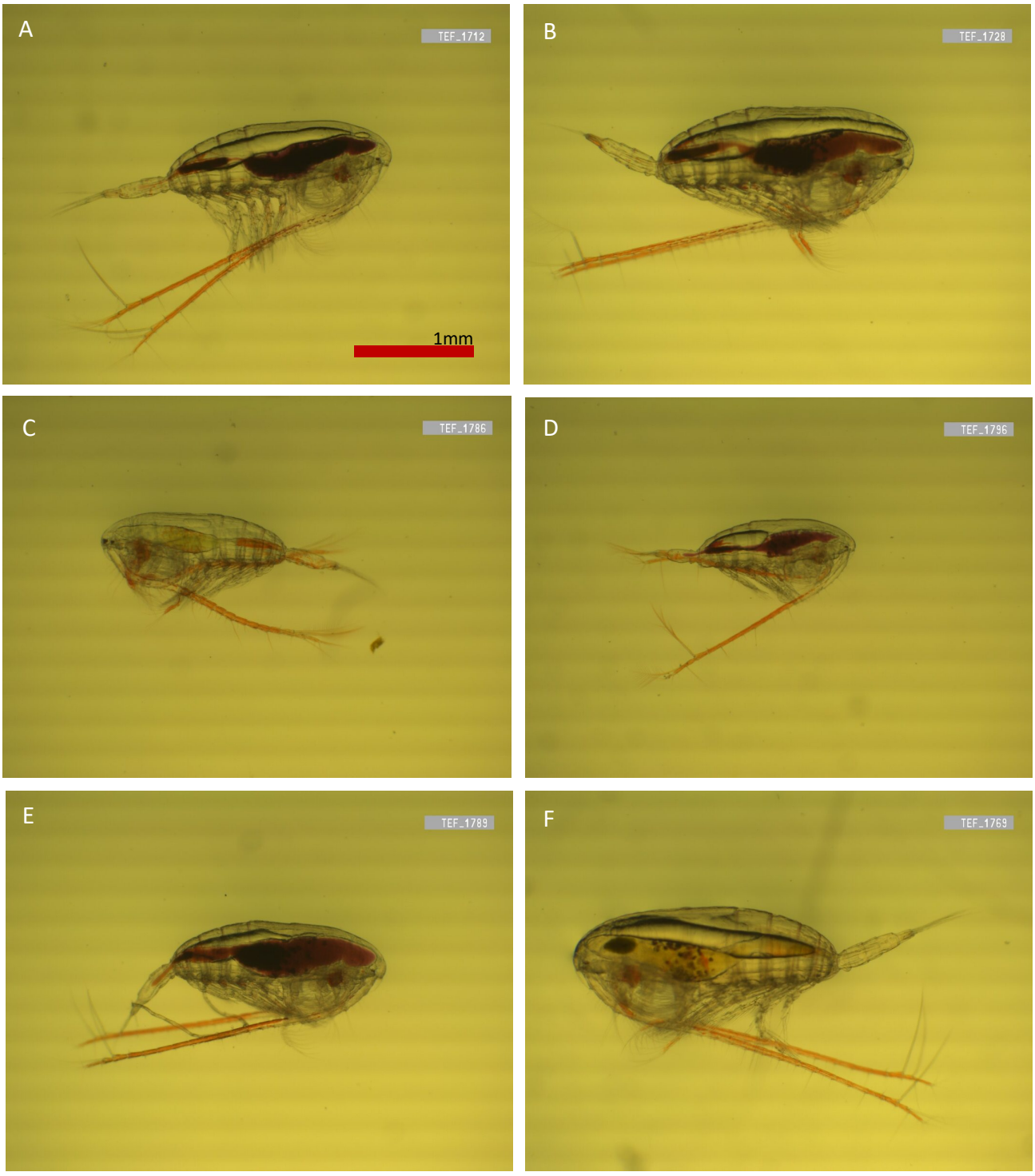

Figure 8: Captured images of TEF 1 (0.001 µg/L). Image A: Normal C3 copepod. Image B: Normal C4 copepod with some deformities on the prosome segment. Image C: Small C2/C3 copepod with possible deformities on the antennas. Image D: Normal small C2 copepod. Image E: Normal C3 with possible early necrosis. Image F: Normal large C4 copepod.

Exposure treatment SC (Solvent control, 0.0 µg/L)

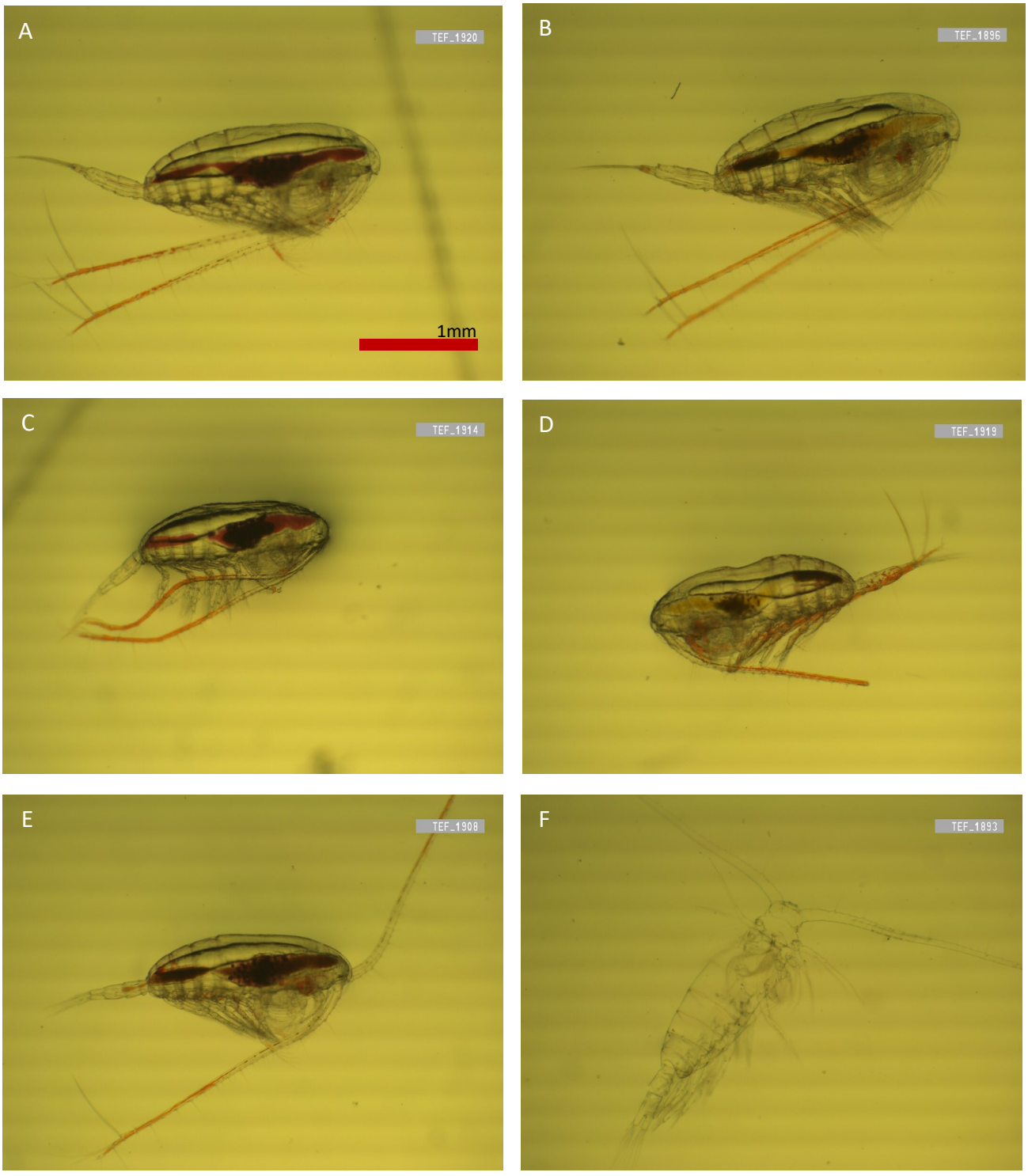

Figure 9: Captured images of solvent control (SC) (0.0 µg/L). Image A: Normal C3 copepod. Image B: Normal C4/C5 copepod. Notice extra cuticle layer over the prosome segments. Image C: Small C3 copepod with deformed antennas. Image D: Abnormal C3 copepod with "groove" in the prosome and broken antenna. Image E: Normal C3 copepod. Image F: Successfully molted exoskeleton of former C3 copepod.

Exposure treatment C (Negative control, 0.0 µg/L)

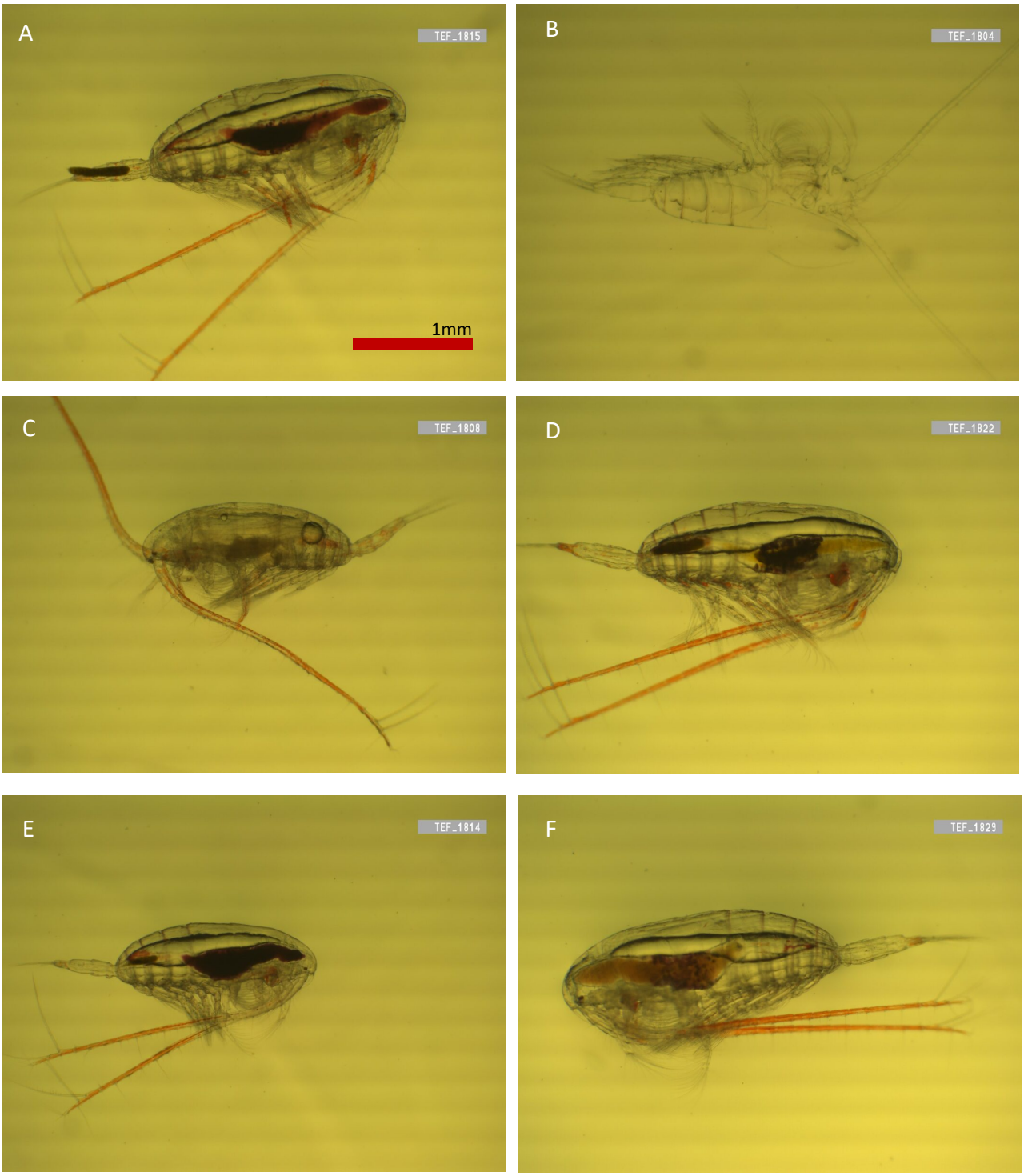

Figure10: Captured images of negative control (C) (0.0 µg/L). Image A: Normal C4 copepod with extra cuticle layer over prosome. Image B: Successfully molted exoskeleton of former C3 copepod. Image C: Dead C3/C4 copepod. Notice extra exoskeleton layer at the head. Image D: Normal large C4 copepod. Notice extra cuticle layer at the prosome and head area. Image E: Normal C3. Image F: normal C4 copepod.

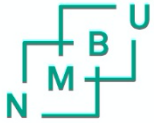

Norges miljø- og biovitenskapelige universitet
Noregs miljø- og biovitskapelege universitet
Norwegian University of Life Sciences

Postboks 5003
NO-1432 Ås
Norway